

การโคลนยีน และการวิเคราะห์ลักษณะของโปรตีน MreB และ FtsZ  
จากเชื้อแบคทีเรียบาซิลลัส ซับทิลิส

ว่าที่ร้อยตรีหญิงสุนารี โชนัด



วิทยานิพนธ์นี้เป็นส่วนหนึ่งของการศึกษาตามหลักสูตรปริญญาวิทยาศาสตรมหาบัณฑิต  
สาขาวิชาชีวเคมี  
มหาวิทยาลัยเทคโนโลยีสุรนารี  
ปีการศึกษา 2558

**GENE CLONING AND CHARACTERIZATION OF  
MREB AND FTSZ FROM *BACILLUS SUBTILIS***

**Sunaree Choknud**



**A Thesis Submitted in Partial Fulfillment of the Requirements for the  
Degree of Master of Science in Chemistry  
Suranaree University of Technology  
Academic Year 2015**

สุนารี โชคนัด : การโคลนยีน และการวิเคราะห์ลักษณะของโปรตีน MreB และ FtsZ จากเชื้อแบคทีเรียบาซิลลัส ซับทิลิส (GENE CLONING AND CHARACTERIZATION OF MREB AND FTSZ FROM *BACILLUS SUBTILIS*). อาจารย์ที่ปรึกษา : อาจารย์ ดร.เสกสิทธิ์ ชำนาญศิลป์, 105 หน้า.

MreB และ FtsZ เป็นโปรตีน โครงสร้างของเซลล์แบคทีเรีย MreB มีความสำคัญสำหรับการควบคุมทิศทางการสร้างผนังเซลล์ ในขณะที่ FtsZ มีความจำเป็นในการแบ่งเซลล์ ไม่นานนี้มีรายงานว่าทั้งสองโปรตีนได้ทำอันตรกิริยากันโดยตรง บริเวณที่มีการสร้างผนังเซลล์ แนะนำให้เห็นว่าโปรตีนทั้งสองทำงานร่วมกันในการแบ่งเซลล์และการสร้างผนังเซลล์ การเกิดเป็นเส้นใยของ MreB และ FtsZ เป็นขั้นตอนแบบพลวัต โดยทั่วไปถูกควบคุมโดยการสลาย ATP และ GTP ตามลำดับ และการเกิดเป็นเส้นใยของ MreB ที่บริเวณผิวภายในเซลล์นั้น ยังต้องการ  $Mg^{2+}$  MreB ทำหน้าที่เป็นโครงสร้างค้ำยันเพื่อเชื่อมโยงเอนไซม์ peptidoglycan synthases โดยการทำอันตรกิริยาผ่านกลุ่มโปรตีนชื่อ penicillin binding proteins FtsZ ไม่ได้มีหน้าที่ในการสร้างผนังเซลล์โดยตรง เช่นเดียวกับ MreB แต่ FtsZ ทำหน้าที่ขับเคลื่อนการสร้างผนังเซลล์ในระหว่างการแบ่งเซลล์ ณ เวลาและสถานที่ที่จำเพาะ ซึ่งอาจสันนิษฐานได้ว่าเป็นผลที่เกิดจากการทำอันตรกิริยากับโปรตีนในกลุ่ม Min ในการกำหนดตำแหน่งของการแบ่งเซลล์ และทำอันตรกิริยากับ MreB ในการกำหนดทิศทางการสร้างแผ่นกั้นเซลล์ (Septum)

การทดลองในวิทยานิพนธ์นี้ ประกอบด้วย การโคลนยีน *mreB-Bs* และ *ftsZ-Bs* การแสดงออกของโปรตีน การทำโปรตีน MreB-BS และ FtsZ-Bs ให้บริสุทธิ์ และการพิสูจน์เอกลักษณ์ของคุณสมบัติการสลายนิวคลีโอไทด์ของโปรตีนทั้ง 2 ชนิด และตรวจสอบผลของ apigenin baicalein luteolin  $\alpha$ -mangostin และ naringenin ซึ่งเป็นสารสกัดจากธรรมชาติ ที่สามารถยับยั้งการแบ่งเซลล์และรบกวนความสมบูรณ์ของผนังเซลล์ แต่ยังไม่ทราบเป้าหมายระดับโมเลกุล โดยวิธี malachite green assay

จากการทดลองพบว่า MreB สามารถสลาย ATP และ GTP ได้ในช่วง pH 5.5 – 8.0 MreB สลาย ATP ได้ดีที่สุดที่ pH 7.0 และสลาย GTP ได้ดีที่สุดที่ pH 6.5 ส่วน FtsZ สามารถสลายได้เฉพาะ GTP ในช่วง pH 5.5 – 8.0 ย่อยสลายได้ดีที่สุดที่ pH 6.5 ผลการศึกษาสารสกัดจากธรรมชาติ

พบว่า apigenin สามารถลดการสลาย GTP ของ FtsZ ได้ร้อยละ 33.3 และ baicalein ร้อยละ 42.5 เมื่อเปรียบเทียบกับผลการศึกษาของ Mayer และ Amann ในปี ค.ศ. 2009 ผลการทดลองนี้ บ่งชี้ว่าการสลายนิวคลีโอไทด์และการเกิดเป็นสายของ MreB-Bs เป็นกระบวนการที่ไม่ขึ้นตรงต่อกัน และยังสนับสนุนรายงานข้างต้นที่ว่า การเกิดเป็นสายของ MreB-Bs ไม่ต้องการการสลาย นิวคลีโอไทด์ ยิ่งไปกว่านั้น ผลการศึกษานี้ถือว่าเป็นการรายงานผลครั้งแรกที่ระบุว่า FtsZ-Bs เป็นเป้าหมายระดับโมเลกุลของ apigenin และ baicalein อย่างไรก็ตาม ยังต้องมีการทำการทดลองเพื่อยืนยัน และศึกษาเพิ่มเติมเกี่ยวกับสมบัติทั้งทางด้านชีวเคมี และ โครงสร้าง เพื่อให้เข้าใจมากขึ้นถึงกระบวนการ และขั้นตอนการทำงานของโปรตีนทั้งสองชนิด เพื่อจะนำมาซึ่งข้อมูลที่เป็นประโยชน์ในการออกแบบยาต่อไป



สาขาวิชาเคมี

ปีการศึกษา 2558

ลายมือชื่อนักศึกษา \_\_\_\_\_

ลายมือชื่ออาจารย์ที่ปรึกษา \_\_\_\_\_

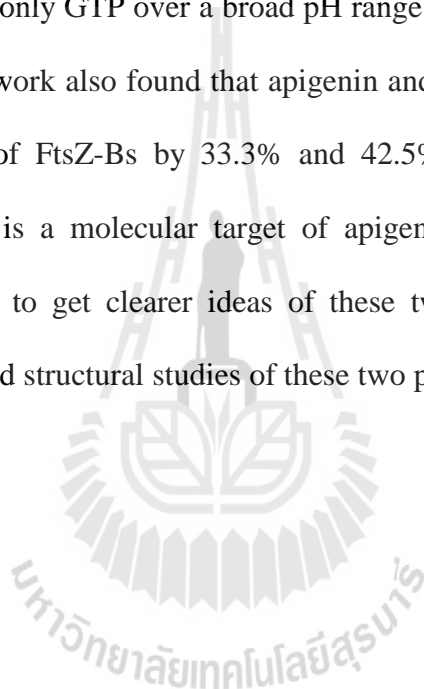
SUNAREE CHOKNUD : GENE CLONING AND CHARACTERIZATION  
OF MREB AND FTSZ FROM *BACILLUS SUBTILIS*. THESIS ADVISOR :  
SAKESIT CHUMNARNSILPA, Ph.D. 105 PP.

BACTERAL CYTOSKELETON/ MREB/ FTSZ/ ATPASE/ GTPASE/ NATURAL  
PRODUCT

MreB and FtsZ are key cytoskeletal proteins of bacteria. MreB plays important roles in bacterial cell wall synthesis while FtsZ is crucial for septum formation and cell division. Interestingly, these two proteins make direct interaction and colocalize at the septum suggesting cooperative functions of these proteins in cell wall synthesis during cell division. Polymerization of MreB and FtsZ is a dynamic process regulated by ATP and GTP hydrolysis, respectively. Polymerization of MreB into filaments at the cell periphery beneath the cell membrane responds to the presence of  $Mg^{2+}$ , and ATP hydrolysis. MreB acts as a scaffold for tethering of peptidoglycan synthases to the cell membrane by a mechanism that relies on penicillin binding proteins. Similar to MreB, FtsZ has no peptidoglycan synthases activity. However, FtsZ drives peptidoglycan synthesis during cell division at the particular time and place, presumably via interaction with Min-family of proteins and MreB.

This thesis included gene cloning, protein expression, protein purification, and nucleotides hydrolysis characterization of the *Bacillus subtilis* versions of these proteins, MreB-Bs and FtsZ-Bs. The work found that MreB-Bs has optimum pH for nucleotide hydrolysis at 7.0, which is different from the optimum pH for the protein polymerization, indicating that these two processes occur independently. This result

supports nucleotide hydrolysis independent polymerization by MreB-Bs, reported by Mayer and Amann, 2009. The work also investigated the effect of apigenin, baicalein, luteolin,  $\alpha$ -mangostin, and naringenin on ATP and GTP-hydrolysis of MreB and FtsZ by malachite green assay. The results show that MreB was able to hydrolyze both ATP and GTP over a broad pH range (5.5 – 8), with the optimum pH for ATP hydrolysis and GTP hydrolysis of 7.0 and 6.5, respectively. On the other hand, FtsZ was able to hydrolyze only GTP over a broad pH range (5.5 – 8), with optimum pH at 6.5. Importantly, this work also found that apigenin and baicalein were able to inhibit the GTPase activity of FtsZ-Bs by 33.3% and 42.5%, respectively. These results suggest that FtsZ-Bs is a molecular target of apigenin and baicalein in cell wall deformation. In order to get clearer ideas of these two proteins for drugs design, further biochemical and structural studies of these two proteins need to be done.



School of Chemistry

Academic Year 2015

Student's Signature \_\_\_\_\_

Advisor's Signature \_\_\_\_\_

**GENE CLONING AND CHARACTERIZATION OF MREB  
AND FTSZ FROM *BACILLUS SUBTILIS***

Suranaree University of Technology has approved this thesis submitted in partial Fulfillment of the requirements for the Master's Degree

Thesis Examining Committee

---

(Assoc. Prof. Dr. Jatuporn Wittayakun)

Chairperson

---

(Dr. Sakesit Chumnarnsilpa)

Member (Thesis Advisor)

---

(Prof. Dr. James R. Ketudat-Cairns)

Member

---

(Asst. Prof. Dr. Panida Khunkaewla)

Member

---

(Prof. Dr. Sukit Limpijumnong)

Vice Rector for Academic Affairs  
and Innovation

---

(Prof. Dr. Santi Maensiri)

Dean of Institute of Science

## AKNOWLEDEMENTS

First and foremost, I would like to thank my thesis advisor, Dr. Sakesit Chumnarnsilpa for the opportunity to conduct my thesis work under his guidance. He has been teaching me the theories and techniques that are involved in all biochemistry, always available for scientific discussion and has emphasized the importance of thinking independently. He provided a pathway for me to follow which allowed me to successfully complete my thesis program.

I expressed my sincere gratitude to Prof. Dr. James R. Ketudat-Cairns for providing me the opportunity to study towards my master degree in Biochemistry. He has away been supported during my time as a graduate student at SUT.

I sincerely thank Assoc. Prof. Dr. Jatuporn Wittayakun, and Asst. Prof. Dr. Panida Khunkaewla for patiently reading this dissertation and providing helpful comments.

Special thanks are extended to all my friends in the School of Biochemistry, Suranaree University of Technology for their help.

I would like to express my deepest gratitude to my family. They were always supporting me, encouraging me and cheering me up with their best wishes.

Finally, I would like to thank School of Biochemistry, Center for Protein Structure, Function and Application, Institute of Science, and Institute of Research and development, Suranaree University of Technology.

Sunaree Choknud

# CONTENTS

	<b>Page</b>
ABSTRACT IN THAI .....	I
ABSTRACT IN IN ENGLISH .....	III
ACKNOWLEDGEMNTS .....	V
CONTENTS.....	VI
LIST OF TABLES .....	X
LIST OF FIGURES .....	XI
LIST OF ABBREVIATIONS AND SYMBOLS .....	XV
<b>CHAPTER</b>	
<b>I INTRODUCTION .....</b>	<b>1</b>
1.1 General introduction .....	1
1.2 Research objectives General introduction.....	3
<b>II BACKGROUND.....</b>	<b>4</b>
2.1 Eukaryotic cytoskeleton proteins .....	4
2.1.1 Microfilaments .....	4
2.1.2 Microtubules .....	8
2.1.3 Intermediate filaments.....	11
2.2 Prokaryotic cytoskeleton proteins .....	14
2.2.1 MreB .....	14
2.2.2 FtsZ .....	16

## CONTENTS (Continued)

	<b>Page</b>
2.2.3 Crescentin.....	18
2.3 MreB and FtsZ interactions.....	21
2.4 Natural products .....	22
2.4.1 Apigenin .....	22
2.4.2 Baicalein.....	24
2.4.3 Luteolin .....	27
2.4.4 $\alpha$ -Mangostin .....	27
2.4.5 Naringenin.....	29
<b>III MATERIALS AND METHODS.....</b>	<b>30</b>
3.1 Materials.....	30
3.1.1 Chemicals.....	30
3.1.2 Instruments and equipment .....	33
3.1.3 Bacterial stain and plasmid .....	33
3.1.4 Oligonucleotides .....	37
3.2 General Methods .....	37
3.2.1 Competent cell preparation .....	37
3.2.2 Heat shock transformation of CaCl <sub>2</sub> competent cell .....	38
3.2.3 Cloning.....	38
3.3 Screening and optimization of protein expression .....	41
3.3.1 Optimization of protein expression.....	41
3.3.2 Screening of protein expression .....	41

## CONTENTS (Continued)

	<b>Page</b>
3.4 Protein purification .....	42
3.5 Nucleotide removal .....	43
3.6 Phosphate release assays .....	43
3.6.1 Effect of pH on nucleotides hydrolysis by the proteins .....	43
3.6.2 Screening of effect of natural products on nucleotides hydrolysis by proteins .....	43
<b>IV RESULTS AND DISCUSSION</b> .....	<b>46</b>
4.1 Cloning.....	46
4.1.1 Amplification of the <i>mreB-Bs</i> and <i>ftsZ-Bs</i> by PCR .....	46
4.1.2 Screening of pTG19-T cloning vector containing the <i>mreB-Bs</i> and <i>ftsZ-Bs</i> by PCR .....	47
4.1.3 Verification of the genes in pTG19-T DNA sequencing .....	48
4.1.4 Cloning and screening of <i>mreB-Bs</i> and <i>ftsZ-Bs</i> into expression plasmid .....	49
4.2 Expressions and purifications of MreB-Bs and FtsZ-Bs .....	50
4.2.1 Optimization of protein expression .....	50
4.2.2 Protein purification.....	53
4.3 Phosphate release assay .....	56
4.3.1 Effect of pH on nucleotides hydrolysis by MreB-Bs .....	58
4.3.2 Effect of pH on nucleotides hydrolysis by FtsZ-Bs .....	63

## CONTENTS (Continued)

	<b>Page</b>
4.4 Screening of natural products effect on nucleotides hydrolysis by the proteins.....	64
4.4.1 Screening of natural products effect on ATP hydrolysis by MreB-Bs .....	64
4.4.1 Screening of natural products effect on GTP hydrolysis by MreB-Bs .....	65
4.4.1 Screening of natural products effect on GTP hydrolysis by FtsZ-Bs .....	66
<b>V CONCLUSION AND FURTHER PERSPECTIVE .....</b>	<b>70</b>
REFERENCES .....	72
APPENDICES .....	86
APPENDIX A SEQUENCE.....	87
APPENDIX B PHOSPHATE RELEASE ASSAY .....	93
APPENDIX C CHEMICAL PREPARATIONS.....	98
CURRICULUM VITAE.....	105

## LIST OF TABLES

<b>Table</b>		<b>Page</b>
2.1	Classification of intermediate filament proteins .....	13
3.1	Chemical reagents and sources .....	30
3.2	Details of primers.....	37
3.3	Chemical compositions of the PCR .....	39
3.4	Cycling parameters of the PCR.....	40
3.5	Composition of ligation reaction of the PCR product into the cloning plasmid .....	40
3.6	Composition of ligation reaction putting inserts into the expression plasmid .....	41
4.1	Characters of polymerization of MreB .....	60

## LIST OF FIGURES

Figure	Page
2.1	Fluorescence images representation of Eukaryotic cytoskeleton.....5
2.2	Representation of the conformational change of G-actin upon polymerization..... 7
2.3	A schematic representation actin polymerization and roles of actin binding proteins and cofilin in promotion of actin dynamic..... 8
2.4	Polymerization of microtubules. Heterdimers of $\alpha$ - and $\beta$ -tubulin assemble to form a short microtubule nucleus ..... 9
2.5	The model of the tubulin dimer show $\alpha$ -tubulin with GTP bound and $\beta$ -tubulin containing GDP and Taxol bound..... 10
2.6	Genetic secondary structures of intermediate filament proteins..... 11
2.7	Schematic models of the prime association reactions occurring between dimers and double dimers ..... 12
2.8	Superimposition crystals structure of MreB (PDB: 1JCE) in blue onto actin (PDB: 3HBT) in grey, including 4 subdomains and ATP binds in a cleft between the domains ..... 15
2.9	Effects of A22 on the morphology of <i>P. aeruginosa</i> ..... 16
2.10	The structure of FtsZ protofilament ..... 17
2.11	The schematic representation of a transverse section of a divisome of <i>E. coli</i> cell ..... 18

## LIST OF FIGURES (Continued)

<b>Figure</b>	<b>Page</b>
2.12 Model for CreS action.....	20
2.13 Composite phase-contrasts image of <i>E. coli</i> cell showed that CreS can produce cell curvature.....	21
2.14 Examples of plants and herbs containing apigenin and luteolin.....	23
2.15 Chemical structure of apigenin.....	23
2.16 Ultrathin sections of log phase CREC grown in cation-adjusted Mueller Hinton broth.....	24
2.17 Appearance of baikal skullcap.....	25
2.18 Chemical structure of baicalein.....	25
2.19 Ultrathin sections of log phase <i>S. pyogenes</i> DMST 30653 grown in cation-adjusted Mueller Hinton broth.....	26
2.20 Chemical structure of luteolin.....	27
2.21 Chemical structure of $\alpha$ -mangostin.....	28
2.22 Appearance of mangosteen fruit ( <i>Garcinia mangostana</i> ).....	28
2.23 Chemical structure of naringenin.....	29
3.1 Map and multiple cloning site sequence of pTG19-T vector.....	35
3.2 Map and multiple cloning site sequence of pSY5.....	36
4.1 Agarose gel electrophoresis analysis of <i>mrB-Bs</i> and <i>FtsZ-Bs</i> amplification...	46
4.2 Agarose gel electrophoresis analysis of <i>mrB-Bs</i> in pTG19 amplification.....	48
4.3 Agarose gel electrophoresis analysis of <i>ftsZ-Bs</i> in pTG19 amplification.....	48

## LIST OF FIGURES (Continued)

<b>Figure</b>	<b>Page</b>
4.4 The mutation of pTG19- <i>ftsZ</i> -Bs on the late base of EcoRI recognition site of the revers primer.....	49
4.5 Agarose gel electrophoresis analysis of <i>mrB</i> -Bs in pSY5 amplification .....	50
4.6 Agarose gel electrophoresis analysis of <i>ftsZ</i> -Bs in pSY5 amplification .....	50
4.7 SDS-PAGE of MreB-Bs expression pattern after induction with different concentrations of IPTG at difference temperatures .....	52
4.8 SDS-PAGE of FtsZ-Bs expression pattern after induction with different concentrations of IPTG at difference temperatures .....	53
4.9 SDS-PAGE of MreB-Bs purification faction, including washes and elution with different imidazole concentrations.....	55
4.10 SDS-PAGE of FtsZ-Bs purification faction, including washes and elution with different imidazole concentrations.....	55
4.11 SDS-PAGE of MreB-Bs and FtsZ-Bs purified after removed nucleotide by 1X8-400Cl Dowex resin .....	56
4.12 Representative of free inorganic phosphate in the malachite green assay.....	57
4.13 pH effect on phosphate release from ATP by MreB-Bs .....	58
4.14 pH effect on phosphate release from GTP by MreB-Bs .....	59
4.15 Phylogenetic tree visualizing the relationship of MreB proteins from various bacteria to each other and yeast actin.....	61
4.16 Crystal structures of MreB in different nucleotide states reveal a propeller twist .....	62

**LIST OF FIGURES (Continued)**

<b>Figure</b>	<b>Page</b>
4.17 pH effect on phosphate release from GTP by FtsZ-Bs.....	64
4.18 Screening of natural products effect on ATP hydrolysis by MreB-Bs.....	66
4.21 Proposed mechanism of straight-to-curved conformational switch.....	67
4.20 Screening of natural products effect on GTP hydrolysis by FtsZ-Bs.....	68
4.19 Screening of natural products effect on GTP hydrolysis by MreB-Bs.....	69



## LIST OF ABBREVIATIONS AND SYMBOLS

A22	S-(3,4-Dichlorobenzyl)isothiourea hydrochloride
ADP	Adenosine diphosphate
ATP	Adenosine triphosphate
ATPase	Adenosine triphosphate hydrolase
bp	Base pair
BSA	Bovine serum albumin
DNA	Deoxyribonucleic acid
DNase	Deoxyribonuclease
dNTP	Deoxy nucleotide triphosphates
DTT	Dithiothreitol
EDTA	Ethylenediaminetetraacetate
EtBr	Ethidium bromide
F	Filament
G	Globular
GDP	Guanosine diphosphate
GTP	Guanosine triphosphate
GTPase	Guanosine diphosphate hydrolase
HEPES	Hydroxyethyl piperazineethanesulfonic acid
Hsp70	70 kilodalton heat shock protein
IF	Intermediate filament
IMAC	Immobilized metal affinity chromatography

**LIST OF ABBREVIATIONS AND SYMBOLS (Continued)**

IPTG	Isopropyl thio- $\beta$ -D-galactoside
kDa	Kilo Dalton
MES	2-(N morpholino)-ethanesulfonic acid
MF	Microfilament
MT	Microtubule
MRSA	Methicillin-resistant <i>Staphylococcus aureus</i>
MWCO	Molecular weight cut off
OD	Optical density
PCR	Polymerase chain reaction
PBP	Penicillin-binding protein
rpm	Revolutions per minute
SDS	Sodium dodecyl sulfate
SDS-PAGE	Polyacrylamide gel electrophoresis with SDS
TEMED	Tetramethylenediamine
Tris	Tris-(hydroxymethyl)-aminoethane
VRE	Vancomycin resistant Enterococci
VRSA	vancomycin-resistant <i>Staphylococcus aureus</i>
X-gal	5-bromo-4-chloro-3-indolyl- $\beta$ -D-galactopyranoside

# CHAPTER I

## INTRODUCTION

### 1.1 General introduction

Cytoskeletal proteins play crucial roles in cellular organization. It was believed those cytoskeletal proteins do not exist in bacteria. Bacterial cell morphology was traditionally assumed to be determined by the external cell wall (Carballido-López, 2006a). It is now known that bacterial cytoskeletons, MreB, FtsZ, are crucial for bacterial survival.

Similar to actin, MreB (an actin ortholog) can assemble into filaments. Assembly of MreB into filaments or polymerization is a dynamics process, which relates to ATP hydrolysis (Mayer and Amann, 2009; Bean and Amann, 2008). The polymerization of MreB is involved in many cellular processes especially in cell wall synthesis (Carballido-López and Errington, 2003), which is crucial for cell elongation and cell division (Fenton and Gerdes, 2013; van den Ent, Amos, and Löwe, 2010).

FtsZ is a tubulin ortholog, which forms a ring-like structure at the mid cell, called the Z-ring. Formation of the Z-ring through polymerization requires GTP hydrolysis. GDP from GTP hydrolysis is used to support the polymer (Löwe, van den Ent, and Amos, 2004). The polymerization of FtsZ is the rate limiting step in septum formation under the membrane at the site of cell division (Erickson, Anderson, and Osawa, 2010). Z-ring is necessary for the localization of a variety of other proteins (Aarsman, Piette, Fraipont *et al.*, 2005).

Both FtsZ and MreB tether peptidoglycan synthases by a mechanism that relies on penicillin binding protein 2, PBP2 (Varma and Yong, 2009). A recent report has shown that direct interactions between FtsZ and MreB are necessary for appropriate cell division in *Escherichia coli*, which suggests a potential mechanism for the coordination of cell elongation and cell division (Fenton and Gerdes, 2013). In the absence of MreB, FtsZ can direct peptidoglycan incorporation into the lateral walls of *E. coli*, which may indicate a more general role in coordination of the peptidoglycan synthases. FtsZ may drive a general form of peptidoglycan synthesis during cell division at a particular time and place. The genesis of cell shape is probably based on a specific geometry of cell wall growth that is directed by MreB (Varma and Yong, 2009).

Bacteria are unicellular microbes. Cell morphology influences bacterial existence. A small cell size increase surface area relative to high surface-to-volume ratio (Capaldo-Kimball and Barbour, 1971). This leads to obvious benefits such as selective pressures-access to nutrients, cell division, predation, and motility (Yang, Blair, and Salama, 2016; Jiang and Sun, 2010). Bacteria usually attach to surfaces through specific cell morphology, which is essential for the overall survival of the bacteria, especially pathogenic ones (Okagaki, Strain, Nielsen *et al.*, 2010).

Together, the preceding information shows that polymerization and direct interactions of MreB and FtsZ are very important for survival of bacteria. The molecular detail and mechanism remain unclear, and understanding of these processes is necessary and will provide fundamental information for controlling bacterial infection and drug design. This study focuses on an investigation of effects of natural products on nucleotide hydrolysis by MreB and FtsZ.

## 1.2 Research objectives

- 1.2.1 To clone and express *mreB* and *ftsZ* of *Bacillus subtilis* in *E. coli*.
- 1.2.2 To purify MreB and FtsZ of *B. subtilis* for biochemical studies.
- 1.2.3 To study the effects of some natural products on nucleotides hydrolysis by MreB and FtsZ of *B. subtilis*.



## **CHAPTER II**

### **BACKGROUND**

#### **2.1 Eukaryotic cytoskeletons**

In eukaryotes, the cytoskeletal proteins play crucial roles in the organization of the cells. The three classes of eukaryotic cytoskeletal fibers are microfilaments, microtubules and intermediate filaments (as show in Figure 2.1). Microfilament, actin filament (F-actin) is a polymer of globular actin or G-actin (Moriyama and Yahara, 2002). Microtubule is a polymer of  $\alpha$ ,  $\beta$ -tubulin heterodimers, while  $\gamma$ -tubulin is not part of the tubulin subunit (Desai and Mitchison, 1997). Lastly, intermediate filaments are homopolymers formed by several classes of cell-specific subunit proteins, including keratins, lamins, and vimentin (Herrmann and Aebi, 2004). A complex filamentous assemblage of microfilaments, microtubules and intermediate filaments form a highly dynamic network that controls a multitude of cell processes, such as cell motility, cell morphology, cell division, cell adhesion.

##### **2.1.1 Microfilament (MF)**

Actin, the monomeric form of MF, is one of the most abundant and highly conserved proteins among eukaryotic cells (Pantaloni, Hill, Carlier *et al.*, 1985). It is a member of a larger superfamily of proteins, which include a group of ATPases such as Hsp70 (Bork, Sander, Valencia *et al.*, 1992).

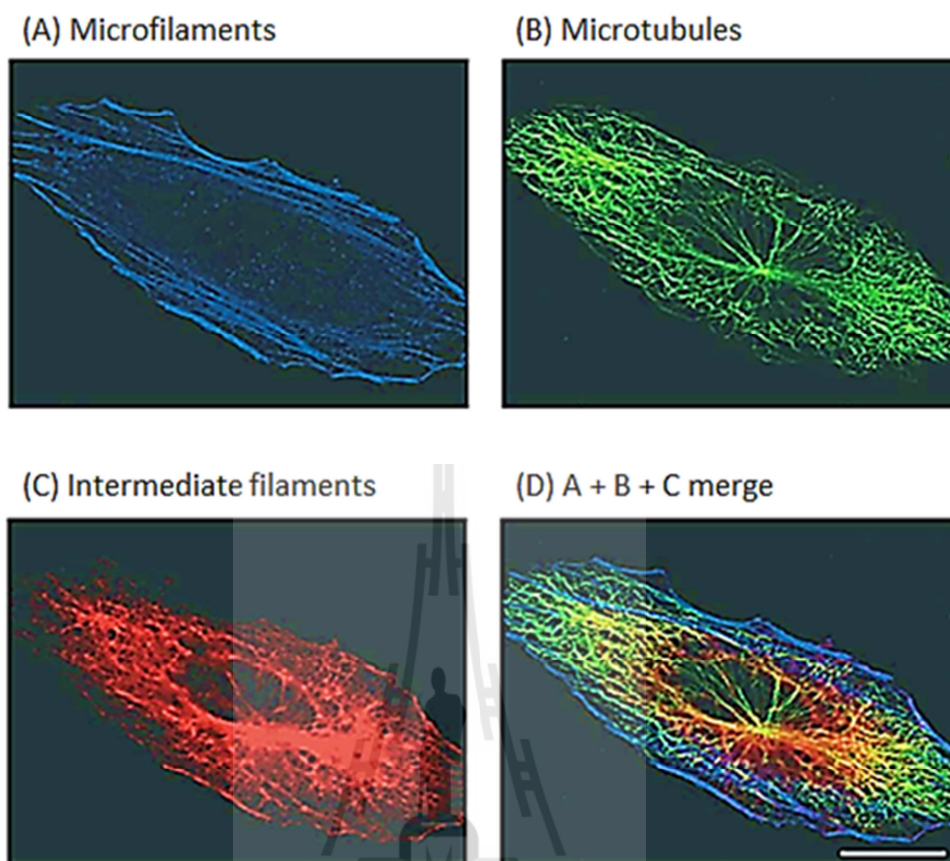


**Figure 2.1** Fluorescence images representation of eukaryotic cytoskeleton. The three major components of the cytoskeleton of Huh7 cultured human hepatocytes were triple-stained with phalloidin to visualize microfilaments (blue, A), anti-tubulin antibody to visualize microtubules (green, B), and anti-K8/K18 antibody to visualize intermediate filaments (red, C). A superimposed image is shown in (D). Scale bar represent 10  $\mu\text{m}$  (Omary, Ku, Tao *et al.*, 2006).

*In vivo*, switching between G-actin and F-actin is a dynamic process, actin dynamics. This process is essential for various cellular processes, including cell motility, cell migration, phagocytosis, vesicular movement, cytokinesis, and

molecular transport (Hoglund, Karlsson, Arro *et al.*, 1980). Actin dynamics is regulated by innate properties of actin itself and by actin-binding proteins, ABS (Schüler, 2001).

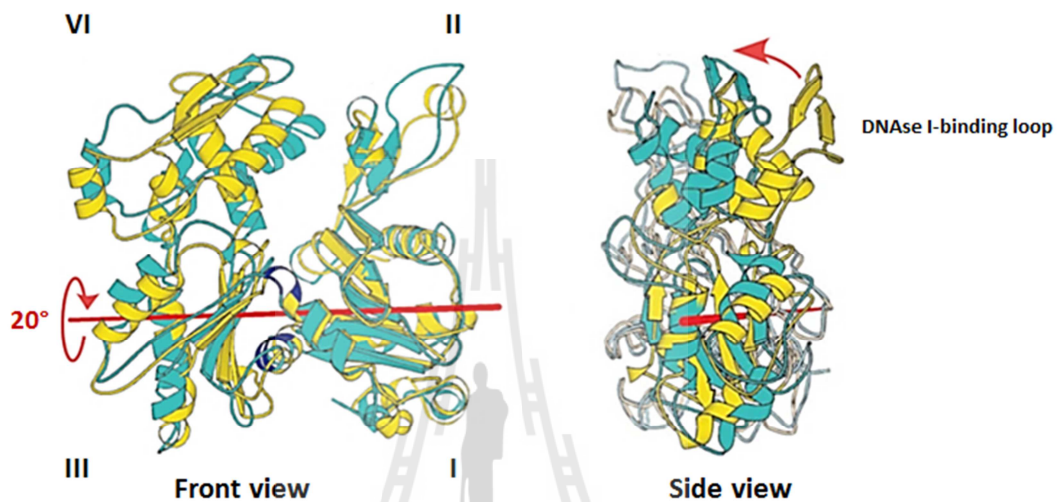


**Figure 2.2** Representation of the conformational change of G-actin upon polymerization. Superimposition the structure of ADP-actin shown in yellow (PDB: 1J6Z; Otterbein, Graceffa, and Dominguez, 2001) onto the structure of ATP-actin excised from a fiber diffraction derived model shown in cyan (Oda, Iwasa, Aihara *et al.*, 2009) demonstrates that subdomains III and IV are rotated with respect to subdomain I and II about the rotation axis (red line) in the direction indicate by the red arrow. The two conformations are related by a 20° rotation of the major domains around an axis passing along the front of subdomain I and the side of subdomain III, and the DNase I-binding, which loop extends to make contacts to an adjacent actin molecule in the filament, is in different position. The rotation is associated with bends of the peptide chain, as indicated in blue.

Superimposition of the crystal structure of G-actin with ADP in nucleotide binding pocket (Otterbein *et al.*, 2001) onto actin monomer (ATP-actin) excised from fiber diffraction of actin filament (Oda *et al.*, 2009) has demonstrated that the conformation of actin in monomeric state is different from the polymeric state (Figure 2.2). It suggests that the conformation of actin affects the polymerization process of actin.

The process of actin polymerization is shown in Figure 2.3. Polymerization of G-actin to form F-actin involves uptake of a divalent salt cation ( $\text{Ca}^{2+}$  or  $\text{Mg}^{2+}$ ) that ATP presented (Blanchoin and Pollard, 2002). G-actins carrying ATP will form a stable nucleus, composing of 2-3 G-actin in the process. During the process of elongation, actin depolymerizing factor (cofilin family) binds to the side of ADP-actin filaments and induces pointed end depolymerization to increase the concentration of G-actin at steady state (Moriyama and Yahara, 2002). In the next step, profilin enhances the exchange of ADP for ATP to recycle G-actins (Pantaloni *et al.*, 1985; Nürnberg, Kitzing, Grosse *et al.*, 2011). The profilin-actin complex assembles exclusively at the barbed end by blocking the barbed ends of major F-actin to increase G-actin at steady state and funnel the flux of G-actins to the non-capped filaments, which take another G-actin in order to start a new cycle of polymerization (Pollard, Blanchoin, Mullins *et al.*, 2000).

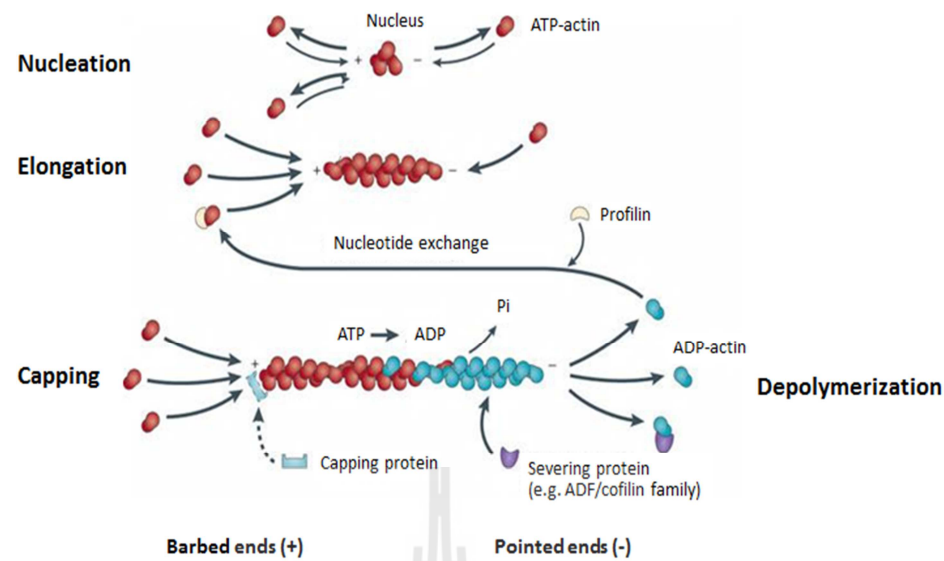


**Figure 2.3** A schematic representation actin polymerization and roles of actin binding proteins: (Adapted from Nürnberg *et al.*, 2011).

### 2.1.2 Microtubules (MT)

Microtubules are long filamentous, tube-shaped protein polymers involve in many essential cellular processes, including cell division, ciliary and flagella motility, intracellular transport, and development and maintenance of cell shape (Jordan and Wilson, 2004).

Microtubules are non-covalent polymers of the two related protein monomers  $\alpha$ - and  $\beta$ -tubulins, in the presence of GTP hydrolysis (Hyman, Salser, Drechsel *et al.*, 1992; Mandelkow and Mandelkow, 1990). Figure 2.4 shows that polymerization of tubulin occurs by a nucleation-elongation mechanism in which the relatively slow formation of a short microtubule or nucleus is followed by rapid elongation of the microtubule at its ends by the reversible addition of tubulin dimers (Ottaviani, Pregnolato, Cangiotti *et al.*, 2012).

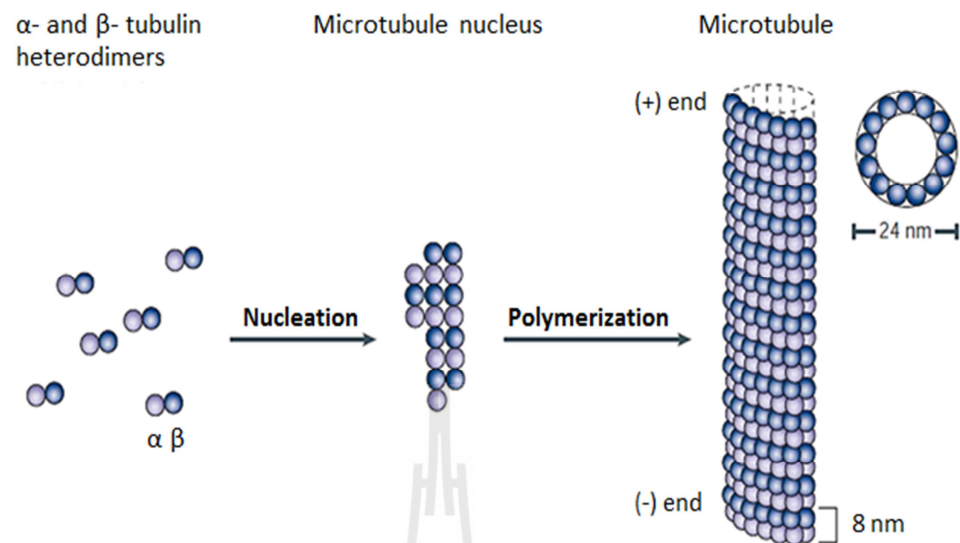


**Figure 2.4** Polymerization of microtubules. Heterdimers of  $\alpha$ - and  $\beta$ -tubulin assemble to form a short microtubule nucleus. Nucleation is followed by elongation at both ends to form a cylinder (plus (+) end with  $\beta$ -tubulin facing, and  $\alpha$ -tubulin facing the minus end (-)) (Adapted from Jordan and Wilson, 2004).

The tubulins show complex polymerization dynamics that use energy provided by GTP, which is in a direct contact with loops T1 to T6 of the GTPase domain (Desai and Mitchison, 1997). Figure 2.5 shows the structure of tubulin in complex with Taxol (Nogales, Whittaker, Milligan *et al.*, 1999). The GTPase domains are showing in red and the activation domains in blue. The core helix that connects the two globular domains in each monomer is yellow and the C-terminal domain on the external surface is green.

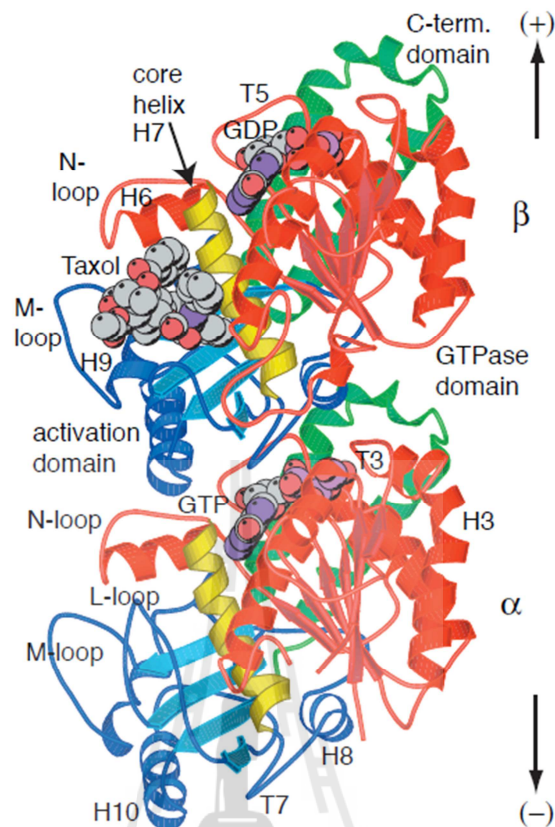


**Figure 2.5** The model of the tubulin dimer show  $\alpha$ -tubulin with GTP bound and  $\beta$ -tubulin containing GDP and Taxol bound. The arrow indicates the direction of the protofilament and microtubule axis (Amos and Schlieper, 2005).

The GTP is sandwiched between the  $\alpha$ - and  $\beta$ -tubulin subunits of each heterodimer, being bound to  $\alpha$ -tubulin by loops T1-T6 and also makes contact with loop T7 of  $\beta$ -tubulin. The nucleotide bound to  $\beta$ -tubulin has been hydrolyzed to GDP through contact with helix H8 and loop T7 of the activation domain of another  $\alpha$ -tubulin subunit. Taxol sits in the pocket of  $\beta$ -tubulin on the inside face of microtubules. In  $\alpha$ -tubulin, this pocket is occupied by the extended L loop (Amos and Schlieper, 2005; Amos, 2004).

### 2.1.1 Intermediate filament (IF)

IFs typically form a network throughout the cytoplasm, surrounding the nucleus and extending out to the cell periphery (Cooper, 2000). They are often anchored to the plasma membrane at cell-cell junctions such as desmosomes, where the external face of the membrane is connected to that of another cell (Osborn and Weber, 1983).

The family of IF proteins include two common traits that define members. Firstly, the (IF) proteins exhibit a characteristic tripartite domain organization. It consists of a highly conserved  $\alpha$ -helical central rod domain (subdomains 1A, 1B, 2A and 2B) flanked by variable N-terminal head and C-terminal tail domains (Eriksson, Dechat, Grin *et al.*, 2009), a generic version of which is shown in Figure 2.6. Secondly, the proteins can self-assemble into cytoskeletal filaments, which usually appear as homogeneous, apolar fibers that have a 10-12 nm diameter (Coulombe, Ma, Yamada *et al.*, 2001).

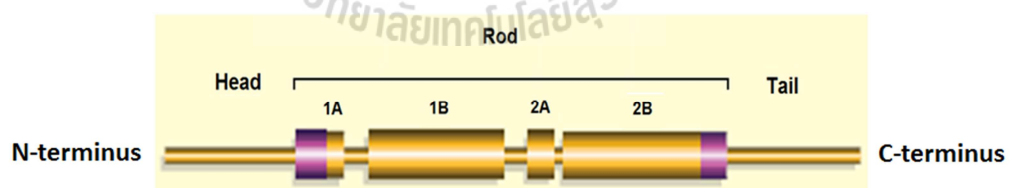


**Figure 2.6** Genetic secondary structures of intermediate filament proteins (Coulombe *et al.*, 2001).

IFs are composed of a variety of proteins that are expressed in different types of cells (Cooper, 2000). The more than 65 different IF proteins are divided into six chemically distinct classes, which are described show in Table 2.1 (Cooper, 2000). At the protein level, polymerization properties define 3 assembly groups (A, B, and C), shown in Figure 2.7. Assembly group A, Keratins assemble from heterodimeric tetramers by lateral and nearly concomitant longitudinal assembly into heterogenous full-width filaments. Assembly group B, Vimentin-type assembly starts from antiparallel, half-staggered double dimers (or tetramers) to form full-width, unit-length filaments. Assembly group C, Lamin dimers associate first into head-to-tail filaments that later laterally associate. The orientation of the two associating filaments is arbitrary (Herrmann and Aebi, 2004; Kim and Coulombe, 2007).

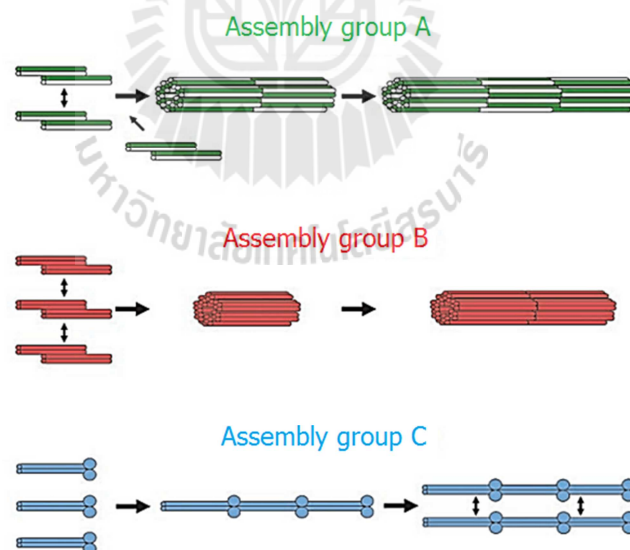


**Figure 2.7** Schematic models of the prime association reactions occurring between dimers and double dimers, respectively, of the three major IF assembly groups (Herrmann and Aebi, 2004).

**Table 2.1** Classification of intermediate filament proteins.

Type	Protein	Size (kD)	Assembly group	Site of expression
I	Acidic keratins (~15 protein)	40–60	A	Epithelial cells
II	Neutral or basic keratins (~15 protein)	50–70	A	Epithelial cells
III	Vimentin	54	B	Fibroblasts, white blood cells, and other
	Desmin	53	B	cell types
	Glial fibrillary acidic protein	51	B	Muscle cells
	Peripherin	57	B	Glial cells Peripheral neurons
IV	Neurofilament protein-L	67	B	Neurons
	Neurofilament protein-M	150	B	Neurons
	Neurofilament protein-H	200	B	Neurons
	$\alpha$ -Internexin	66	B	Neurons
V	Nuclear lamins	60–75	C	Nuclear lamina of all cell types
VI	Nestin	200	B	Stem cells of central nervous system

## 2.2 Prokaryotic cytoskeleton proteins

In recent years, scientists have found that bacteria present a number of cytoskeletal structures. The most understood bacterial cytoskeleton proteins, FtsZ, MreB and crescentin are orthologs of the three major types of eukaryotic cytoskeletal proteins actin, tubulin, and intermediate filament, respectively. These proteins play essential roles in dictating cell shape, motility, chromosome separation and cell division.

### 2.2.1 MreB

In rod shape bacteria, the cytoskeletal protein MreB is an actin orthologue that plays important roles in several cellular functions in bacteria, especially regulation of cell shape (Bean, Flickinger, Westler *et al.*, 2009; Fenton and Gerdes, 2013). The *mreB* gene is located in the gene cluster *mre* (murein cluster e). Bioinformatics analysis indicated that MreB has a sequence pattern in common with the actin superfamily (van den Ent *et al.*, 2001). The crystal structure of *Thermotoga maritima* MreB1 revealed that actin is the most related protein to MreB, in overall structure, as shown in Figure 2.8 (van den Ent *et al.*, 2001).

MreB plays an important role in regulation of cell shape (van den Ent *et al.*, 2010). Mutation of *mreB* causes *E. coli* to lose its normal rod-shape to become a spherical shape (Doi *et al.*, 1988; Yamachika *et al.*, 2012). In *E. coli*, MreB polymerizes into filament bundles in a reversible process, which responds to ions ( $Mg^{2+}$ ) and nucleotides (ATP) (van den Ent *et al.*, 2001). This suggests that polymerization proceeds with a nucleation step in much the same way as that of eukaryotic actin (Nurse and Marians, 2012).

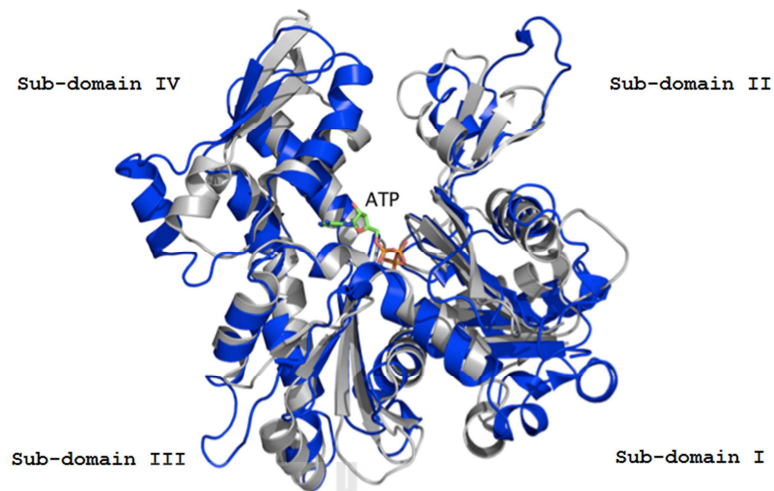


**Figure 2.8** Superimposition of the crystal structure of MreB (PDB: 1JCE) in blue onto actin (PDB: 3HBT) in grey. Both structures include 4 subdomains and ATP binds in a cleft between the domains.

The early study by Bean and colleagues (Bean *et al.*, 2009) has shown that S-(3,4-Dichlorobenzyl) isothiourrea (A22) increases the critical concentration for ATP-bound MreB assembly from 500 nM to approximately 2000 nM. Suggesting that A22 acts as a competitive inhibitor of ATP binding to MreB, and MreB is unable to polymerize when bound to A22. The structure of MreB of *Caulobacter crescentus* complex with A22 shows that A22 binds closely to the nucleotide in MreB, presumably preventing nucleotide hydrolysis and destabilizing double protofilaments (van den Ent *et al.*, 2014). *In vivo* study has shown that A22 inhibits growth and induces a morphological change of *P. aeruginosa*, as shown in Figure 2.9 (Cowles and Gitai, 2010; Yamachika *et al.*, 2012).

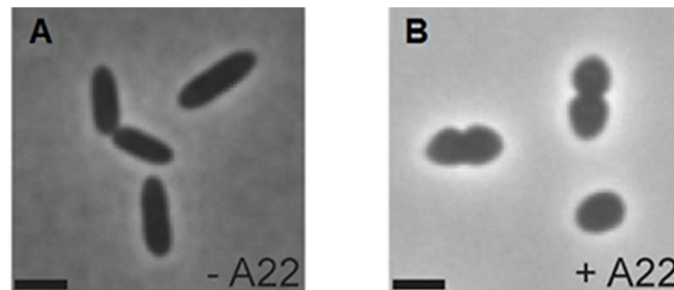


**Figure 2.9** Effects of A22 on the morphology of *P. aeruginosa*. A22 absent (A) A22 present (B). Scale bars represent 2  $\mu\text{m}$  (Cowles and Gitai, 2010).

### 2.2.2 FtsZ

The tubulin orthologue, Filamenting temperature-sensitive mutant Z (FtsZ) is one of the major cytoskeletal protein present in eubacteria, and is also found in archae and chloroplasts (Erickson, Anderson, Osawa *et al.*, 2010; Löwe, van den Ent, Amos *et al.*, 2004). FtsZ forms a dynamic ring-like structure, called the Z-ring at mid cell, under the membrane, at the site of cell division. It is necessary for the localization of various proteins that are required for cell division (Erickson *et al.*, 2010).

FtsZ forms polymers, with the GTPase active-site split across two monomers. One monomer provides the GTP-binding site and the other, through its T7 loop, nucleotide hydrolysis, as illustrated in Figure 2.10 (Erickson and Osawa, 2010). The polymers contain a substantial amount of GTP, which suggests that hydrolysis occurs with some lag following assembly. After the polymerization, the polymer condenses to form a Z-ring. Some models suggest that rearrangement of FtsZ drives

condensation of the ring and generates adequate force to pinch the cell at the site of the division plane (Lan *et al.*, 2009).

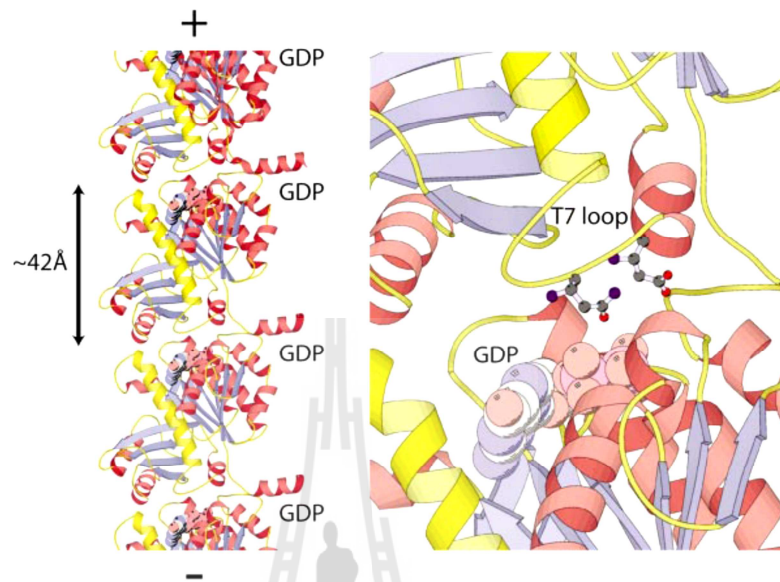


**Figure 2.10** The structure of FtsZ protofilament. FtsZ forms a chain of molecules with the GDP bound between two subunits. Residues in loop T7 contact the nucleotide directly and are required for hydrolysis (Löwe *et al.*, 2004).

The divisome of *E. coli* is nucleated initially by the assembly of FtsZ, and then the rest of the ring proteins are incorporated sequentially: FtsA, ZipA, FtsK, FtsQBL, FtsW, FtsEX, and finally FtsN. ZipA and FtsA interact with and stabilize the Z ring at the inner membrane, as showed in Figure 2.11 (Aarsman, Piette, Fraipont *et al.*, 2005). The divisome contains essential cell division proteins, such as the peptidoglycan synthases PBP1B and PBP3, and amidase enzymes (Ami) with their activators (EnvC), as well as proteins of the Tol-Pal complex for constriction of the outer membrane. Activity of the PBPs is regulated in part by outer membrane-

anchored lipoproteins (LpoB) and lytic transglycosylase (LT). Cells lacking functional FtsZ are unable to divide and instead grow as filaments (Typas, Banzhaf, Gross *et al.*, 2011).

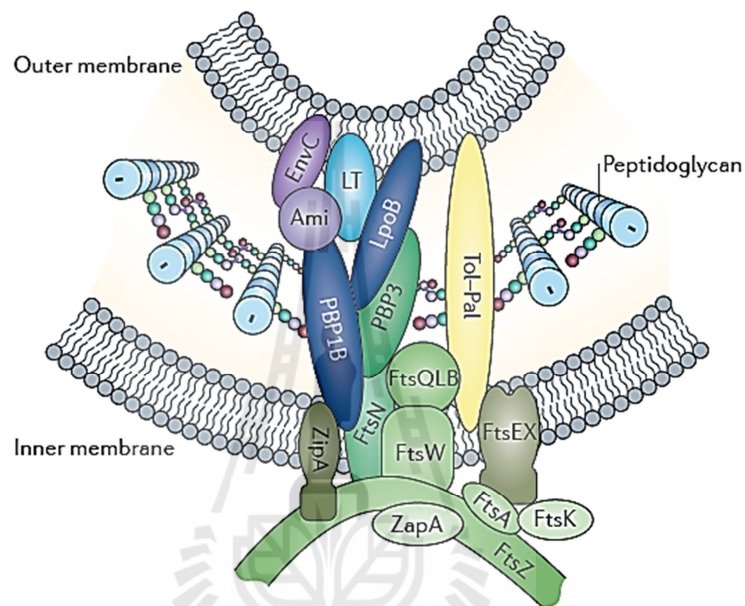


**Figure 2.11** The schematic representation of a transverse section of a divisome of *E. coli* cell. The complex is composed of FtsA, ZipA, FtsK, FtsQBL, FtsW, FtsEX, FtsN, PBP1B, PBP3, Ami, EnvC, Tol-Pal, LpoB, and LT (Typas *et al.*, 2011).

### 2.2.3 Crescentin

Crescentin (CreS) is the only IF orthologue identified in prokaryotic cells at the moment (Shih and Rothfield, 2006), based on structural prediction and *in vitro* polymerization properties (Charbon, Cabeen, Jacobs-Wagner *et al.*, 2009). The amino acid sequence of CreS has a distinct seven-residue repeat that is predicted to

form coiled-coil structures (Herrmann and Aebi, 2004). Because of the dominating coiled-coil repeat, sequence comparisons are unreliable, but CreS shares some important overall features with eukaryotic IF (Herrmann and Aebi, 2004; Margolin, 2004). Analysis has revealed that the domain organization of CreS is similar to eukaryotic IF, suggesting that CreS probably is a prokaryotic homologue of IF (Michie and Löwe, 2006).

CreS forms a polymer along the cell-length direction, localizes at the inner curvature of the cell, and attaches to the cytoplasmic side of the cell membrane (Gitai, 2005). CreS filament, when detached from the cell membrane through antibiotic treatment, collapses into a helix (Cabeen *et al.*, 2009). This suggests CreS affixed to the cell membrane in a stretched configuration form in untreated cells, and may generate a constricting force on the cell wall, as shown in the model action of CreS shown in Figure 2.12.

CreS forms filaments to generate the curved cell morphology in comma-shaped *Caulobacter crescentus* that were identified in a screen for *C. crescentus* transposon insertion mutations that affected cell shape (Briegel, Dias Jensen *et al.*, 2006). Loss of the structural gene for CreS, leads to a change in cell shape from comma to rod (Ausmees and Wagner, 2003). Previous report indicated bacterial cells lacking CreS lose their curved morphology and adopt a straight rod-like shape, the mechanism of CreS induced curvature is likely to be simply mechanical. The difference of cell morphology is shown in Figure 2.13 (Charbon *et al.*, 2009).

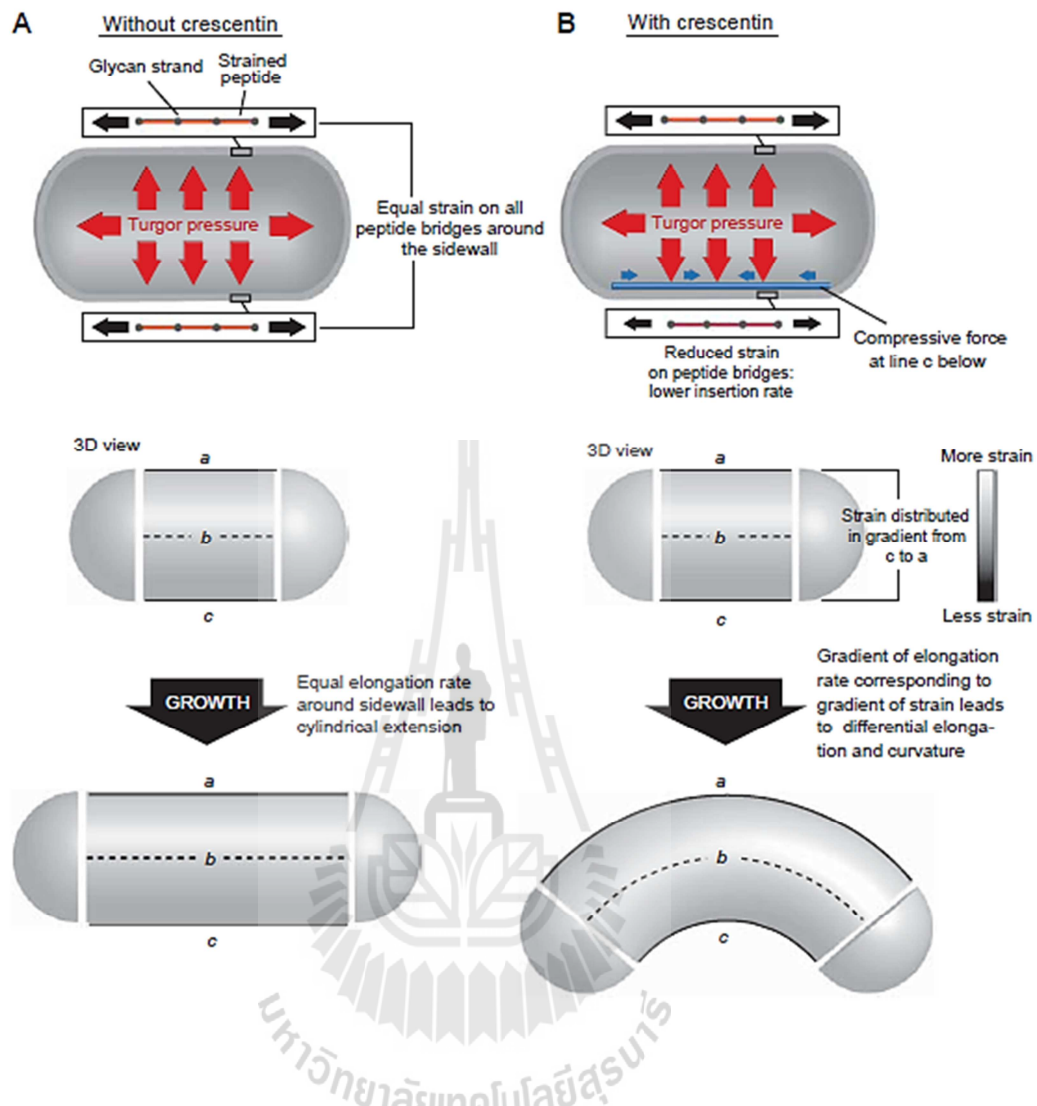


**Figure 2.12** Model for CreS action. A rod-shaped cell lacking CreS, turgor pressure strains peptide bridges (A). A cell with a CreS structure, which is affixed to the cell membrane in a stretched configuration (B). This in turn produces a compressive force on the cell wall. Cell elongation under these conditions produces a gradient of cell lengths, from line a to line c (Cabeen *et al.*, 2009).

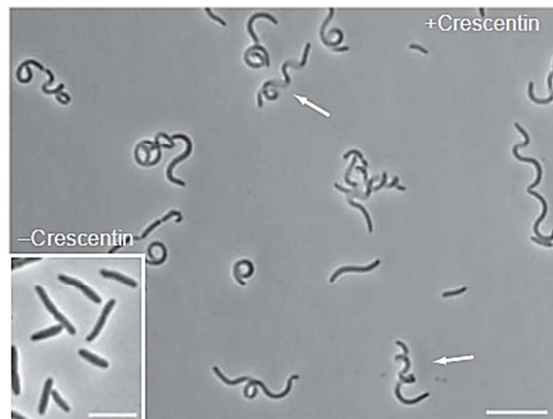


**Figure 2.13** Composite phase-contrast image of *E. coli* cells showed that CreS can produce cell curvature; with CreS indicate elongated and helical cells while without CreS indicate rod shape of *E. coli* (Cabeen *et al.*, 2009).

### 2.3 MreB and FtsZ interactions

The process of cell elongation is controlled by MreB, which localizes components of the peptidoglycan synthesis along the lateral cell wall, thereby governing the geometry during cell wall growth (Carballido-López, 2006b). During cell division on the inner membrane at the middle of the cell, it triggers invagination by attracting a set of proteins to form a septal Z ring was formed with the tubulin homologue FtsZ (Gaballah, Kloeckner, Otten *et al.*, 2011).

Recent studies by Fenton and Gerdes suggest that direct interaction of MreB and FtsZ is crucial for septum synthesis during cell division. *In vivo* study by bacterial two hybrid analysis suggests MreB-FtsZ crosslink. Mutagenesis showed that D258 of MreB interacts with the C-terminus of FtsZ. The MreB/FtsZ interaction localizes the Z-ring and supports septum formation (Fenton and Gerdes, 2013).

## 2.4 Natural products

A natural product is a chemical compound produced by a living organism and originating in nature. Natural products can also be produced by total synthesis or semi-synthesis processes. The products as long as a key role can be played in traditional medicine or other complementary and integrative health practices. The ideas are effect of small molecule that mediated by specific interactions of the drug molecule with biological macromolecules.

### 2.4.1 Apigenin

Apigenin (4',5,7-trihydroxyflavone), is a dietary flavonoid which is found in a wide variety of plants and herbs, including parsley, celery, rosemary, oregano, thyme, basil, and coriander (Figure 2.14). It is a natural product belonging to the flavone class. The chemical structure of apigenin is shown in Figure 2.15. Apigenin shows promising biological effects, such as prevention and therapy of prostate cancer, suppression of tumorigenesis and angiogenesis in melanoma (Caltagirone, Rossi, Poggi *et al.*, 2000) and breast, skin, and colon carcinomas (Wang, Heideman, Chung *et al.*, 2000).

Apigenin also has antimicrobial activity against oral pathogen agents (Cha, Kim, Cha *et al.*, 2016). Ceftazidime is bactericidal in action, exerting its effect on target cell wall proteins and causing inhibition of cell wall synthesis. Recent report by Eumkeb (2012) has shown that the cells were treated with ceftazidime presenting elongated of shape and damaged cell wall especially at the cells polar. On the other hand, apigenin also causes cell elongation without disrupting cell wall integrity at the

poles of the cells as ceftazidime, as show in Figure 2.16 (Eumkeb and Chukrathok, 2013).



**Figure 2.14** Examples of plants and herbs containing apigenin and luteolin.

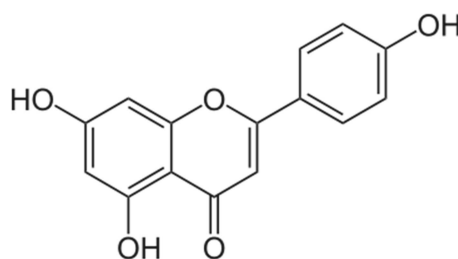


**Figure 2.15** Chemical structure of apigenin.

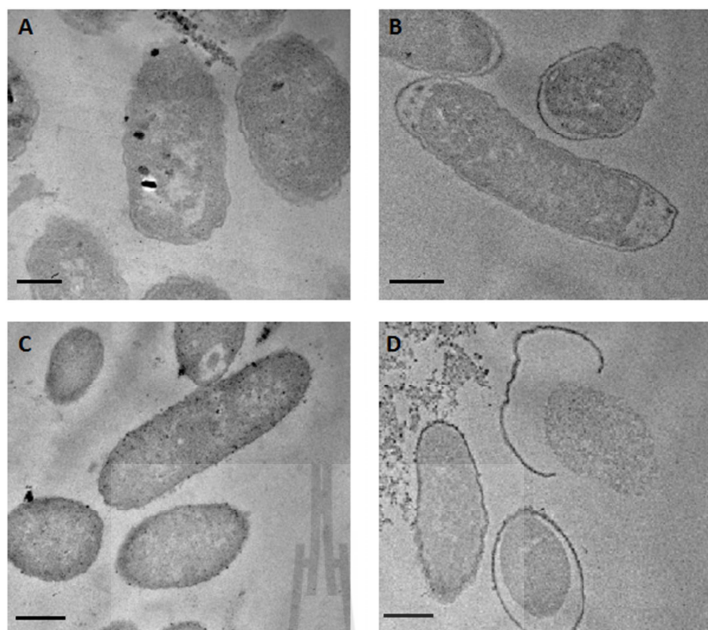


**Figure 2.16** Ultrathin sections of log phase CREC grown in cation-adjusted Mueller Hinton broth containing: drug-free (A), 20 µg/ml ceftazidime (B), 10 µg/ml apigenin (C), 3 µg/ml ceftazidime and 3 µg/ml apigenin (D). Scale bars represent 0.5 µm (Eumkeb and Chukrathok, 2013).

#### 2.4.2 Baicalein

Baicalein (5,6,7-trihydroxyflavone) is a type of flavonoid, a major flavone of baikal skullcap (*Scutellariae baicalensis*, Figure 2.17). The chemical structure of baicalein show as Figure 2.18. The ability of baicalein showed significant cytotoxicity against the hepatocellular carcinoma cells and moderate cytotoxicity against immortalized human hepatocytes (Zheng, Yin, Grahn *et al.*, 2014), and act as an anti-inflammatory agent (Hsieh, Hall, Ha *et al.*, 2007). The baicalein has a potential adjuvant role in clinical bactericidal therapy for severe enterococcal

infection that demonstrated baicalein and gentamicin can act synergistically in inhibiting vancomycin-resistant *Enterococcus* (Chang, Li, Tang *et al.*, 2007). It also demonstrated strong antibacterial activity against clinically isolated methicillin and vancomycin-resistant *Staphylococcus aureus* that baicalein could be employed as a natural antibacterial agent against multidrug-resistant pathogens infection (Lee, Jung, Cha *et al.*, 2015).



**Figure 2.17** Appearance of baikal skullcap. It is member of the mint family (Lamiaceae) that is a perennial found in sandy mountain soils in northeast China and adjacent Russia, Korea, Mongolia, and Japan (Foster, 2004).

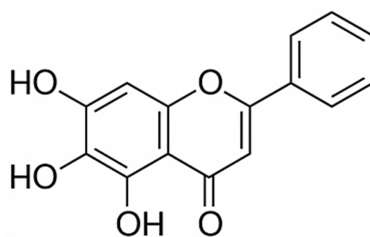


**Figure 2.18** Chemical structure of baicalein.

Baicalein is a potential synergistic adjunct to ceftazidime for the treatment of *S. pyogenes* infections. It acts by exerting inhibition activity against  $\beta$ -lactamase. Compared with the controls (drug-free), combining ceftazidime with baicalein caused peptidoglycan and morphological damage (Figure 2.19) (Siriwong, Pimchan, Naknarong *et al.*, 2015).

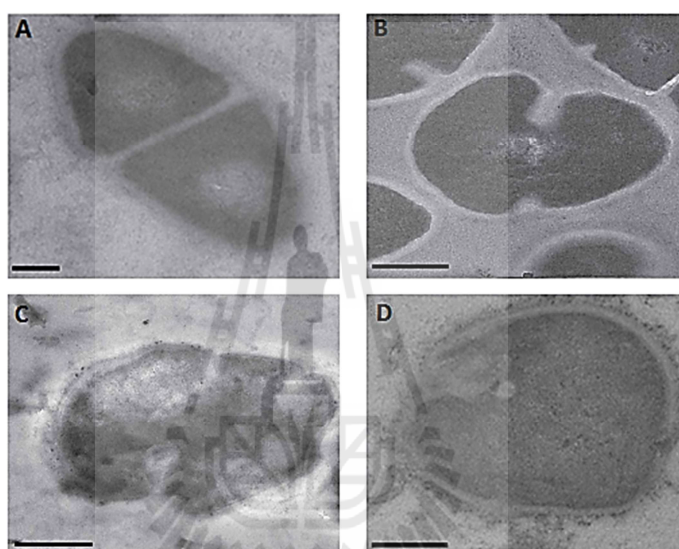


**Figure 2.19** Ultrathin sections of log phase *S. pyogenes* DMST 30653 grown in cation-adjusted Mueller-Hinton broth with lysed horse blood (2.5 %v/v) containing: Drug-free (A), 0.25  $\mu\text{g/ml}$  ceftazidime (B), 128  $\mu\text{g/ml}$  baicalein (C), 0.09  $\mu\text{g/ml}$  ceftazidime and 24  $\mu\text{g/ml}$  baicalein. Scale bars represent 0.5  $\mu\text{m}$  (Siriwong *et al.*, 2015).

### 2.4.3 Luteolin

Luteolin, 3',4',5,7-tetrahydroxyflavone (Figure 2.20), is a common flavonoid that exists in many types of plants, including fruits, vegetables, and

medicinal herbs, such as celery, parsley, thyme, oregano, and rosemary (Figure 2.14), broccoli, green pepper, navel oranges, and olive oil. The hydroxylated flavone derivative is a strong antioxidant and radical scavenger. (Evans, Miller, Paganga *et al.*, 1996). Luteolin activates both the extrinsic and intrinsic apoptosis pathways (Horinaka, Yoshida, Shiraishi *et al.*, 2005). Luteolin is potent to inhibit angiogenesis (Bagli, Stefanidou, Morbidelli *et al.*, 2004), to prevent carcinogenesis, to reduce tumor growth (Fang, Zhou, Shi *et al.*, 2007) and to sensitize tumor cells to the cytotoxic effects of some anticancer drugs, which suggests that this flavonoid has cancer chemopreventive and chemotherapeutic potential (López-Lázaro, 2009). It also plays a role in inhibition of fatty acid synthase activity (Coleman, Bigelow, Cardelli *et al.*, 2009).

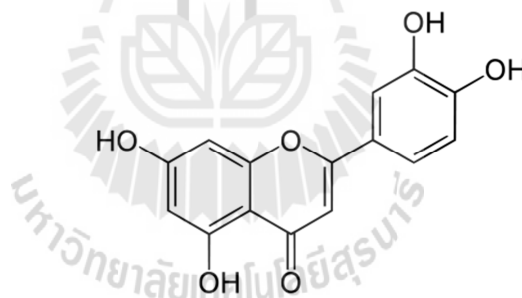


**Figure 2.20** Chemical structure of luteolin.

#### 2.4.4 $\alpha$ -Mangostin

Alpha-mangostin is a natural xanthonoid that belongs to the family of xanthenes (Figure 2.21). It is a pigment from mangosteen (Figure 2.22). The xanthenone derivative has been shown to induce apoptosis via inhibiting fatty acid synthase (Quan, Wang, Ma *et al.*, 2012).  $\alpha$ -Mangostin was found to be active against

vancomycin-resistant enterococci (VRE) and methicillin-resistant *Staphylococcus aureus* (MRSA) with synergism between alpha-mangostin and gentamicin (GM) against VRE, and  $\alpha$ -mangostin and vancomycin hydrochloride (VCM) against MRSA (Sakagami, Inuma, Piyasena *et al.*, 2005). The direct interactions of  $\alpha$ -mangostin with the *S. aureus* membrane are responsible for the rapid concentration-dependent membrane disruption and bactericidal action (Koh, Qiu, Zhu *et al.*, 2013).

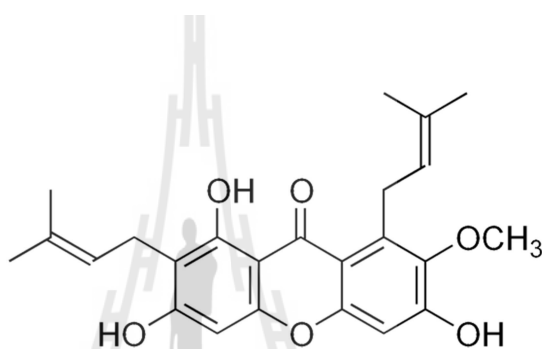


**Figure 2.21** Chemical structure of  $\alpha$ -mangostin.



**Figure 2.22** Appearance of mangosteen fruit (*Garcinia mangostana*). It is found particularly in the South-East Asian regions.

### 2.4.5 Naringenin

Naringenin is a flavanone, a type of flavonoid (Figure 2.23). It can be found in grapefruits, oranges and tomato skin. The pharmacological properties of naringenin, which has many potential applications, include an antioxidant effect (Andrade, Carvalho, Cunico *et al.*, 2010), hepatoprotective (Lee, Yoon and Moon., 2004), anti-inflammatory (Bodet, La, Epifano *et al.*, 2008), antiviral (Nahmias, Goldwasser, Casali *et al.*, 2008), antihypertensive (Saponara, Testai, Lozzi *et al.*, 2006) and antimutagenic effects (Renugadevi and Prabu, 2009). In addition naringenin displayed additive effects when combined with the different antibiotics at sub-inhibitory concentrations against multidrug resistant *Staphylococcus aureus* (Ng'uni, Mothlalamme, Daniels *et al.*, 2015) and inhibited the growth of gram-positive and gram-negative bacteria (Andrade *et al.*, 2010).

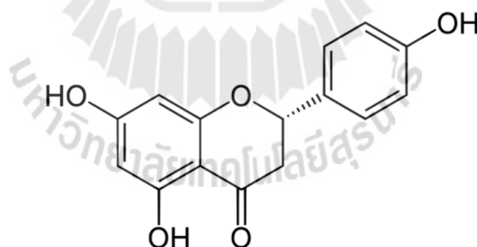


**Figure 2.23** Chemical structure of naringenin.

# CHAPTER III

## MATERIALS AND METHODS

### 3.1 Materials

#### 3.1.1 Chemicals

Chemical reagents and sources used in this work are listed in Table 3.1

**Table 3.1** Chemical reagents and sources.

Reagent	Source
<ul style="list-style-type: none"><li>• Coomassie brilliant blue R250</li></ul>	Acros Organics
<ul style="list-style-type: none"><li>• Dithiothreitol (C<sub>4</sub>H<sub>10</sub>O<sub>2</sub>S<sub>2</sub>)</li><li>• Ethidium bromide (C<sub>21</sub>H<sub>20</sub>BrN<sub>3</sub>)</li><li>• Malachite green (C<sub>23</sub>H<sub>25</sub>ClN<sub>2</sub>)</li><li>• Methanol (CH<sub>3</sub>HO)</li><li>• Perchloric acid (HClO<sub>4</sub>)</li><li>• Triton X-100</li></ul>	
<ul style="list-style-type: none"><li>• Ammonium persulfate (NH<sub>4</sub>)<sub>2</sub>S<sub>2</sub>O<sub>4</sub></li><li>• Glycerol (C<sub>3</sub>H<sub>8</sub>O<sub>3</sub>)</li><li>• Sodium chloride (NaCl)</li><li>• Magnesium chloride (MgCl<sub>2</sub>)</li><li>• Sodium dodecyl sulfate (NaC<sub>12</sub>H<sub>25</sub>SO<sub>4</sub>)</li></ul>	CARLO ERBA

**Table 3.1** Chemical reagents and sources (Continued).

<b>Reagent</b>	<b>Source</b>
<ul style="list-style-type: none"> <li>• Potassium chloride(KCl)</li> <li>• Tris(hydroxymethyl)aminomethane (NH<sub>2</sub>C(CH<sub>2</sub>OH)<sub>3</sub>)</li> <li>• Hydrochloric acid (HCl)</li> <li>• Ethylenediaminetetraacetic acid (C<sub>10</sub>H<sub>16</sub>N<sub>2</sub>O<sub>8</sub>)</li> <li>• Sodium molybdate (Na<sub>2</sub>MoO<sub>4</sub>)</li> <li>• Sodium acetate (CH<sub>3</sub>COONa)</li> </ul>	CARLO ERBA
<ul style="list-style-type: none"> <li>• Bacto-agar</li> <li>• Peptone</li> <li>• Yeast extract</li> </ul>	HiMedia
<ul style="list-style-type: none"> <li>• Adenosine triphosphate</li> <li>• Guanosine triphosphate</li> <li>• Ampicillin</li> <li>• Bovine serum albumin</li> <li>• Isopropyl-β-D thiogalactopyranosid</li> <li>• Lysozyme</li> <li>• N, N-Methylenebisacrylamide</li> <li>• Acrylamide</li> <li>• 4-(2 Hydroxyethyl)-1-piperazineethanesulfonic acid</li> <li>• 2-(N morpholino)-ethanesulfonic acid</li> <li>• Apigenin (≥97% purity)</li> <li>• Baicalein (98% purity)</li> </ul>	Sigma-Aldrich

**Table 3.1** Chemical reagents and sources (Continued).

<b>Reagent</b>	<b>Source</b>
<ul style="list-style-type: none"> <li>• Luteolin (<math>\geq 98\%</math> purity)</li> <li>• <math>\alpha</math>-Mangostin (<math>\geq 98\%</math> purity)</li> <li>• Naringenin (<math>\geq 95\%</math> purity)</li> </ul>	Sigma-Aldrich
<ul style="list-style-type: none"> <li>• Restriction enzymes               <ul style="list-style-type: none"> <li>– EcoRI</li> <li>– SfiI</li> <li>– XhoI</li> <li>– SalI</li> </ul> </li> </ul>	ThermoScience
<ul style="list-style-type: none"> <li>• Agarose</li> <li>• Deoxyribonucleotide triphosphate</li> <li>• DNA ladder VC 100 bp plus</li> <li>• <i>Taq</i> DNA polymerase</li> <li>• T4-DNA ligase</li> <li>• Protein maker</li> <li>• Tetramethylethylenediamine</li> </ul>	Vivantis

### 3.1.2 Instruments and equipment

3.1.2.1 TC-PLUS thermal cycler (Techne)

3.1.2.2 DNA gel electrophoresis apparatus (Amersham)

3.1.2.3 Vertical gel electrophoresis apparatus (Bio-RAD)

3.1.2.4 Innova 4300 shaker incubator (Brunswick Scientific)

3.1.2.5 Sorvall legend XFR centrifuge (ThermoScience)

3.1.2.6 Nano drop 2000 spectrophotometer (ThermoScience)

3.1.2.7 Labsystems iEMS Microplate Reader MF (MTX LabSystems)

### 3.1.3 Bacterial stains and plasmids

3.1.3.1 Bacterial template

*Bacillus subtilis* (TISTR No. 001, Thailand Institute of Scientific and Technological Research, Thailand).

3.1.3.2 *Escherichia coli* strains

1.) *E. coli* DH5 $\alpha$

*E. coli* strains DH5 $\alpha$  is suitable for cloning of genes. The mutations that the DH5 $\alpha$  has are: F $^{-}$   $\Phi$ 80lacZ $\Delta$ M15  $\Delta$ (lacZYA-argF) U169 recA1 endA1 hsdR17(rK-mK+) supE44 $\lambda^{-}$  thi-1 gyrA96 relA1 (Taylor, Walker, McInnes *et al.*, 1993). These mutations allow for blue-white screening, lower endonuclease degradation (which ensures higher plasmid transfer rates), increase insert stability and improve the quality of plasmid DNA preparation.

2.) *E. coli* BL21(DE3)

*E. coli* strains BL21(DE3) is used for performing protein expression that utilizes the T7 RNA polymerase promoter to direct high-level expression (Studier and Moffatt, 1986). The mutations that the BL21 has are: F $^{-}$  ompT gal dcm lon hsdS<sub>B</sub>(r<sub>B</sub> $^{-}$  m<sub>B</sub> $^{-}$ )  $\lambda$ (DE3). These expression strains naturally lack the Lon protease, which can degrade recombinant proteins. In addition, these strains are engineered to be deficient for a second protease, the OmpT protein (Grodberg and Dunn, 1988).

### 3.1.3.3 Plasmid

#### 1.) pTG19-T cloning plasmid

pTG19-T is a plasmid designed for rapid and efficient cloning of PCR products with 3'-dA overhangs (Figure 3.1). The linearized plasmid was engineered with a multiple cloning site in the gene for  $\beta$ -galactosidase (also known as lacZ) (Langley, Villarejo, Fowler *et al.*, 1975). Successful cloning of foreign DNA into the multiple cloning sites interrupts lacZ the genes producing a non-functional  $\beta$ -galactosidase enzyme. An unsuccessful cloning will produce a functional enzyme (Langley *et al.*, 1975). The ligated plasmid without a foreign gene produces the functional enzyme that is able to hydrolyze X-gal, which creates a blue colony on LB agar plate supplemented by X-gal and IPTG.

#### 2.) pSY5 expression plasmid

The pSY5 plasmid was modified from pET-21d(+), designed by the (Robert C Robinson group), Institute of Molecular and Cell Biology (IMCB), A\*Star, Singapore. This plasmid enables expression the protein under the control of the T7 promoter. The pSY5 encodes an N-terminal, His8-tag, followed by a human rhinovirus 3C protease cleavage site ahead of the N-terminus of the protein.

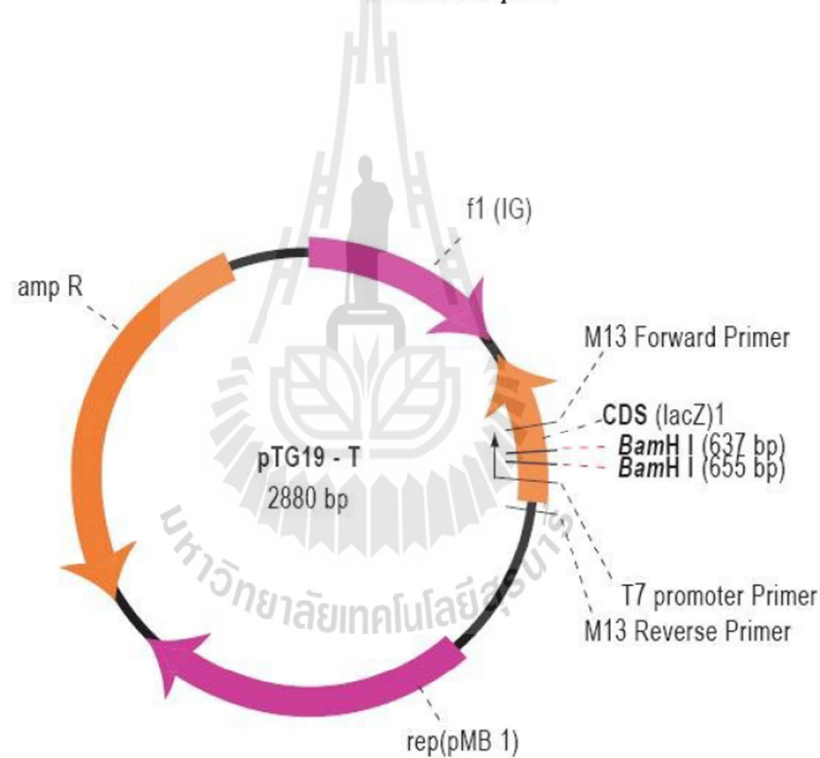
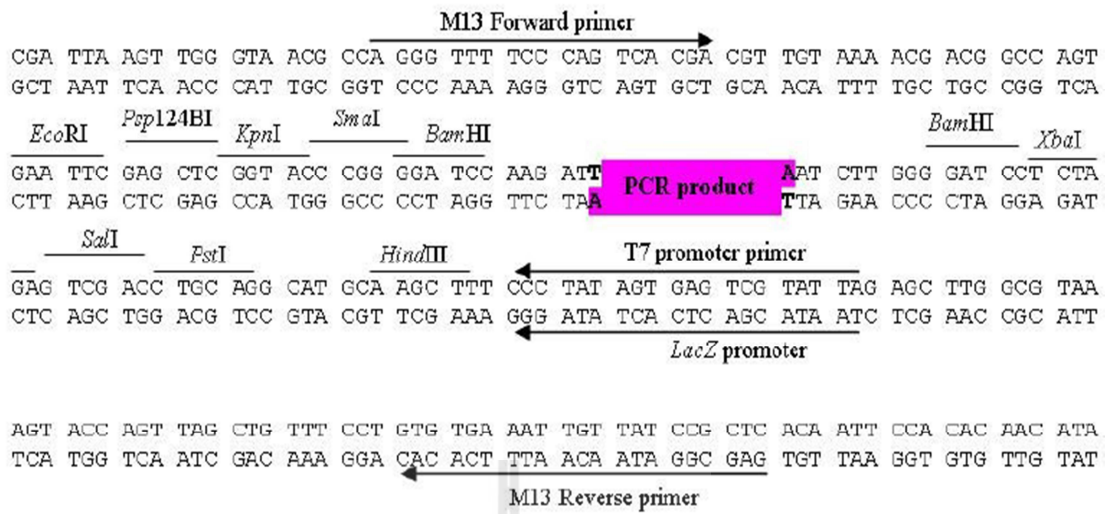
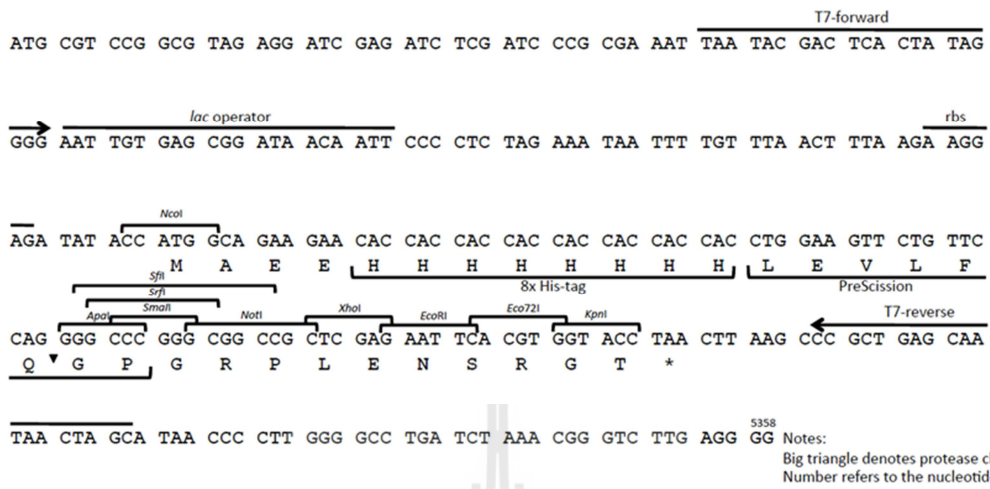


**Figure 3.1** Map and multiple cloning site sequence of pTG19-T vector.

8x His – PreScission – MCS



Expression vector based on pET-21d(+) (Novagen, cat no 69743-3).

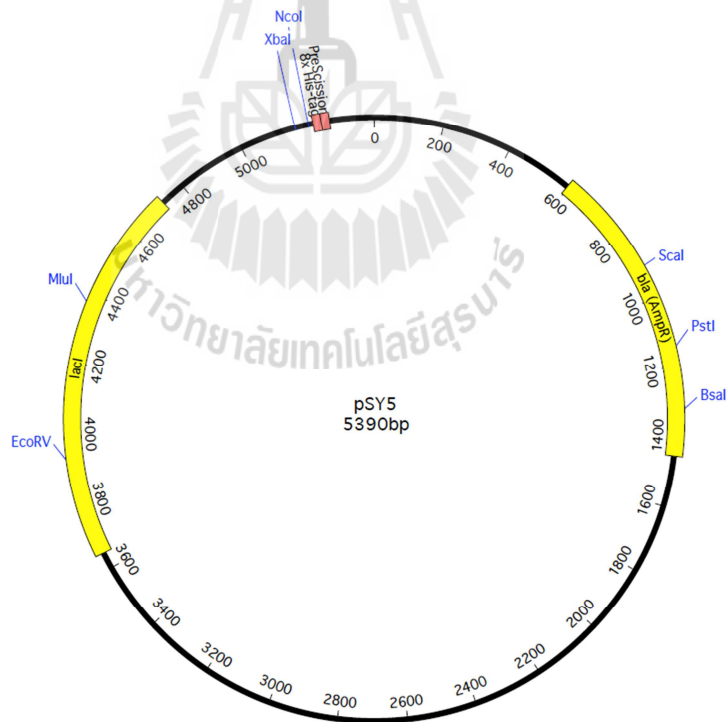


Figure 3.2 Map and multiple cloning site sequence of pSY5.

### 3.1.4 Oligonucleotides

The oligonucleotides (primers) used for genes amplification were purchased from Sigma-Aldrich (Singapore) Co., Ltd. and are shown in Table 3.1.

**Table 3.2** Details of primers.

Construction	Primer	Sequence	Cloning site
pTG19-mreB-Bs, pSY5-mreB-Bs	MreB-Bs Fwd	5' ggcccgggcccgatgttg gaattggtagtagagac 3'	SfiI
pTG19-mreB-Bs, pSY5-mreB-Bs	MreB-Bs Rev	5' gaattctatctagtttccttg aaaagat ggatgtgctcc 3'	EcoRI
pTG19-ftsZ-Bs, pSY5-ftsZ-Bs	FtsZ-Bs Fwd	5' ggcccgggcccgatgttg gagtcgaaac 3'	SfiI
pTG19-ftsZ-Bs, pSY5-ftsZ-Bs	FtsZ-Bs Rev	5' gaattcttagccgcttattac ggttcttaagaatg 3'	EcoRI

## 3.2 General Methods

### 3.2.1 CaCl<sub>2</sub> Competent cell preparation

The *E. coli* DH5 $\alpha$  and BL21(DE3) were grown in 5 ml LB medium (10 g/l peptone, 5 g/l yeast extract, 5 g/l NaCl) at 37 °C, 200 rpm for 16 – 18 hours as a starter, then 1 ml starter was inoculated to 100 ml LB and cultured at 37 °C, 200 rpm until the optical density at 600 nm reached 0.4 – 0.5. The cell pellet was collected by centrifugation at 3,000 xg, for 10 minutes, at 4 °C. The pellet was suspended in 10 ml of cold 0.1 M CaCl<sub>2</sub>, gently mixed and stored on ice for 10 minutes. The cell

suspension was centrifuged at 3,000 xg, for 10 minutes, at 4 °C, the supernatant discarded, and 2 ml of cold 15% glycerol in 0.1 M CaCl<sub>2</sub> was added, and the cell suspension was mixed very well and aliquot into the micro centrifuge tubes with 100 µl per tube. The tubes of competent cells were used immediately or kept at -80 °C.

### 3.2.2 Heat shock transformation of CaCl<sub>2</sub> competent cell

One hundred microliters of competent cell in 1.5 ml micro centrifuge tube was thawed on ice. One microliter of plasmid (or ~100 ng) was added to the cell and mixed by gently stirring the pipette tip. Incubation of the cells continued on ice for 30 minutes. The cells were heat pulsed at 42 °C for 45 seconds followed by 2 minutes incubation on ice. The LB medium (0.9 ml) was added to each tube of cells and the tubes were incubated at 37 °C for 1 hour. A sample of 50 µl was plated out on agar plates with appropriate antibiotics for selection. Plates were incubated at 37 °C overnight.

### 3.2.3 Cloning

DNA encoding the genes of *mreB* (Gene ID: 936759) and *ftsZ* (Gene ID: 935971) of *B. subtilis* were amplified by polymerase chain reaction (PCR). All forward primers contained a SfiI recognition site and reverse primers containing an EcoRI recognition site (Table 3.2). Chemical compositions of the PCR and thermo-cycler program are shown in Tables 3.3 and 3.4. The genes were amplified directly from *B. subtilis* cell by using *Taq* DNA polymerase. PCR products were cleaned by PCR Clean-up Kit. The concentration of cleaned PCR products was measured by Nano drop spectrophotometer. The cleaned PCR products were ligated into pTG19-T plasmid by using T4 ligase. The details of the ligation reaction are shown in Table 3.5. The reaction was incubated at 22 °C for 1 hour. The ligation product was

transformed into *E. coli* DH5 $\alpha$ . The transformation reaction was spread onto an LB agar plate containing 100  $\mu$ g/ml ampicillin, 1 mM IPTG, and 50  $\mu$ g/ml X-gal.

**Table 3.3** Chemical compositions of the PCR.

Composition	Volume ( $\mu$ l)	Final concentration
10 $\times$ S buffer	2.5	1x
dNTPs (0.2 mM each dNTP)	2.5	0.2 mM
2 mM MgCl <sub>2</sub>	2.0	2.0 mM
5 $\mu$ M Primer forward	2.5	0.5 mM
5 $\mu$ M Primer reverse	2.5	0.5 mM
DNA template	2.0	-
Taq DNA polymerase	0.25	1U
Distilled water	10.75	-
<b>Total reaction volume</b>	<b>25 <math>\mu</math>l</b>	

The constructs were confirmed by DNA sequencing (Macrogen, Korea) with the M13 forward primer and M13 reverse primer. The plasmid containing *mreB-Bs* was named pTG19-*mreB-Bs* and the plasmid containing *ftsZ-Bs* was named pTG19-*ftsZ-Bs*. The verified pTG19-*mreB-Bs* plasmid was digested and the *mreB-Bs* insert cloned into pSY5 at SfiI and EcoRI cloning sites (Table 3.6). The plasmid containing *mreB-Bs* was named pSY5-*mreB-Bs*. The verified pTG19-*ftsZ-Bs* was digested with SfiI and SalI and the insert cloned into pSY5 at SfiI and XhoI cloning sites (Table 3.6). The plasmid containing *ftsZ-Bs* was named pSY5-*ftsZ-Bs*.

**Table 3.4** Cycling parameters of the PCR.

<b>Step</b>	<b>Temperature (°C)</b>	<b>Time (min)</b>	
Initial Denaturation	95	5	
Denaturation	95	0.30	← 30 cycles
Annealing	68	0.30	
Extension	72	1.30	
Polish extension	72	5	

**Table 3.5** Composition of ligation reaction of the PCR product into the cloning plasmid.

<b>Composition</b>	<b>Volume (μl)</b>
pTG19 (25ng/μl)	2
Fresh PCR product (55ng/μl)	1
10X Buffer Ligase	1
T4 DNA Ligase (200u/μl)	0.2
Distilled water	5.8
<b>Total Volume</b>	<b>10 μl</b>

**Table 3.6** Composition of ligation reaction putting inserts into the expression plasmid.

<b>Composition</b>	<b>Volume (<math>\mu</math>l)</b>
pSY5 (25 ng/ $\mu$ l)	4
Gene insert (20 ng/ $\mu$ l)	3
10X Buffer Ligase	1
T4 DNA Ligase (200 U/ $\mu$ l)	0.2
Distilled water	1.8
<b>Total Volume</b>	<b>10 <math>\mu</math>l</b>

### 3.3 Screening and optimization of protein expression

#### 3.3.1 Screening of protein expression

The pSY5-*mreB-Bs* and pSY5-*ftsZ-Bs* plasmids were transformed into *E. coli* BL21(DE3) cells (expression cells). Ten single-colonies were selected from each transformation plate (pSY5-*mreB-Bs* or pSY5-*ftsZ-Bs*). Each single-colony was inoculated in 10 ml of LB media containing 100  $\mu$ g/ml ampicillin. The bacterial cultures were incubated at 37 °C, 200 rpm in a shaker incubator for 16 hours. Then, 2.5 ml (5%) of each starter culture was inoculated in 47.5 ml of LB media containing 100  $\mu$ g/ml ampicillin. The cells were grown at 37 °C, 200 rpm in a shaker incubator until optical density at 600 nm reached 0.6 – 0.8. The cultures were induced with 1 mM IPTG and incubated at 20 °C, 200 rpm in shaker incubator for 16 hours.

The induction cells were harvested by centrifugation at 3,000 xg for 15 minutes. The cell pellets were suspended in 1 ml of 50 mM Tris-HCl, pH 8, 150 mM NaCl, and 0.1 mg/ml lysozyme incubated at 37 °C for 30 minutes. The lysate were

clarified by centrifugation at 12,000 xg for 10 minutes. The supernatant was applied to 20  $\mu$ l of Ni<sup>2+</sup>-NTA resin and gently shaken for 10 minutes. The resin were washed with 50 mM Tris-HCl, pH 8.0, 20 mM imidazole, and 500 mM NaCl. The soluble protein was verified by SDS-PAGE.

### **3.3.2 Optimization of protein expression**

The best expression clones were inoculated in 10 ml of LB media containing 100  $\mu$ g/ml ampicillin. The starter cultures were incubated at 37 °C, 200 rpm in shaker incubator for 16 hours. Then, 2.5 ml of starter culture was inoculated in 47.5 ml of LB media containing 100  $\mu$ g/ml ampicillin. The cells were cultured in LB media containing 100  $\mu$ g/ml ampicillin until the optical density at 600 nm reached 0.6 – 0.8. The optimum concentration of IPTG and temperature for the protein expression were investigated by varying the concentration of IPTG from 0.25 – 1.00 mM, and temperature from 20 – 30 °C. The cell induced were collected by centrifugation at 3,000 xg and suspended in 50 mM Tris-HCl, pH 8.0, 150 mM NaCl, and 0.1 mg/ml lysozyme. The cell suspensions were incubated at 37 °C for 30 minutes and the lysate was clarified by centrifugation at 12,000 xg for 10 minutes. The supernatant was applied to 20  $\mu$ l of Ni<sup>2+</sup>-NTA resin. The resin was washed with 50 mM Tris-HCl, pH 8.0, 20 mM imidazole, and 500 mM NaCl. The soluble protein was verified by SDS-PAGE.

## **3.4 Protein purification**

The expression cell pellets were suspended in 50 mM Tris-HCl, pH 8.0, and 150 mM NaCl and lysed by sonication. The lysate was clarified by centrifugation at 12,000 xg for 30 minutes. The supernatant was applied to a Ni<sup>2+</sup>-NTA column. The

proteins were purified by Ni<sup>2+</sup>-NTA with stepwise elution using imidazole concentrations of 0, 20, 40, 60, 80, 100, 120, 140, 160, 180, 200, 220, and 240 mM in 500 mM NaCl and 50 mM Tris-HCl, pH 8. The pure proteins were dialyzed against buffer containing 50 mM Tris-HCl, pH 8.0, and 150 mM NaCl. The proteins were concentrated by a 30 kDa molecular mass cut off (MWCO) Centricon centrifugal filter.

### **3.5 Nucleotide removal**

To examine the effects of concentration of nucleotide on the polymerization of MreB-Bs and FtsZ-Bs, nucleotides were removed from the proteins by treating the proteins in Dowex resin following Bean and Amann (2008). The proteins were mixed with 1/4 its volume of 50% Dowex resin (1X8-400Cl) slurry in 10 mM Tris-HCl, pH 8.0. The reaction was incubated on ice for 15 minutes with gentle mixing every 2 – 3 minutes, the mixture was centrifuged at 4 °C at 10,000xg for 2 minutes and the supernatant transferred to a separate tube. This procedure was carried out three times to ensure complete nucleotide removal.

### **3.6 Phosphate release assays**

#### **3.6.1 Effect of pH on nucleotides hydrolysis by the proteins**

The ATP hydrolysis and GTP hydrolysis activity of MreB-Bs at different pH values was investigated by the malachite green assay of released phosphate (Carter and Karl, 1982) by buffering the reaction with sodium acetate, pH 5.5, MES pH 6.0, MES, pH 6.5, HEPES, pH 7.0, Tris-HCl, pH 7.5 and, Tris-HCl, pH 8.0.

The effect of pH on nucleotides hydrolysis by MreB-Bs was tested by mixing 5  $\mu$ M MreB-Bs in 50 mM buffer, 100 mM NaCl, 4 mM MgCl<sub>2</sub>, and 0.2 mM ATP or GTP (van den Ent *et al.*, 2001).

The effect of pH on nucleotides hydrolysis by FtsZ-Bs was tested by mixing 10  $\mu$ M FtsZ-Bs in 50 mM Buffer, 200 mM KCl, 5 mM MgCl<sub>2</sub>, and 0.2 mM ATP or GTP (Matsui, Han, Yu *et al.*, 2013).

The reactions were stopped by adding an equal volume of cold 0.6 M perchloric acid. Two volumes of filtered malachite green solution (0.15 g malachite green, 1 g sodium molybdate, 0.25 g Triton X-100 in 500 ml 0.7 M HCl) was added to the supernatants and the mixtures incubated at room temperature for 15 minutes. The absorbance at 620 nm was read by spectrophotometer. The phosphate concentrations were calculated from the standard curve plot (Appendix B), (Geladopoulos *et al.*, 1991).

### **3.6.2 Screening of natural products effect on nucleotides hydrolysis by the proteins**

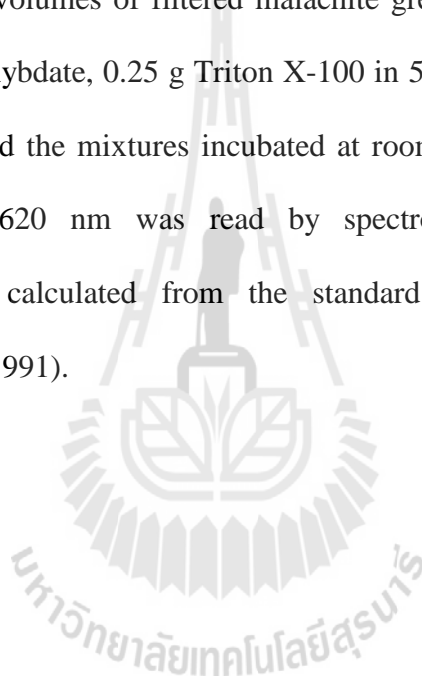
#### **3.6.2.1 Screening of natural products effect on nucleotides hydrolysis of MreB-Bs**

MreB-Bs (5  $\mu$ M) was mixed in 50 mM Tris-HCl, pH 7.5, 100 mM NaCl, 4 mM MgCl<sub>2</sub> and 200  $\mu$ M of one natural products (apigenin, baicalein, luteolin,  $\alpha$ -mangostin, or naringenin), and 200  $\mu$ M ATP or GTP was added and incubated for 1 hour.

### 3.6.2.2 Screening of natural products effects on nucleotides hydrolysis by FtsZ-Bs

FtsZ-Bs (10  $\mu$ M) was mixed in 50 mM MES, pH 6.5, 200 mM KCl, 5 mM  $\text{MgCl}_2$  and 200  $\mu$ M of one natural products (apigenin, baicalein, luteolin,  $\alpha$ -mangostin, or naringenin), and 200  $\mu$ M GTP was added and incubated for 1 hour.

The reaction was stopped by adding an equal volume of cold 0.6 M perchloric acid. Two volumes of filtered malachite green solution (0.15 g malachite green, 1 g sodium molybdate, 0.25 g Triton X-100 in 500 ml 0.7 M HCl) were added to the supernatants and the mixtures incubated at room temperature for 15 minutes. The absorbance at 620 nm was read by spectrophotometer. The phosphate concentrations were calculated from the standard curve plot (Appendix B), (Geladopoulos *et al.*, 1991).



## CHAPTER IV

### RESULTS AND DISCUSSION

#### 4.1 Cloning

##### 4.1.1 Amplification of *mreB*-Bs and *ftsZ*-Bs by PCR

DNA encoding the genes of *mreB* and *ftsZ* of *B. subtilis* were amplified from the *B. subtilis* cells by *Taq* DNA polymerase with the pair of gene specific primers (Table 3.2). The best annealing temperature for the two genes was 62 °C. The PCR products with the expected sizes of *mreB*-Bs (1,041 bp) and *ftsZ*-Bs (1149 bp) were obtained, as show in Figure 4.1.

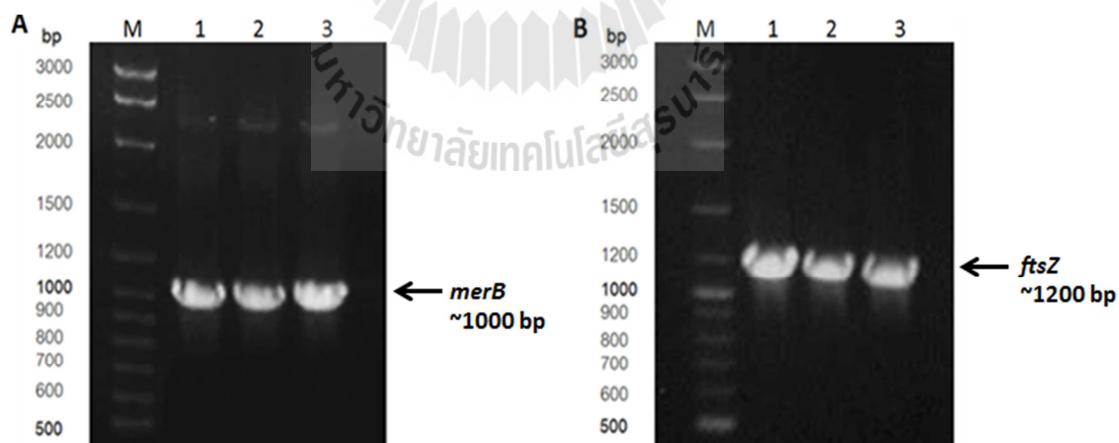


**Figure 4.1** Agarose gel electrophoresis analysis of *mreB*-Bs and *ftsZ*-Bs amplification: Lane M; DNA ladder (VC 100 bp plus, Vivantis), (A) lanes 1–3; PCR product of *mreB*-Bs, (B) lanes 1–3; PCR product of *ftsZ*-Bs.

#### 4.1.2 Screening of pTG19-T cloning vector containing the *mreB-Bs* and *ftsZ-Bs* by PCR

The purified PCR products were ligated into pTG19-T cloning vector by using T4 ligase. The ligation products were transformed into *E. coli* DH5 $\alpha$ . The transformation reaction was spread on LB agar plate supplemented by 2% (w/v) X-gal and 1 mM IPTG. The ligated plasmid without a foreign gene produces the functional enzyme that is able to hydrolyze X-gal, which creates a blue colony on the agar plate. Thus, the blue colony is a clone without insert and then the white colony is a positive clone (the clone with non-functional  $\beta$ -galactosidase). However, false white colonies can occur but doesn't have insert is possible, because single 3'-dT overhangs on the vector may be degraded.

Therefore, colony PCR was performed by using the sets of cloning primers to screen and verify the plasmid containing gene insert. Figure 4.2 shows that clones numbers 2 – 8 yielded the PCR product with the size of *mreB-Bs* (1,041 bp), suggesting the presence of the insert of *mreB-Bs* in the pTG19. In the same way, Figure 4.3 shows that clones numbers 1, 3 – 6, and 10 produced the PCR products with the expected size of *ftsZ-Bs* (1149 bp), suggesting the insert of *ftsZ-Bs* in the pTG19.

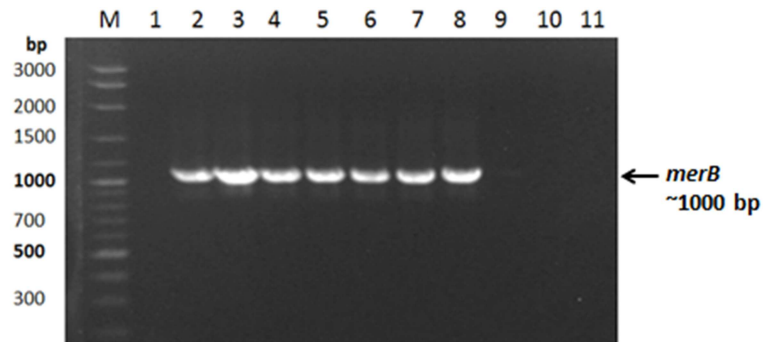


**Figure 4.2** Agarose gel electrophoresis analysis of *mreB-Bs* in pTG19 amplification: Lane M, DNA ladder; lanes 1 – 11, PCR products that show the presence or absence of *mreB-Bs* in pTG19-T clones numbers 1 – 11.

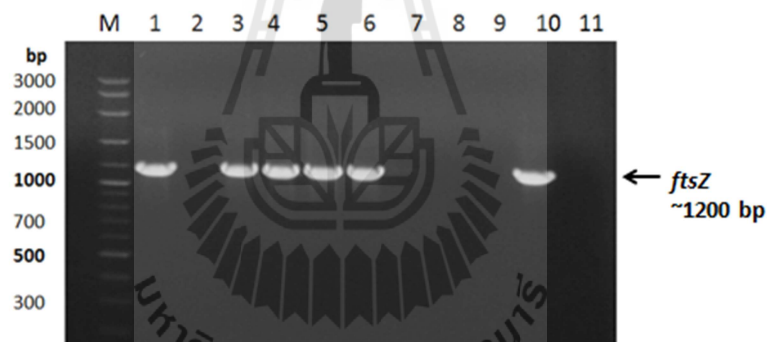


**Figure 4.3** Agarose gel electrophoresis analysis of *ftsZ-Bs* in pTG19 amplification: Lane M, DNA ladder; lane 1 – 11, PCR products that show the presence or absence of *ftsZ-Bs* in pTG19-T clones numbers 1 – 11.

#### 4.1.4 Verification of the genes in pTG19-T DNA sequencing

The sequencing was carried out by Macrogen Inc. (Korea), (the details are shown in Appendix A). The pTG19 containing genes *ftsZ-Bs* was sequenced by using the M13 universal primers in both directions. The result showed that the pSY5-

*mreB*-Bs contains the *mreB*-Bs without mutation. However, the pTG19-*ftsZ*-Bs contained the mutation on the reverse primer (FtsZ-Bs Rev) at the late base of the EcoRI recognition site (from C to A, show in Figure 4.4). However, the Sall restriction site on the pTG19-*ftsZ*-Bs after the mutated EcoRI site remains intact. We decided to use Sall instead of EcoRI, because of the compatibility of the cohesive end of Sall and XhoI recognition sites (on the cloning site of pSY5). As a result, the construct was actually cloned into pSY5 at the SfiI and XhoI recognition sites.

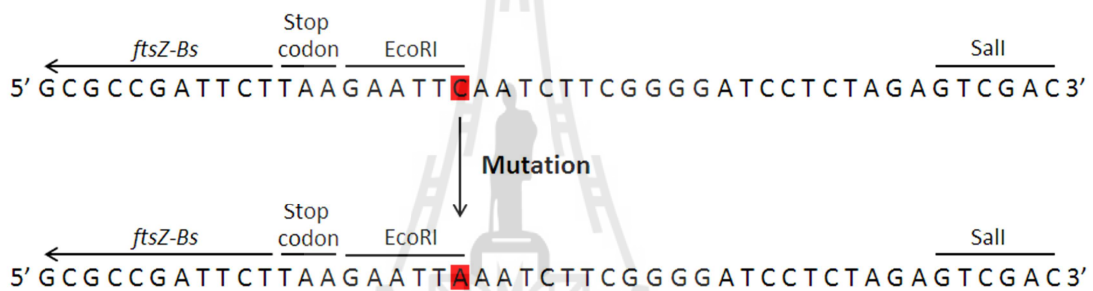


**Figure 4.4** The mutation of pTG19-*ftsZ*-Bs on the late base of EcoRI recognition site of the reverse primer.

#### 4.1.3 Cloning and screening of *mreB*-Bs and *ftsZ*-Bs into expression plasmid (pSY5)

The verified genes were excised from the cloning plasmids (pTG19-*mreB* and pTG19-*ftsZ*-Bs) and ligated into the expression plasmid. The ligation products were transformed into *E. coli* DH5 $\alpha$ . PCR using the sets of cloning primers were performed to screen the *E. coli* DH5 $\alpha$  clones containing *mreB*-Bs and *ftsZ*-Bs in pSY5. Figure 4.5 shows that clone numbers 1 – 10 gave the PCR product with the expected size of *mreB*-Bs (1,041 bp), suggested the insert of *mreB*-Bs in the pSY5.

The PCR product with the expected size of *ftsZ-Bs* (1149 bp) of clones 1, 2, 4, 6 – 10 suggested the *ftsZ-Bs* in these pSY5 (Figure 4.6).

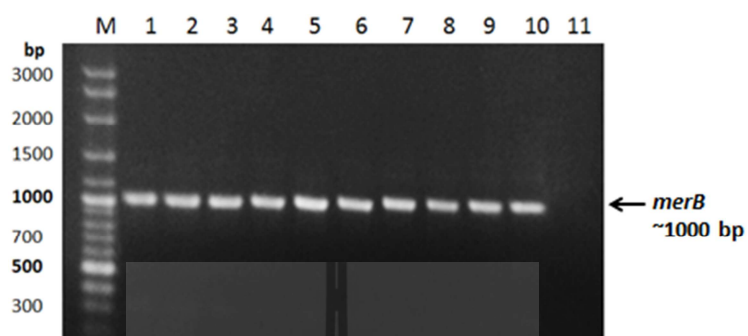


**Figure 4.5** Agarose gel electrophoresis analysis of *mreB-Bs* in pSY5 amplification: Lane M, DNA ladder; lanes 1 – 10: PCR products that show the presence of *mreB-Bs* in pSY5 clones numbers 1 – 10.

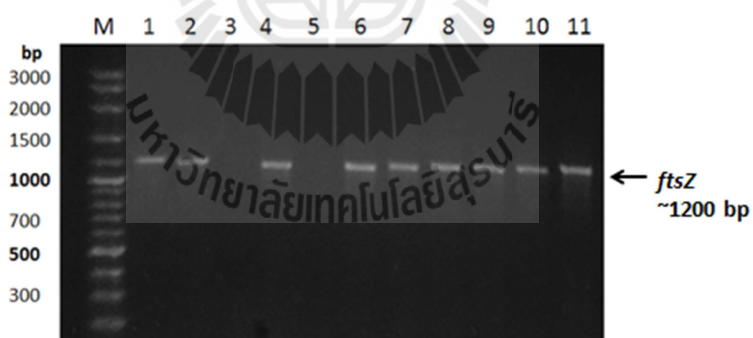


**Figure 4.6** Agarose gel electrophoresis analysis of *ftsZ-Bs* in pSY5 amplification: Lane M, DNA ladder; lanes 1 – 11, PCR products that show the presence or absence of *ftsZ-Bs* in pSY5 clones numbers 1 – 11.

## 4.2 Expressions and Purifications of MreB-Bs and FtsZ-Bs

### 4.2.1 Optimization of protein expression

Expressed His8-tagged proteins can be purified and detected easily because the string of 8 his8-tidine residues binds to IMAC ( $\text{Ni}^{2+}$ -NTA), under specific buffer conditions. The expression plasmids containing the target genes, pSY5-*mreB*-Bs and pSY5-*ftsZ*-Bs, were transformed into the expression strain, *E. coli* BL21(DE3). The expression cells were screened for the best clones in terms of expression by a small scale purification using  $\text{Ni}^{2+}$ -NTA.

The expressions of selected clones were optimized by varying the IPTG concentration and induction temperature. The protein expressions levels were analyzed by a small scale purification using  $\text{Ni}^{2+}$ -NTA followed by SDS-PAGE. The patterns of proteins expressed from cell lysates from expression of MreB-Bs are show in Figures 4.7A and the protein bound with  $\text{Ni}^{2+}$ -NTA resins shown in Figure 4.7B. The black arrow indicates the protein with the 36 kDa.

The protein expression patterns of FtsZ-Bs were analyzed by SDS-PAGE. The cell lysates are shown in Figures 4.8A and the protein bound with  $\text{Ni}^{2+}$ -NTA resin is shown in Figures 4.8B. The black arrow indicates the protein with the 38 kDa. The over expressions of MreB-Bs and FtsZ-Bs are not significantly different in every test condition. According to the screening tests, the optimal condition of the expression was selected at lower IPTG concentration (0.25 mM) and lower temperature (20 °C).

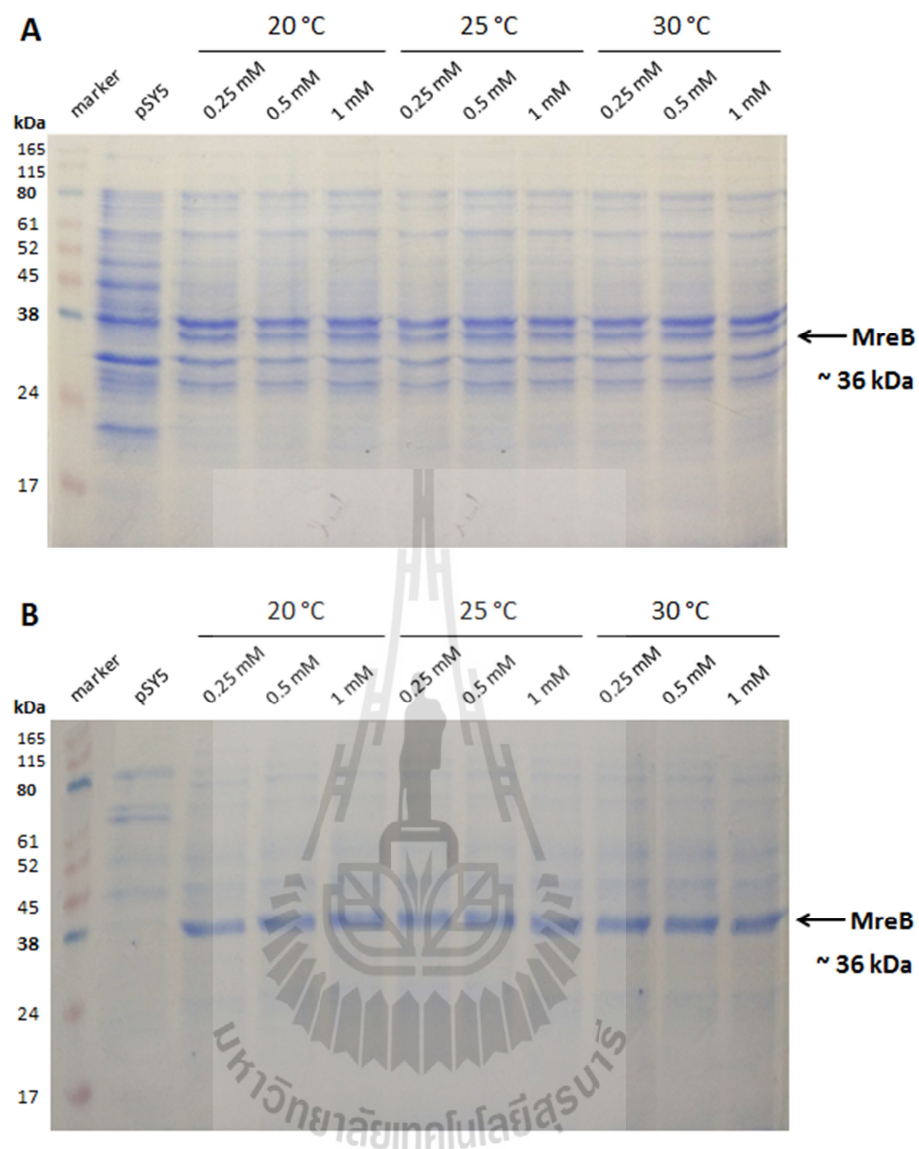


**Figure 4.7** SDS-PAGE of MreB-Bs expression pattern after induction with different concentrations of IPTG (0.25, 0.50, and 1.00 mM) at difference temperatures (20, 25, and 30 °C). (A) Cell lysated, and (B) proteins bound to Ni<sup>2+</sup>-NTA resin. The black arrow indicates MreB-Bs.

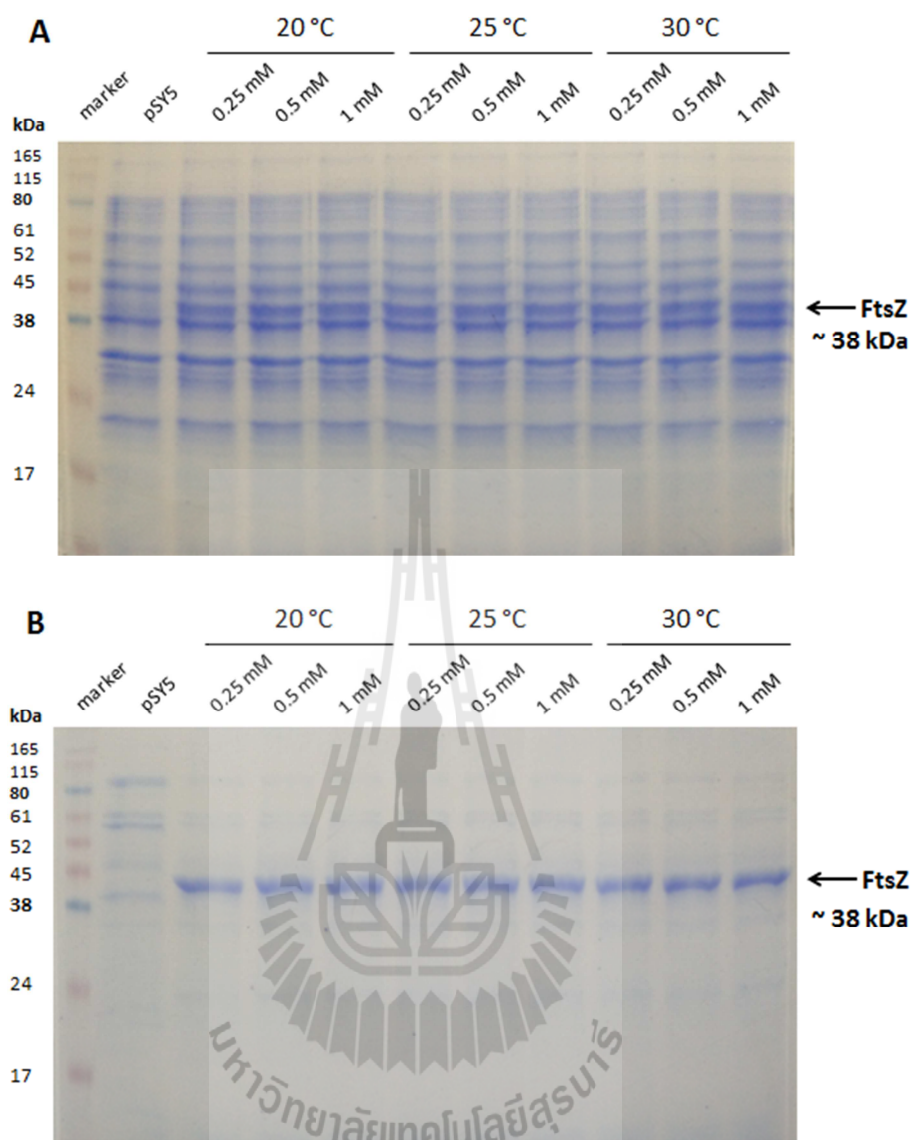


**Figure 4.8** SDS-PAGE of FtsZ-Bs expression pattern after induction with different concentrations of IPTG (0.25, 0.50, and 1.00 mM) at difference temperatures (20, 25, and 30 °C). (A) Cell lysated, and (B) proteins bound to Ni<sup>2+</sup>-NTA resin. The black arrow indicates FtsZ-Bs.

#### 4.2.2 Protein purification

The selected clones were expressed in the optimal condition (0.25 mM IPTG at 20 °C). The proteins were purified by Ni<sup>2+</sup>-NTA with stepwise elution using imidazole concentrations of 0, 20, 40, 60, 80, 100, 120, 140, 160, 180, 200, 220, and 240 mM in 500 mM NaCl and 50 mM Tris-HCl, pH 8. The MreB-Bs was released out from the resin at the concentration of imidazole from 100 – 240 mM (Figure 4.9). At fractions of 100 – 120 mM imidazole were discarded due to their containing a significant amount of contaminating proteins. The FtsZ-Bs was released out from the resin at the concentration of imidazole from 80 – 180 mM (Figure 4.10). However, the fraction at 80 mM imidazole was discarded, since it contaminated a significant amount of contaminated protein.

The fractions of 140 – 240 mM imidazole of MreB-Bs and the fractions with 100 – 180 mM imidazole of FtsZ-Bs appeared to be more than 95% pure based on SDS-PAGE profiles and were saved for the further experiments. Totally, approximately 1 mg of MreB-Bs, and approximately 2 mg of the FtsZ-Bs were obtained from 1 L of *E. coli* BL21(DE3) culture. Each protein was pooled and concentrated and removed nucleotides were removed by adsorption to Dowex resin. The proteins then were analyzed by SDS-PAGE, as shown in Figure 4.11.

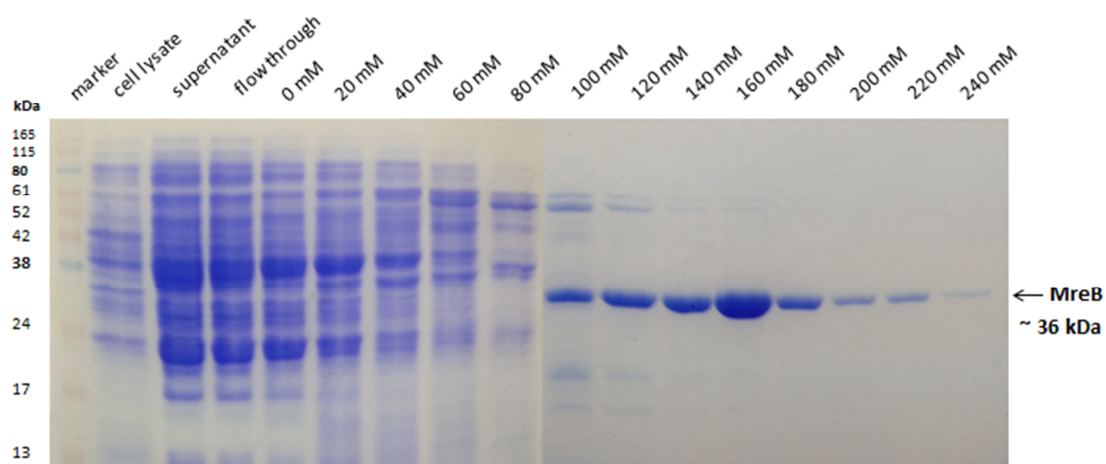


**Figure 4.9** SDS-PAGE of MreB-Bs purification fraction, including washes and elution with different imidazole concentrations. The black arrow indicates the MreB-Bs with an approximate size of 36 kDa.



**Figure 4.10** SDS-PAGE of FtsZ-Bs purification fraction, including washes and elution with different imidazole concentrations. The black arrow indicates the MreB-Bs with an approximate size of 38 kDa.

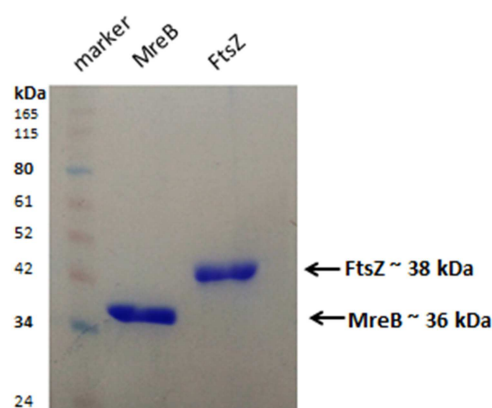


**Figure 4.11** SDS-PAGE of MreB-Bs and FtsZ-Bs purified after removed nucleotide by 1X8-400Cl Dowex resin. The black arrows indicate MreB-Bs (approximately size 36 kDa and FtsZ-Bs approximate size 38 kDa).

### 4.3 Phosphate release assay

The phosphate release assay is a simplified method based on free inorganic phosphate determination. The liberation of orthophosphate from ATP and GTP was generated by ATPases and GTPases. The technique is simple and cost effective functional assay for this class of enzymes.

Malachite green assay is a colorimetric method for measuring free inorganic phosphate. The assay is based on the formation of malachite green molybdophosphoric acid complex that absorbs light at 620-640 nm. It is directly related to the free inorganic phosphate concentration (Figure 4.12) (D'Angelo, Crutchfield, and Vandiviere *et al.*, 2001). This application is a reliable and suitable means of quantifying minimal amounts of 1 – 100  $\mu$ M of inorganic phosphate and amenable to high-throughput screening applications (Attin, Becker, Hannig *et al.*,

2005). This includes quantification of phosphorylation and phosphate release from protein phosphatase substrates (Maehama, Taylor, Slama *et al.*, 2000).

Releasing orthophosphate is a key factor in the control of MreB and FtsZ function. ATPase activity is a consequence of MreB polymerization. After the ATP hydrolysis, free inorganic phosphate is released from the protein filament. During the course of MreB polymerization, there is a lag between polymerization and phosphate release (Esue, Cordero, Wirtz *et al.*, 2005). This indicates that ATP hydrolysis occurs after MreB monomers are assembled into filaments (Esue *et al.*, 2005). Likewise, the GTP-dependent assembly of FtsZ into protofilaments is followed by hydrolysis of GTP to GDP by an active site formed between two associated FtsZ monomers (Pacheco-Gómez, Roper, Dafforn *et al.*, 2011).



**Figure 4.12** Representative of free inorganic phosphate in the malachite green assay. The samples containing malachite green molybdophosphoric acid complex present green color, the absence present yellow color, (yellow-green gradient bar shows increasing of inorganic phosphate ion concentration).

The ATP and GTP hydrolysis activities of MreB-Bs and FtsZ-Bs at different pH were investigated by the malachite green assay. The reactions under the condition were described in the method section 3.4.

### 4.3.1 Effect of pH on nucleotides hydrolysis by MreB-Bs

#### 4.3.1.1 Effect of pH on ATP hydrolysis by MreB-Bs

MreB-Bs hydrolyzed ATP over a wide pH range. The inorganic phosphate 6.80, 16.50, 14.90, 31.11, 33.70, and 33.24  $\mu\text{M}$  were released from ATP in the experiment at pH 5.5, 6.0, 6.5, 7.0, 7.5, and 8.0, respectively (Figure 4.13).

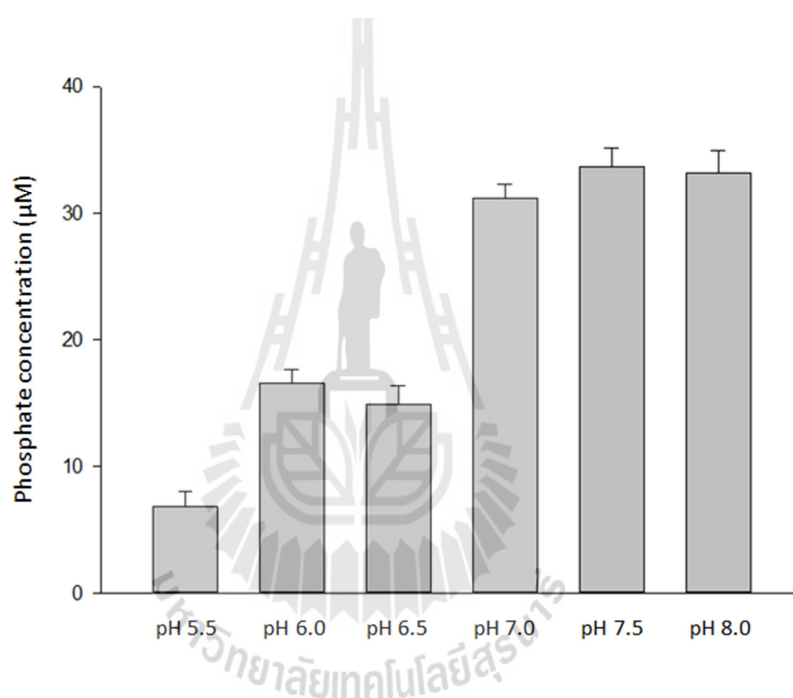


**Figure 4.13** pH effect on phosphate release from ATP by MreB-Bs.

#### 4.3.1.2 Effect of pH on GTP hydrolysis by MreB-Bs

MreB-Bs hydrolyzed GTP over a wide pH range. The inorganic phosphate concentrations of 20.64, 28.64, 44.43, 39.81, 25.77, and 25.26  $\mu\text{M}$  were released from ATP in the experiment at pH 5.5, 6.0, 6.5, 7.0, 7.5, and 8.0, respectively (Figure 4.14).

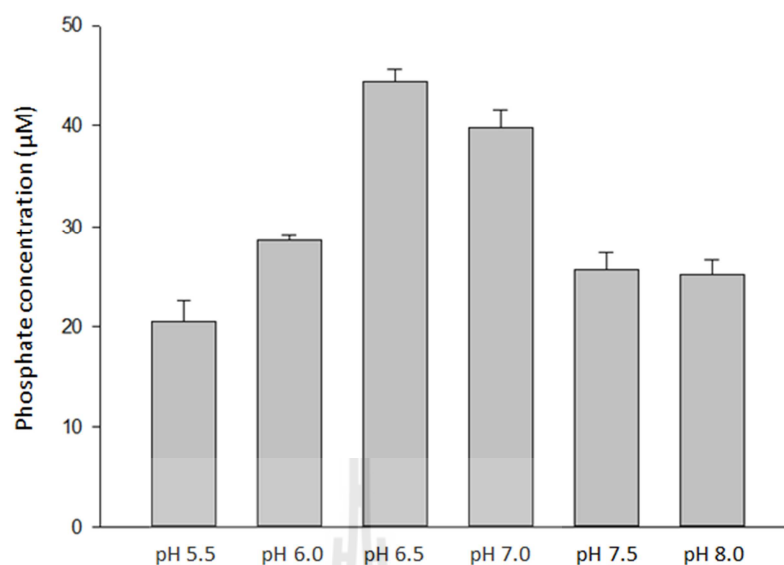


**Figure 4.14** pH effect on phosphate release from GTP by MreB-Bs.

MreB is a member of a larger superfamily of proteins carrying ATPase activity (van den Ent *et al.*, 2001) that can bind and hydrolyze both ATP and GTP. Our study found that the ATPase activity of MreB-Bs was favored at higher pH 7.0 – 8.0, but strongly favored at pH 7.5, while the GTPase activity was most favored at pH 6.5 – 7.0, but and highest at pH 6.5. The nucleotide hydrolysis characteristics of MreB-Bs was similar to that from other species that have been reported, however nucleotide hydrolysis by MreB-Bs is not necessary for polymerization, as in other study species, as shown in Table 4.1.

**Table 4.1** Characters of polymerization of MreB.

MreB	pH range	Optimal pH	Ion		NTP		Critical concentration ( $\mu\text{M}$ )	NTPase dependent polymerization	Gram/ Morphology	Reference
			Mg <sup>2+</sup>	Ca <sup>2+</sup>	ATP	GTP				
<i>T. maritime</i> (MreB-Tm)	4 – 9.5	6 – 7	Yes	Yes	Yes	Yes	5	Yes	Negative/ rod-shape enveloped	van den Ent <i>et al.</i> , 2001 Bean and Amann, 2009
<i>B. subtilis</i> (MreB-Bs)	5.5 – 8	5.5	Yes	Yes	Yes	Yes	0.9	No	Positive/ rod-shaped	Mayer and Amann, 2009
<i>C. pneumonia</i> (MreB-Cp)	5.5 – 7	6.5	Yes	N/A	Yes	Yes	N/A	No	Negative/ rod-shaped	Gaballah <i>et al.</i> , 2011
<i>E. coli</i> (MreB-Ec)	N/A	7	Yes	Yes	Yes	Yes	1.5	Yes	Negative/ coccobacilli	Nurse and Mariani, 2012
<i>C. crescentus</i> (MreB-Cc)	N/A	8	Yes	N/A	Yes	N/A	N/A	Yes	Negative/ curved rod	van den Ent <i>et al.</i> , 2014

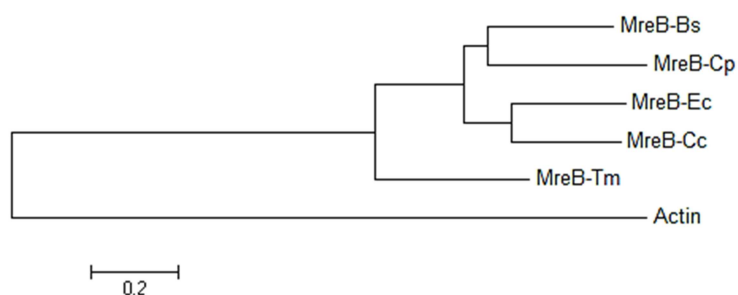


**Figure 4.15** Phylogenetic tree visualizing the relationship of MreB proteins from various bacteria to each other and yeast actin. The tree was produced from the protein sequence alignment by using MEGA6. Yeast actin (GI: 170986), MreB-Bs (GI: 760457758), MreB-Cp (GI: 15618759), MreB-Ec (GI: 751252054), MreB-Cc (GI: 221234549), MreB-Tm (GI: 15988309).

The effect of pH on nucleotide hydrolysis by MreB has never been studied before. This study found that the optimum pH of the nucleotides hydrolysis by MreB-Bs was different from the optimum pH of the previously reported polymerization of the protein (Mayer and Amann, 2009). The result suggests that the two processes may be independent, which supports the earlier report that the polymerization of MreB-Bs does not require nucleotide hydrolysis (Mayer and Amann, 2009).

MreB shares ~57% sequence identity among bacteria which, is less than its orthologue, actin. Actin is one of the most conserved proteins in eukaryotes, sharing ~90% sequence identity. The conformational changes of actin regard to ADP- and ATP-binding are innate properties of actin, which affect the polymerization process. The biochemical characters (Table 4.1) and the primary

structure analysis (Figure 4.15) classified MreB into two groups. The first group, which requires the nucleotides hydrolysis for the polymerization, comprises MreB-Tm, MreB-Ec, and MreB-Cc. The structural study (van den Ent *et al.*, 2014) has demonstrated that the conformational changes of MreB-Cc result from the nucleotides binding.

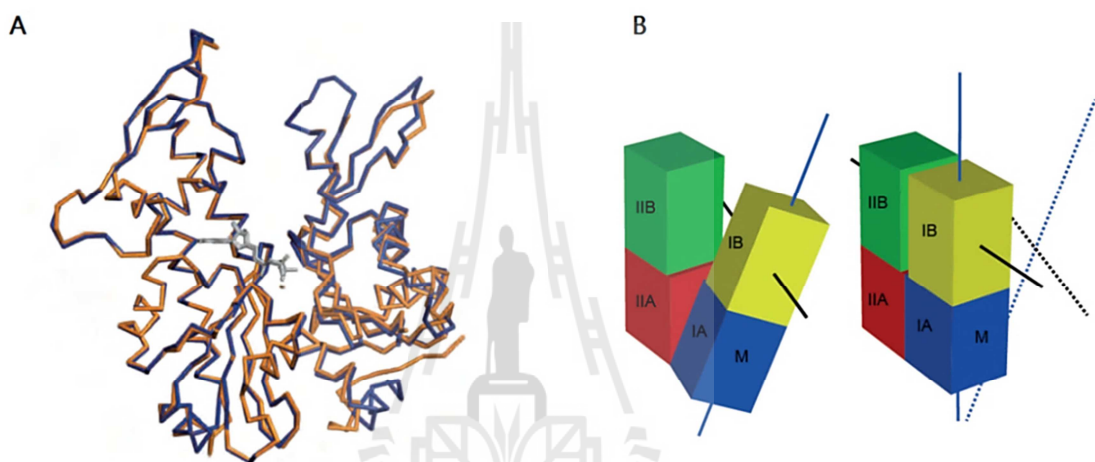


**Figure 4.16** Crystal structures of MreB in different nucleotide states reveal a propeller twist. (A) Superposition of ADP-MreB-Cc (orange) and AMPPNP-MreB-Cc (blue), a small movement of domain IB initiates the propeller twist observed upon polymerization. (B) Schematic drawing showing the propeller twists in MreB. The interdomain cleft narrows due to the movement of domain I towards domain II that is accompanied by a rotation of domain I resulting in flattening of the interfilament interface, M is indicated the membrane binding site (van den Ent, Izoré, Bharat *et al.*, 2014).

This study proposed that the structure of MreB-Cc is an innate property that regulates the polymerization process, similar to actin. The second group consisting of MreB-Bs and MreB-Cp does not require the nucleotides hydrolysis for the polymerization. Biochemical studies (Mayer and Amann, 2009) have shown that MreB-Bs has very low critical concentration for the polymerization (Table 4.1) and monovalent cation ( $K^+$ ) inhibits the polymerization (Bean and Amann, 2009; Mayer and Amann, 2009). Together, this information suggests that MreB-Bs adopts a unique structure that has high affinity for polymerization. This unique structure is not affected by nucleotide binding.

#### **4.3.2 Effect of pH on nucleotides hydrolysis by FtsZ-Bs**

##### **4.3.2.1 Effect of pH on ATP hydrolysis by FtsZ-Bs**

ATP hydrolysis by FtsZ-Bs was not detected, since there was no release of free phosphate from ATP. The data are shown in Appendix B.

##### **4.3.2.2 Effect of pH on GTP hydrolysis of FtsZ-Bs**

FtsZ-Bs hydrolyzed GTP over a wide pH range. The inorganic phosphate concentrations of 9.00, 13.71, 14.81, 11.15, 9.76, and 11.42  $\mu\text{M}$  were released from GTP in the experiment at pH 5.5, 6.0, 6.5, 7.0, 7.5, and 8.0, respectively (Figure 4.17).

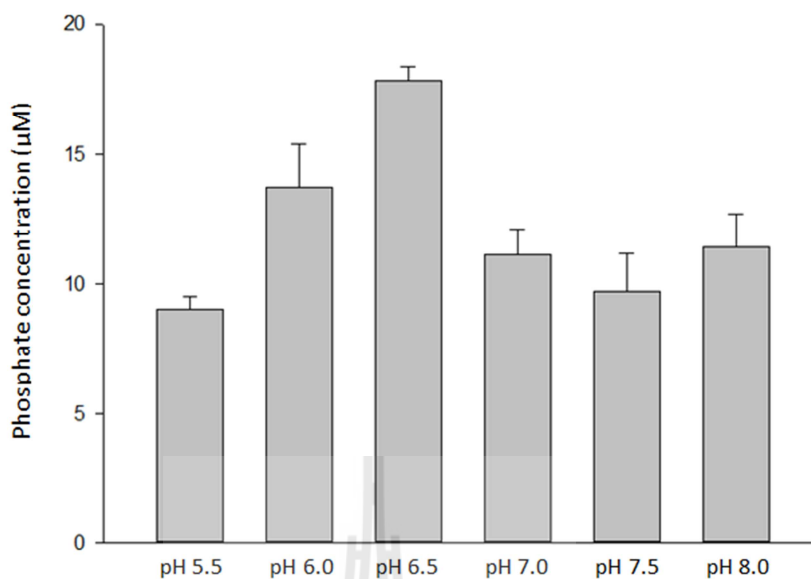


**Figure 4.17** pH effect on phosphate release from GTP by FtsZ-Bs.

FtsZ exhibits the GTP-dependent assembly, in which GTP is hydrolyzed to GDP by the active-site GTPase split across two monomers (Pacheco-Go´mez *et al.*, 2011). Our experiment found that ATP hydrolysis of FtsZ-Bs was not detectable, indicating that there was no release of free phosphate from ATP. The GTPase activity occurred over a wide pH range (5.5 – 8.0), but was highest at pH 6.5. The GTP hydrolysis character of FtsZ-Bs was similar to that reported earlier (Król and Scheffers, 2013).

## **4.4 Screening of natural products effects on nucleotides hydrolysis by the proteins**

The effects of natural products on nucleotides hydrolysis by the proteins were screened against apigenin, baicalein, luteolin,  $\alpha$ -mangostin, and naringenin. Lysozyme and BSA were used as negative controls that there are has no nucleotide hydrolysis activity. The reactions were performed under optimal pH and condition as described in the methods section 3.4.

### **4.4.1 Screening of natural products effect on ATP hydrolysis by MreB-Bs**

The effects of the natural products on ATP hydrolysis by MreB-Bs were screened by the malachite green assay in the presence and absence of the natural products (as described in section 3.4). Free phosphates at the final concentrations of 32.22, 31.51, 32.76, 30.57, 32.04, and 29.34  $\mu$ M, were released from ATP in the assay containing apigenin, baicalein, luteolin,  $\alpha$ -mangostin, and naringenin, respectively, compare to in the control reaction (Figure 4.18). Statistical analysis was used to analyze *p*-value (Appendix B). The results showed that the liberation of free phosphates from ATP in the presence of the natural products was not significantly different from that without the natural products shows no statistically significant (Appendix B). It indicated that the natural products have no effect on ATP hydrolysis by MreB-Bs under the conditions tested.

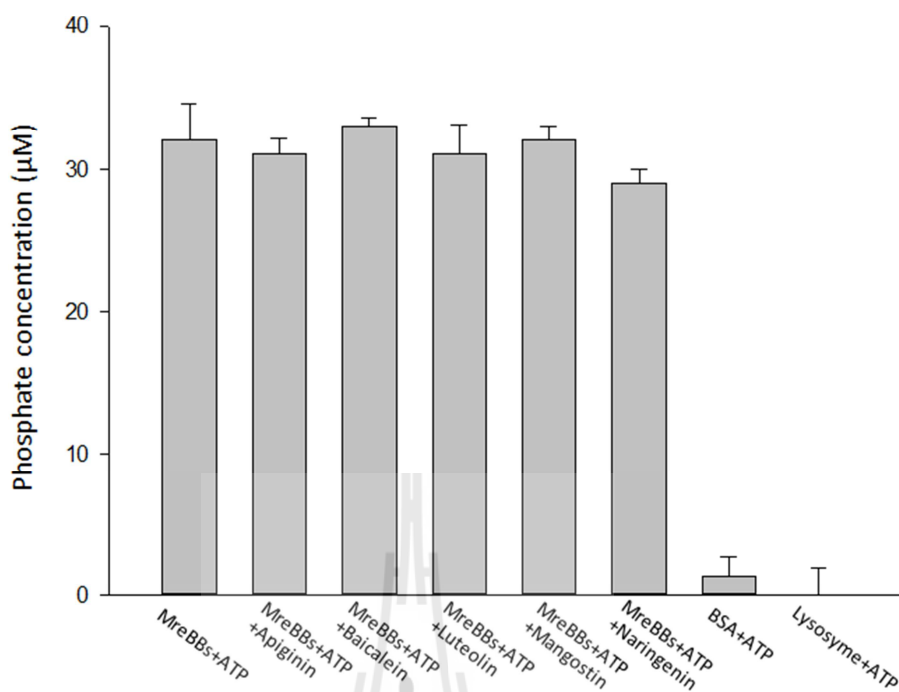


**Figure 4.18** Screening of natural products effect on ATP hydrolysis by MreB-Bs.

#### 4.4.2 Screening of natural products effects on GTP hydrolysis by MreB-Bs

The effects of the natural products on GTP hydrolysis by MreB-Bs were screened by the malachite green assay in the presence and absence of the natural products (as described in section 3.4). The final free phosphate concentrations were 38.37, 36.38, 35.51, 37.12, 35.74, and 38.93 µM, when phosphate was released from GTP in the reactions with apigenin, baicalein, luteolin,  $\alpha$ -mangostin, and naringenin, respectively compared to 38.37 µM (Figure 4.19). The results were showed that the liberation of free phosphates from the reaction in the presence of the natural products was not significantly different compare with the reaction without the natural products (Appendix B). This indicated that the natural products have no effect on GTP hydrolysis by MreB-Bs.

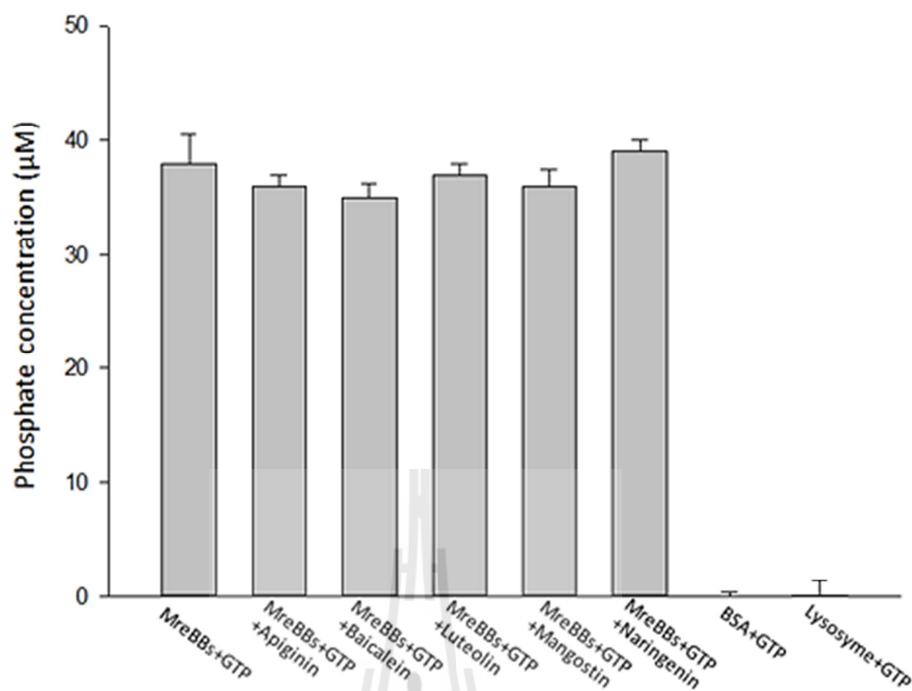


**Figure 4.19** Screening of natural products effect on GTP hydrolysis by MreB-Bs.

#### 4.4.3 Screening of natural products effect on GTP hydrolysis by FtsZ-Bs

The effects of the natural products on GTP hydrolysis by FtsZ-Bs were screened by the malachite green assay in the presence and absence of the natural products (as described in section 3.4). The free phosphate concentrations of 8.38, 7.22, 13.25, 12.78, and 12.72  $\mu\text{M}$  were obtained from release of phosphate from GTP in the reaction containing apigenin, baicalein, luteolin,  $\alpha$ -mangostin, and naringenin, respectively, (Figure 4.19) compared to 12.56  $\mu\text{M}$  in the reaction absence of the natural products. The *p*-value indicated that the amount of phosphate liberated from GTP by FtsZ-Bs in the presence of luteolin,  $\alpha$ -mangostin, and naringenin showed no statistically significant difference compared to the control without the natural products. It suggested that luteolin,  $\alpha$ -mangostin, and naringenin have no effect on

GTP hydrolysis property of FtsZ-Bs. On the other hand, apigenin and baicalein significant decreased the GTPase activity of FtsZ-Bs to 33.3% and 42.5%, respectively.

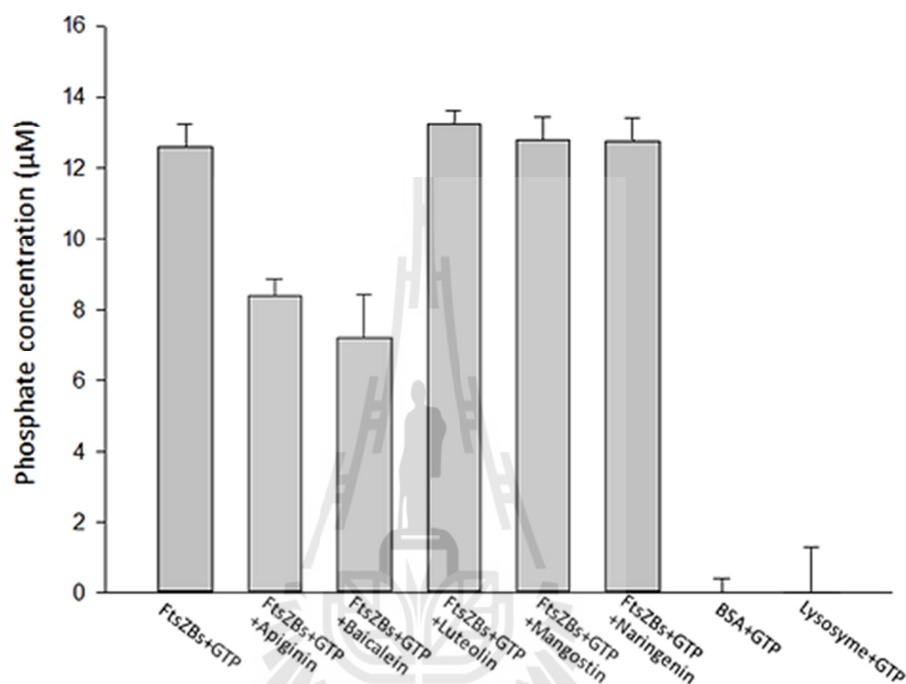


**Figure 4.20** Screening of natural products effect on GTP hydrolysis by FtsZ-Bs

GTP hydrolysis occurs during the polymerization by one FtsZ molecule providing the GTP-binding site to a second molecule, and then the T7 loop provides the catalytic residues to cleave GTP into GDP and  $P_i$ . The results from the malachite green released phosphate assay indicated FtsZ-Bs has interaction with apigenin and baicalein, but the site of interaction is unclear.

Possibly, the position may be anywhere on the protein that affects GTP binding or interferes with the polymerization mechanism, as proposed in Figure 4.21. This includes any possible allosteric sites on the molecule, such as the GTP binding

site at the N-terminal subdomain, T7 loop and H6-H7 loop on H7 helix, and binding site at the C-terminal subdomain.

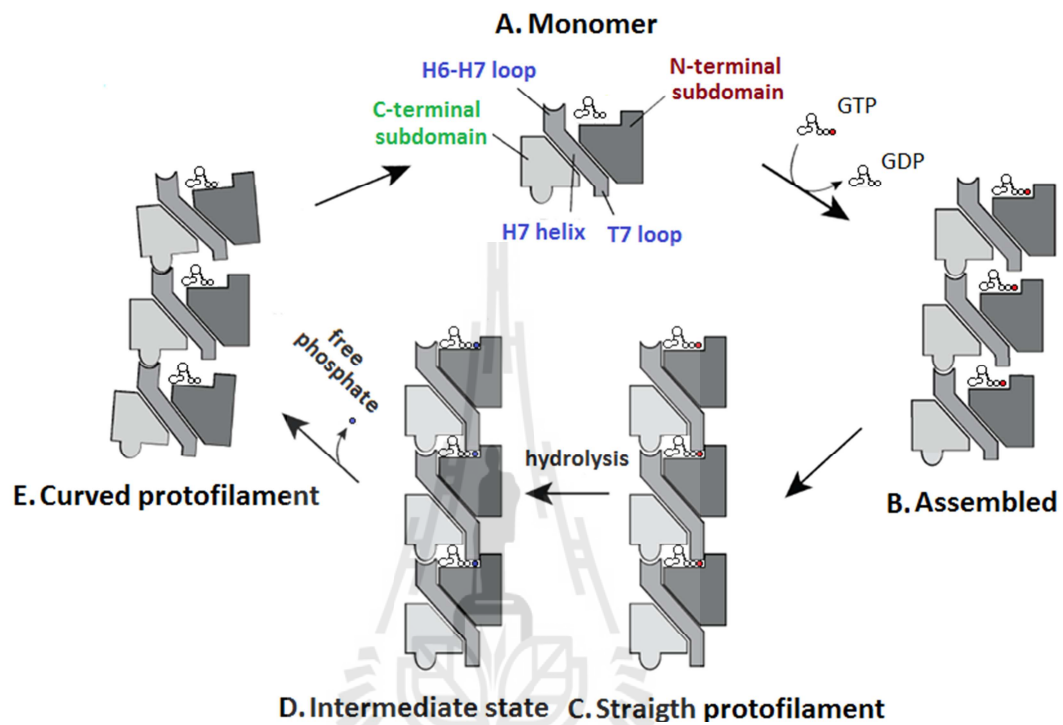


**Figure 4.21** Proposed mechanism of straight-to-curved conformational switch. FtsZ bound with GDP is a soluble monomer in the R (Relaxed) state (A). When FtsZ is bound to GTP, FtsZ is assembled (B). The intermolecular interactions between bound GTP and the T7 loop of the second molecule induce a structural change of the molecule from the R to the T (Tense) state to form the straight protofilament (C). In the straight protofilament, the catalytic residues in the upper subunit hydrolyze GTP to GDP and an intermediate state of FtsZ with GDP in the straight protofilament is formed (D). After releasing phosphate, the FtsZ molecule returns to the R state, and the straight protofilament changes to a curved protofilament. Finally, the curved protofilament is disassembled to monomeric FtsZ (E) (Matsui, Han *et al.*, 2013).

## CHAPTER V

### CONCLUSION AND FUTURE PERSPECTIVE

DNA encoding *mreB* and *ftsZ* of *B. subtilis* were cloned into the pSY5 plasmids and expressed in *E. coli* BL21(DE3). The proteins were purified by Ni<sup>2+</sup>-NTA with stepwise elution. Batch production of the proteins yielded approximately 1 mg of MreB-Bs, and approximately 2 mg of the FtsZ-Bs from 1 L of *E. coli* BL21(DE3) culture.

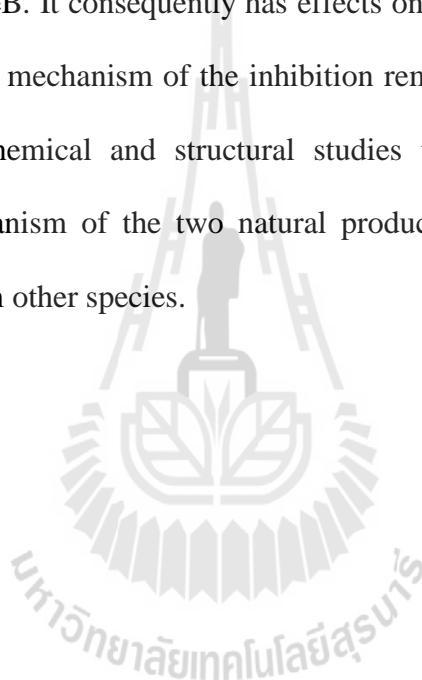
MreB-Bs was able to hydrolyze both ATP and GTP over a broad pH range (5.5 – 8.0). The optimum pH values for ATP and GTP hydrolysis were at pH 7.0 and pH 6.5, respectively. The results demonstrated that MreB-Bs has the optimum pH for nucleotide hydrolysis that is different from the reported optimum pH for protein polymerization (Mayer and Amann, 2009). Apigenin, baicalein, luteolin,  $\alpha$ -mangostin, and naringenin showed no effect on both ATP and GTP hydrolysis of MreB-Bs.

FtsZ-Bs was unable to hydrolyze ATP, but hydrolyzed GTP over a broad pH range (5.5 – 8.0), with the optimum pH at 6.5. This work found that apigenin and baicalein inhibited GTP hydrolysis by FtsZ-Bs. Apigenin decrease GTPase activity of FtsZ-Bs to 33.3% while baicalein decreased the GTPase activity of FtsZ-Bs by 42.5%.

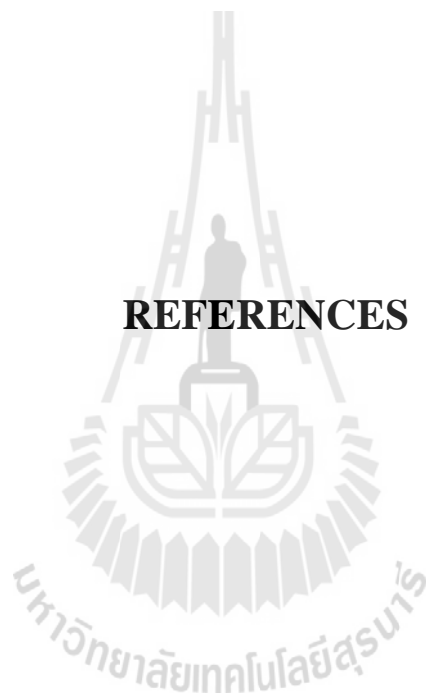
Together, the results suggest that MreB-Bs adopts a unique structure that is not different between the nucleotide-free and the nucleotides-bound states bound to (GTP,

GDP, ATP, or ADP), suggesting an optimum structure for the polymerization of MreB. However, the structures of MreB-Bs alone and with nucleotides are not yet determined. Thus, structural investigation of MreB-Bs is needed.

Evidently, FtsZ is one molecular targets of apigenin and baicalein. We speculated that the interactions between apigenin and baicalein and FtsZ may interfere with the polymerization of the protein (Z-ring formation) and/or disrupt interaction between FtsZ and MreB. It consequently has effects on cell wall synthesis during cell division. However the mechanism of the inhibition remains unclear. We now plan to perform further biochemical and structural studies to verify and investigate the interaction and mechanism of the two natural products on the GTPase activity of FtsZ-Bs and FtsZ from other species.



## REFERENCES



## REFERENCES

- Aarsman, E., Piette, A., Fraipont, C., Vinkenvleugel, M., Nguyen-Distèche, M., and Blaauwen, T. (2005). Maturation of the *Escherichia coli* divisome occurs in two steps. **Molecular Microbiology**. 55(6): 1631 – 1645.
- Amos, A., and Schlieper, D. (2005). Microtubules and maps. **Advances in Protein Chemistry**. 71: 257 – 298.
- Amos, A. (2004). Bending at microtubule interfaces. **Chemistry & Biology**. 11(6): 745 – 747.
- Andrade, C., Carvalho, J., Cunico, M., Lordello, A., Higaskino, C., Almeida, S., Dias, J., Kerber, V., Miguel, M., and Miguel, O. (2010). Antioxidant and antibacterial activity of extracts, fractions and isolated substances from the flowers of *Acacia podalyriifolia* A. Cunn. ex G. Don. **Brazilian Journal of Pharmaceutical Science**. 46: 715 – 721.
- Attin, T., Becker, K., Hannig, C., Buchalla, W., and Wiegand, A. (2005). Suitability of a malachite green procedure to detect minimal amounts of phosphate dissolved in acidic solutions. **Clinical Oral Investigations**. 9(3): 203 – 207.
- Ausmees, N., and Wagner, C. (2003). Spatial and temporal control of differentiation and cell cycle progression in *Caulobacter crescentus*. **Annual Reviews in Microbiology**. 57(1): 225 – 247.

- Bagli, E., Stefaniotou, M., Morbidelli, L., Ziche, M., Psillas, K., Murphy, C., and Fotsis, T. (2004). Luteolin inhibits vascular endothelial growth factor-induced angiogenesis; inhibition of endothelial cell survival and proliferation by targeting phosphatidylinositol 3'-kinase activity. **Cancer Research**. 64(214): 7936 – 7946.
- Bean, G., Flickinger, S., Westler, W., McCully, M., Sept, D., Weibel, D., and Amann, K. (2009). A22 disrupts the bacterial actin cytoskeleton by directly binding and inducing a low-affinity state in MreB. **Biochemistry**. 48(22): 4852 – 4857.
- Bean, G., and Amann, J. (2008). Polymerization properties of the *Thermotoga maritima* actin MreB: roles of temperature, nucleotides, and ions. **Biochemistry**. 47(2): 826 – 835.
- Blanchoin, L., and Pollard, T. D. (2002). Hydrolysis of ATP by polymerized actin depends on the bound divalent cation but not profilin. **Biochemistry**. 41(2): 597 – 602.
- Bodet, C., La, D., Epifano, F., and Grenier, D. (2008). Naringenin has anti-inflammatory properties in macrophage and ex vivo human whole-blood models. **Journal of Periodontal Research**. 43(4): 400 – 407.
- Bork, P., Sander, C., and Valencia, A. (1992). An ATPase domain common to prokaryotic cell cycle proteins, sugar kinases, actin, and Hsp70 heat shock proteins. **Proceedings of the National Academy of Sciences of the United States of America**. 89(16): 7290 – 7294.
- Briegel, A., Dias, D., Li, Z., Jensen, R., Frangakis, A., and Jensen, G. (2006). Multiple large filament bundles observed in *Caulobacter crescentus* by electron cryotomography. **Molecular Microbiology**. 62(1): 5 – 14.

- Cabeen, M., Charbon, G., Vollmer, W., Born, P., Ausmees, N., Weibel, D., and Jacobs-Wagner, C. (2009). Bacterial cell curvature through mechanical control of cell growth. **The European Molecular Biology Organization Journal**. 28(9): 1208 – 1219.
- Caltagirone, S., Rossi, C., Poggi A., Ranelletti, FO., Natali, PG., Brunetti, M., Aiello, FB., and Piantelli, M. (2000). Flavonoids apigenin and quercetin inhibit melanoma growth and metastatic potential. **International Journal of Cancer**. 87: 595 – 600.
- Capaldo-Kimball, F., and Barbour, S. (1971). Involvement of Recombination Genes in Growth and Viability of *Escherichia coli* K-12. **Journal of Bacteriology**. 106(1): 204 – 212.
- Carballido-López, R. (2006a). The bacterial actin-like cytoskeleton. **Microbiology and Molecular Biology Reviews**. 70(4): 888 – 909.
- Carballido-López, R. (2006b). Orchestrating bacterial cell morphogenesis. **Molecular Microbiology**. 60(4): 815 – 819.
- Carballido-López, R., and Errington, J. (2003). A dynamic bacterial cytoskeleton. **Trends in Cell Biology**. 13(11): 577 – 583.
- Carter, G., and Karl, W. (1982). Inorganic phosphate assay with malachite green: an improvement and evaluation. **Journal of Biochemical and Biophysical Methods**. 7(1): 7 – 13.
- Cha, S., Kim, G., and Cha, J. (2016). Synergistic antimicrobial activity of apigenin against oral pathogens. **International Journal of Engineering Research & Science**. 2(1): 27 – 37.

- Chang, P., Li, H., Tang, H., Liu, J., Wang, J., and Chuang, Y. (2007). In vitro synergy of baicalein and gentamicin against vancomycin-resistant *Enterococcus*. **Journal of Microbiology, Immunology and Infection**. 40(1): 56 – 61.
- Charbon, G., Cabeen, M., and Jacobs-Wagner, C. (2009). Bacterial intermediate filaments: *in vivo* assembly, organization, and dynamics of crescentin. **Genes & Development**. 23(9): 1131 – 1144.
- Coleman, D., Bigelow, R., and Cardelli, J. (2009). Inhibition of fatty acid synthase by luteolin post-transcriptionally downregulates c-met expression independent of proteosomal/lysosomal degradation. **Molecular Cancer Therapeutics**. 8(1): 214 – 224.
- Cooper, G. (2000). The Cell: A Molecular Approach 2nd edition. **American Society Microbiology**. Washington and Sinauer association, Sunderland, MA.
- Coulombe, P. A., Ma, L., Yamada, S., and Wawersik, M. (2001). Intermediate filaments at a glance. **Journal of Cell Science**. 114(24): 4345 – 4347.
- Cowles, K. N., and Gitai, Z. (2010). Surface association and the MreB cytoskeleton regulate pilus production, localization and function in *Pseudomonas aeruginosa*. **Molecular Microbiology**. 76(6): 1411 – 1426.
- D'Angelo, E., Crutchfield, J., and Vandiviere, M. (2001). Rapid, sensitive, microscale determination of phosphate in water and soil. **Journal of Environmental Quality**. 30(6): 2206 – 2209.
- Desai, A., and Mitchison, J. (1997). Microtubule polymerization dynamics. **Annual Review of Cell and Developmental Biology**. 13(1): 83 – 117.

- Doi, M., Wachi, M., Ishino, F., Tomioka, S., Ito, M., Sakagami, Y., and Matsuhashi, M. (1988). Determinations of the DNA sequence of the *mreB* gene and of the gene products of the *mre* region that function in formation of the rod shape of *Escherichia coli* cells. **Journal of Bacteriology**. 170(10): 4619 – 4624.
- Erickson, P., Anderson, E., and Osawa, M. (2010). FtsZ in bacterial cytokinesis: cytoskeleton and force generator all in one. **Microbiology and Molecular Biology Reviews**. 74(4): 504 – 528.
- Erickson, P., and Osawa, M. (2010). Cell division without FtsZ a variety of redundant mechanisms. **Molecular Microbiology**. 78(2): 267 – 270.
- Eriksson, P., Dechat, T., Grin, B., Helfand, B., Mendez, M., Pallari, H., and Goldman, D. (2009). Introducing intermediate filaments: from discovery to disease. **The Journal of Clinical Investigation**. 119(7): 1763 – 1771.
- Esue, O., Cordero, M., Wirtz, D., and Tseng, Y. (2005). The assembly of MreB, a prokaryotic homolog of actin. **Journal of Biological Chemistry**. 280: 2628 – 2635.
- Eumkeb, G., and Chukrathok, S. (2013). Synergistic activity and mechanism of action of ceftazidime and apigenin combination against ceftazidime-resistant *Enterobacter cloacae*. **Phytomedicine**. 20: 262 – 269.
- Evans, A., Miller, J., and Paganga, G. (1996). Structure-antioxidant activity relationships of flavonoids and phenolic acids. **Free Radical Biology and Medicine**. 20(7): 933 – 956.
- Fang, J., Zhou, Q., Shi, L., and Jiang, H. (2007). Luteolin inhibits insulin-like growth factor 1 receptor signaling in prostate cancer cells. **Carcinogenesis**. 28(3): 713 – 723.

- Fenton, K., and Gerdes, K. (2013). Direct interaction of FtsZ and MreB is required for septum synthesis and cell division in *Escherichia coli*. **The European Molecular Biology Organization Journal**. 32(13): 1953 – 1965.
- Foster, S. (2004). The secret garden: important Chinese herbs in American horticulture: a photo essay. **American Botanical Council**. 64: 44 – 51.
- Gaballah, A., Kloeckner, A., Otten, C., Sahl, G., and Henrichfreise, B. (2011). Functional analysis of the cytoskeleton protein MreB from *Chlamydomonas reinhardtii*. **PLoS One**. 6(10): e25129.
- Geladopoulos, T. P., Sotiroudis, T. G., and Evangelopoulos, A. E. (1991). A malachite green colorimetric assay for protein phosphatase activity. **Analytical Biochemistry**. 192(1): 112 – 116.
- Gitai, Z. (2005). The new bacterial cell biology: moving parts and subcellular architecture. **Cell**. 120(5): 577 – 586.
- Grodberg, J., and Dunn, J. (1988). *ompT* encodes the *Escherichia coli* outer membrane protease that cleaves T7 RNA polymerase during purification. **Journal of Bacteriology**. 170(3): 1245 – 1253.
- Herrmann, H., and Aebi, U. (2004). Intermediate filaments: molecular structure, assembly mechanism, and integration into functionally distinct intracellular scaffolds. **Annual Review of Biochemistry**. 73(1): 749 – 789.
- Hoglund, S., Karlsson, R., Arro, E., Fredriksson, A., and Lindberg, U. (1980). Visualization of the peripheral weave of microfilaments in glia cells. **Journal of Muscle Research and Cell Motility**. 1(2): 127 – 146.

- Horinaka, M., Yoshida, T., Shiraishi, T., Nakata, S., Wakada, M., Nakanishi, R., Nishino, H., Matsui, H., and Sakai, T. (2005). Luteolin induces apoptosis via death receptor 5 upregulation in human malignant tumor cells. **Oncogene Journal**. 24(48): 7180 – 7189.
- Hsieh, J., Hall, K., Ha, T., Li, C., Krishnaswamy, G., and Chi, S. (2007). Baicalein inhibits IL-1 $\beta$ - and TNF- $\alpha$ -induced inflammatory cytokine production from human mast cells via regulation of the NF- $\kappa$ B pathway. **Clinical and Molecular Allergy**. 5(1).
- Hyman, A., Salser, S., Drechsel, D., Unwin, N., and Mitchison, T. (1992). Role of GTP hydrolysis in microtubule dynamics: information from a slowly hydrolyzable analogue, GMPCPP. **Molecular Biology of the Cell**. 3(10): 1155 – 1167.
- Jiang, H., and Sun, S. X. (2010). Morphology, growth, and size limit of bacterial cells. **Physical Review Letters**. 105(2): 028101.
- Jordan, A., and Wilson, L. (2004). Microtubules as a target for anticancer drugs. **Nature Reviews Cancer**. 4(4): 253 – 265.
- Kim, S., and Coulombe, P. (2007). Intermediate filament scaffolds fulfill mechanical, organizational, and signaling functions in the cytoplasm. **Genes & Development**. 21(13): 1581 – 1597.
- Koh, J., Qiu, S., Zou, H., Lakshminarayanan, R., Li, J., Zhou, X., Tang, C., Saraswathi, P., Chandra Verma, C., Donald, H., Tan, L., Liu, S., and Beuerman, R. (2013). Rapid bactericidal action of alpha-mangostin against MRSA as an outcome of membrane targeting. **Biochimica et Biophysica Acta**. 1828(2): 834 – 844.

- Króll, E., and Scheffers, D. J. (2014). FtsZ Polymerization Assays: Simple Protocols and Considerations. **Journal of Visualized Experiments**. 81: e50844
- Lan, G., Daniels, R., Dobrowsky, M., Wirtz, D., and Sun, X. (2009). Condensation of FtsZ filaments can drive bacterial cell division. **Proceedings of the National Academy of Sciences of the United States of America**. 106(1): 121 – 126.
- Langley, K., Villarejo, M., Fowler, A., Zamenhof, P., and Zabin I. (1975). Molecular basis of beta-galactosidase alpha-complementation. **Proceedings of the National Academy of Sciences of the United States of America**. 72(4): 1254 – 1257.
- Lee, Y., Jung, E., and Cha, J. (2015). Synergistic effect between baicalein and antibiotics against clinic methicillin and vancomycin-resistant *Staphylococcus aureus*. **Chemotherapy: Open Access**. 4(1).
- Lee, M., Yoon, S., and Moon, J. (2004). The flavonoid naringenin inhibits dimethylnitrosamine – induced liver damage in rats. **Biological and Pharmaceutical Bulletin**. 27(1): 72 – 76.
- López-Lázaro. (2009). Distribution and biological activities of the flavonoid luteolin. **Mini Reviews in Medicinal Chemistry**. 9(1): 31 – 59.
- Löwe, J., van den Ent, F., and Amos, L. A. (2004). Molecules of the bacterial cytoskeleton. **Annual Review of Biophysics and Biomolecular Structure**. 33: 177 – 198.
- Maehama, T., Taylor, G., Slama, J., and Dixon, J. (2000). A sensitive assay for phosphoinositide phosphatases. **Analytical Biochemistry**. 279(2): 248 – 250.
- Mandelkow, E., and Mandelkow, E. (1990). Microtubular structure and tubulin polymerization. **Current Opinion in Cell Biology**. 2(1): 3 – 9.

- Margolin, W. (2004). Bacterial shape: concave coiled coils curve *Caulobacter*. **Current Biology**. 14(6): 242 – 244.
- Matsui, T, Han, X., Yu, J., Yao, M., and Tanaka, I. (2013). Structural change in FtsZ induced by intermolecular interactions between bound GTP and the T7 loop. **Journal of Biological Chemistry**. 289(6): 3501 – 3509.
- Mayer, J., and Amann, K. (2009). Assembly properties of the *Bacillus subtilis* actin, MreB. **Cell Motility and the Cytoskeleton**. 66(2): 109 – 118.
- Michie, K., and Löwe, J. (2006). Dynamic filaments of the bacterial cytoskeleton. **Annual Review of Biochemistry**. 75: 467 – 492.
- Moriyama, K., and Yahara, I. (2002). Human CAP1 is a key factor in the recycling of cofilin and actin for rapid actin turnover. **Journal of Cell Science**. 115(8): 1591 – 1601.
- Nahmias, Y., Goldwasser, J., Casali, M., Poll, V., Wakita, T., Chung, R. T., and Yarmush, L. (2008). Apolipoprotein  $\beta$ -dependent hepatitis C virus secretion is inhibited by the grapefruit flavonoid naringenin. **Hepatology**. 47(5): 1437 – 1445.
- Ng'uni, T., Mothlalamme, T., Daniels, R., Klaasen, J., and Fielding, B. (2015). Additive antibacterial activity of naringenin and antibiotic combinations against multidrug resistant *Staphylococcus aureus*. **African Journal of Microbiology Research**. 9(23): 1513 – 1518.
- Nogales, E., Whittaker, M., Milligan, R. A., and Downing, K. H. (1999). High-resolution model of the microtubule. **Cell**. 96(1): 79 – 88.
- Nürnberg, A., Kitzing, T., and Grosse, R. (2011). Nucleating actin for invasion. **Nature Reviews Cancer**. 11(3): 177 – 187.

- Nurse, P., and Mariani, K. J. (2012). Purification and Characterization of *Escherichia coli* MreB. **The Journal of Biological Chemistry**. 288: 3469 – 3475.
- Oda, T., Iwasa, M., Aihara, T., Maéda, Y., and Narita, A. (2009). The nature of the globular- to fibrous-actin transition. **Nature**. 457(7228): 441 – 445.
- Okagaki, H., Strain, K., Nielsen, N., Charlier, C., Baltes, J., Chrétien, F., Heitman, J., Dromer, F., and Nielsen, K. (2010). Cryptococcal cell morphology affects host cell interactions and pathogenicity. **PLoS Pathogens**. 6(6): e1000953
- Omary, M., Ku, N., Tao, G., Toivola, D., and Liao, J. (2006). Heads and tails' of intermediate filament phosphorylation: multiple sites and functional insights. **TRENDS in Biochemical Sciences**. 31(7): 383 – 394.
- Osborn, M., and Weber, K. (1983). Tumor diagnosis by intermediate filament typing: a novel tool for surgical pathology. **Journal of Technical Methods and Pathology**. 48(4): 372 – 394.
- Ottaviani, F., Pregolato, M., Cangiotti, M., Fiorani, L., Fattori, A., and Danani, A. (2012). Spin probe analysis of microtubules structure and formation. **Archives of Biochemistry and Biophysics**. 522(1): 1 – 8.
- Otterbein, R., Graceffa, P., and Dominguez, R. (2001). The crystal structure of uncomplexed actin in the ADP state. **Science**. 293(5530): 708 – 711.
- Pacheco-Gómez, R., Roper, D., Dafforn, T., and Rodger A. (2011). The pH dependence of polymerization and bundling by the essential bacterial cytoskeletal protein FtsZ. **PLoS One**. 6(6): e19369.
- Pantaloni, D., Hill, T. L., Carlier, M.-F., and Korn, E. D. (1985). A model for actin polymerization and the kinetic effects of ATP hydrolysis. **Proceedings of the**

**National Academy of Sciences of the United States of America.** 82(21): 7207 – 7211.

Pollard, T. D., Blanchoin, L., and Mullins, R. D. (2000). Molecular mechanisms controlling actin filament dynamics in nonmuscle cells. **Annual Review of Biophysics and Biomolecular Structure.** 29(1): 545 – 576.

Quan, X., Wang, Y., Ma, X., Liang, Y., Tian, W., Ma, Q., Jiang, H., and Zhao, Y. (2012).  $\alpha$ -Mangostin induces apoptosis and suppresses differentiation of 3T3-L1 cells via inhibiting fatty acid synthase. **PLoS One.** 7(3): e33375.

Renugadevi, J., and Prabu, M. (2009). Naringenin protects against cadmium-induced oxidative renal dysfunction in rats. **Toxicology.** 256(4): 128 – 134.

Sakagami, Y., Iinuma, M., Piyasena, G., and Dharmaratne, R. (2005). Antibacterial activity of alpha-mangostin against vancomycin resistant Enterococci (VRE) and synergism with antibiotics. **Phytomedicine.** 12(3): 203 – 208.

Saponara, S., Testai, L., Lozzi, D., Martinotti, E., Martelli, A., Chericoni, S., Sgaragli, G., Fusa, F., and Calderone, V. (2006). (+/-) Naringenin as large conductance  $\text{Ca}^{2+}$  activated  $\text{K}^+$  ( $\text{BK}_{\text{ca}}$ ) channel opener in vascular smooth muscle cells. **British Journal of Clinical Pharmacology.** 149(8): 1013 – 1021.

Schüler, H. (2001). ATPase activity and conformational changes in the regulation of actin. **Biochimica et Biophysica Acta (BBA)-Protein Structure and Molecular Enzymology.** 1549(2): 137 – 147.

Shih, L., and Rothfield, L. (2006). The bacterial cytoskeleton. **Microbiology and Molecular Biology Reviews.** 70(3): 729 – 754.

- Siriwong, S., Pimchan, T., Naknarong, W., and Eumkeb, G. (2015) Mode of action and synergy of ceftazidime and baicalein against *Streptococcus pyogenes*. **Tropical Journal of Pharmaceutical Research**. 14(4): 641 – 648.
- Studier, A., and Moffatt, A. (1986). Use of bacteriophage T7 RNA polymerase to direct selective high-level expression of cloned genes. **Journal of Molecular Biology**. 189(1): 113 – 130.
- Taylor, G., Walker, C., and McInnes, R. (1993). *E. coli* host strains significantly affect the quality of small scale plasmid DNA preparations used for sequencing. **Nucleic Acids Research**. 21(7): 1677 – 1678.
- Typas, A., Banzhaf, M., Gross, C. A., and Vollmer, W. (2011). From the regulation of peptidoglycan synthesis to bacterial growth and morphology. **Nature Reviews in Microbiology**. 10(2): 123 – 136.
- van den Ent, F., Izoré, T., Bharat, T., Johnson, C., and Löwe J. (2014). Bacterial actin MreB forms antiparallel double filaments. **eLife**. 3: e02634.
- van den Ent, F., Johnson, M., Persons, L., de Boer, P., and Löwe, J. (2010). Bacterial actin MreB assembles in complex with cell shape protein Rod Z. **The European Molecular Biology Organization Journal**. 29(6): 1081 – 1090.
- van den Ent, F., Amos, L. A., and Löwe, J. (2001). Prokaryotic origin of the actin cytoskeleton. **Nature**. 413(6851): 39 – 44.
- Varma, A., and Yong, K. (2009). In *Escherichia coli*, MreB and FtsZ direct the synthesis of lateral cell wall via independent pathways that require PBP 2. **Journal of Bacteriology**. 191(11): 3526 – 3533.

- Wang, W., Heideman, L., Chung, C., Pelling, J., Koehler, K., and Birt, D. (2000). Cell-cycle arrest at G2/M and growth inhibition by apigenin in human colon carcinoma cell lines. **Molecular Carcinogenesis**. 28: 102 – 110.
- Yamachika, S., Sugihara, C., Tsuji, H., Muramatsu, Y., Kamai, Y., and Yamashita, M. (2012). Anti-*Pseudomonas aeruginosa* compound, 1, 2, 3, 4-tetrahydro-1, 3, 5-triazine derivative, exerts its action by primarily targeting MreB. **Biological and Pharmaceutical Bulletin**. 35(10): 1740 – 1744.
- Yang, D., Blair, K., and Salama, N. (2016). Staying in shape: the impact of cell shape on bacterial survival in diverse environments. **Microbiology and Molecular Biology Reviews**. 80(1): 187 – 203.
- Zheng, H., Yin, H., Grahn, H., Ye, F., Zhao, R., and Zhang, Y. (2014). Anticancer effects of baicalein on hepatocellular carcinoma cells. **Phytotherapy Research**. 28(9): 1342 – 1348.

# APPENDICES



# APPENDIX A

## SEQUENCE

### Gene sequence of *mreB-Bs*

NCBI Reference Sequence: NC\_000964.3

atgtttggaattggtgctagagaccttggtatagatcttgaactgcgaatacgttgttttgtaaaggaaaaggaattgtgt  
gagagagccgtcagttgtcgtttgcagacggatacgaatcgttgcgtgcggaaatgatgcgaaaaatatgattgga  
cggacaccgggcaactggtggctcttcgcccgatgaaagacggcgttatcgtgattatgaaacaacggcgacgatgat  
gaaatattacatcaatcaggccataaaaaataaaggcatgtttgccagaaaaccatatgtaatggtatgtgtcccatcaggca  
ttacagctgttgaagaacgcgctgttatcgtatgcgacaagacaggcgggagcgcgtgacgcgtatccgattgaagagcctt  
ttgccgcagcaatcggagccaatctgccagtttgggaaccgactggaagcatggtgttgatcggggcggtacgaca  
gaagtgcgattatttccctcggagcatcgtaacgtctcagtcacccgtgtagccggtgatgagatggatgacgcgattat  
caactacatcagaaaaacgtacaatctgatgatcggtgaccgtacggctgaagcgattaaaatggaaatcggatctgcaga  
agctcctgaagaatccgacaacatggaaatccgcggccgcgatttctcacaggttggcgaaaacaattgaaattacagg  
aaaagagatttctaacgctctacgcgacactgtatctacaattgtcgaagcagtgaagagcacactcgaaaaaacaccgctt  
gagcttgagcagatatcatggacagaggtatagtgttaaccggcggcggagcgttttgcgcaatttggacaaagtcac  
agcgaagaacaataatgccggtccttatgccgaagatccgcttgattgtgtagcgtatcggaaacagggaagcactgga  
gcacatccatctttcaagggaactagataa

### Protein sequence of MreB-Bs

mfgigardlgidltantlvfvkkgkivvrepvvalqtdtkisivavgndaknmigrtpgnvvalrpmkdgviadyett  
 atmmkyyinqaiknkgmfarkpyvmvcvpsgitaveeravidatrqagardaypieepfaaaiganlpvweptgs  
 mvvdigggttevaiislggivtsqirvagdemddaiinyirktylnmigdrtaeaikmeigsaeapeesdnmeirgrd  
 lltglpktieitgkeisnalrdtvstiveavkstlektppelaadimdrgivltgggallrnldkvisetkmpvliaedpldc  
 vaigtgkalehihlfkgr

### Gene sequence of *ftsZ*-Bs

NCBI Reference Sequence: NC\_000964.3

atgttgagttcgaacaacatagacggcttagcatcaattaaagtaatcggagtaggagggcggcggtaacaacgccgtt  
 aaccgaatgattgaaaatgaagtgcaaggagtagagtatatcgcggtaaacacggacgctcaagctttaacctgtcaaaa  
 gcagaagtgaaaatgcaaatcggcgcaaagctgactagaggattgggagcaggtgcgaatccggaagtcgggaaaaaa  
 gccgctgaagaaagcaaagagcagattgaagaagcacttaaggtgctgacatggtattcgtgacagctggtatggcgcg  
 cggaacaggaacaggtgccgcaccggttcgcacaaatcgcgaaagacttaggcgattaacagtcggcggttgacaa  
 gaccgtttacctcgaaggacgcaaaagacagcttcaggctgcagggcgaatctcggcaatgaaagaagcggtgatac  
 actgatcgtgatcccgaacgaccgtatccttgaattgtgataaaacacaccgatgcttgaagcattccgcgaagcggat  
 aacgtacttcgccaaggggtcaaggtatttctgacttgattgctacacctggtcttatcaacctgactttgctgatgtgaaaac  
 aatcatgtcaaaacaaaggatctgcttgatgggtatcggattgctactgggaaaatcgcgcggcagaggcagcaaaaaa  
 agcaattccagcccgttcttgaagcggccattgacgggtgcgcaaggcgtcctcatgaacatcactggaggaacaaacct  
 cagcctatatgaggttcaggaagcagcagacattgtcgttcggcgtctgatcaagacgtaaacatgatttcgggtctgttatt  
 aatgaaaatctaaaagatgagattgtggtgacagtgattgcaaccggttatcgaacaagagaaggacgtgacgaagcct  
 cagcgtccaagcttaaatcaagcatcaaaacacacaatcaaagtgtccgaagcgtgagccaaaacgtgaggaacctca  
 gcagcagaacacagtaagccgtcacttcacagccggctgatgatacgttgacatcccacattcttaagaaaccgtaat  
 aaacgcggctaa

## Protein sequence of FtsZ-Bs

mlefetnidglasikvigvggggnnavnrmienevqgveyiavntdaqalnlskaevkmqigakltrlgaganpev  
 gkkaeeskeqieealkgadmfvtagmgggtgtgaapviaqiakdlgaltvgvtrpftfeqrqlqaaggisamk  
 eavdtlivpndrileivdkntpmleafreadnvlrqvqgisdiatpmlinldfadvktimsnkgsalmgigiatgenr  
 aaeaakkaissplleaaidgaqgvlmnitggtlnslyevqeaadivasasdqdvnmifgsvinenlkdeivvtviatgfi  
 eqekdvtkpqrpslnqsikthnqsvpkreepqqntvsrhtsqpaddtldiptflrnkrkg

## Sequencing result

>140804-07\_D19\_MreB-Bs\_T7promoter.ab1 1613

gtgggacgatacaattccctctagaataatgttgaactttaagaaggagatataccatggcagaagaacaccaccacca  
 ccaccaccaccacctggaagtctgtccagggccccggcggccgatgttggaattggtgctagagaccttggtataga  
 tcttggaactgcgaatacgttgtttgtaaaaggaaaaggaaattgttgagagagccgtcagttgtcgtttgcagacgga  
 tacgaaatcaattgctgctgctggaaatgatgcgaaaaatagattggacggacaccggcaacgtggtggctctgcgcc  
 gatgaaagacggcgttatcgtgattatgaaacaacggcgcacgatgatgaaatattacatcaatcaggccataaaaaataaa  
 ggtatgtttgccagaaaaccatagtaatgtatgtgccatcaggcattacagctgttgaagaacgcgctgttatcgtgacg  
 acaagacagcgggagcgcgtgacgcgtatccgattgaagagcctttgccgcagcaatcggggccaatctgccagttg  
 ggaaccgactggaagcatggtgttgatcggggcggtagcagagaagttgcgattattccctcggaggcatcgtaac  
 gtctcagtcaatccgtgtagccggtgatgagatggatgacgcgattatcaactacatcagaaaaacgtacaatctgatgatc  
 ggtgaccgtacggctgaagcgattaaaatggaaatcggatctgcagaagctcctgaagaatccgacaacatgaaatccg  
 cggacgcgatttgctgacaggtctgccgaaaacaattgaaattacaggaaaagagatttctaagtcttacgcgacactgtat  
 ctacaattgtcgaagcagtgaaagcacaactcgaaaaaacaccgctgagcttgacagagatcatggacagaggtata  
 gtgtaaccggcggcggagcgttttgcaatttgacaaagtcacagcgaagaacaaaaatgccggtccttatcgcc  
 gaagatccgcttgattgtgtagcgtatcggaaacagggaaagcactggaacacatccatctttcaagggaaaactagatag  
 aattcacgtgttacctaacttaagcccgtgaacaataactagcataacccttggggcctctaacggggccttgaggggt

ttttgctgaaaggaggaactatattcgggattggcgaattgggaccgccctggaccgggccttaaacccggggcgggtg  
 tgggggggtacccccaccgtgaccgctacctttgccagggcctaaggccctcctttttcttttcttttccccccgt  
 tccccgggttcccccaaacgctaaaaagggggggctccttagaggggcgataatgggtttggggcctccccccac  
 aaaaaatftttggggggagggtgtcccagggggcgccccctcaaaaaagttttctcctttttggggaggcctttttatgg  
 gagtgtgtccggggaaaacacaacccccccccctttcttttatggaaaa

**>140804-07\_F19\_MreB-Bs\_T7terminator.ab1 1186**

gaaatgtccgtgaattctatctagttttccctttgaaagatggatgtgctccagtgtttccctgtccgatcgtacacaatca  
 agcggatcttcggcgataaggaccggcattttgtttcttcgctgatgactttgtccaaattgcgcaaaagcgtccgcccc  
 ggtaaacactatacctctgtccatgatactgtgcaagctcaggcgggtttttcgagtgtgctcttactgcttcgacaattgt  
 agatacagtgctgcgtagagcattagaaatctcttttctgtaatttcaattgttttcggcagacctgcagcaaatcgcgtccg  
 cggatttccatgtgtcggattcttcaggagcttctgcagatccgatttccatttaatcgttcagccgtacggtcaccgatcat  
 cagattgtacgttttctgatgtagttgataatcgcgtcatccatctcatcaccggctacacggattgactgagacgttacgatg  
 cctccgagggaaataatcgaacttctgtcgtaccgccccgatatcaacaacctgctccagtcgggtcccaactggca  
 gattggccccgattgtcggcggcaaaaggctcttcaatcggatacgcgtcacgcgtccccgctgtcttgcgcacgataac  
 agcgcgttctcaacagctgtaatgcctgatgggacacataccattacataggtttctggcaaacatacctttatftttatggc  
 ctgattgatgtaatafttcatcatcgtcggcgttgttcataatcagcgataacgccgttcttcatcggggcgagagccaccacg  
 ttgcccgggtgctcgtccaatcatatfttgcacatfttccgacagcgacaattgatttctgtatccgtctgcaaagcgacaactg  
 acggctctctcacaacaattccttttcttttacaaaaacaagcgtattcgcagttccaagatctataccaaggtctctagcacc  
 aattccaacatcggccgcccgggcctggaacagacttcaagtgggggggggggggggggggggggggggggggggggttttt  
 agttcctctttttttcccatcttttttgcacttttccatgagcttacctctcttattcccatccctcccccttttttaaaa

>141009-07\_B10\_pTG19-ftsZBs\_M13R-pUC.ab1 1873

ccagcttctatac gactcactatagg gaaagcttgc atgcctgc aggtcgactc tagaggatccc aagattga attccttag  
ccgcgtttattac ggtttctta agaatgtcgg gatgtca agcgtatc atcagcc ggctgtg aagtatg acggctt actgtgttct  
gtgtctg aggtcctc acgtttgg ctcacgctt cggaacactt tgattgtg ttttgatg ctttgatt aagcttgg acgctga  
ggcttcgtc acgtcctt ctcttggc gataaagcc ggttgca atcactgtc accacaatc tcatcttt agattttc attaataaca  
gaaccgaaa atcatgttt acgtctt gatcagac gccgaagc gacaatgt ctgctgctt cctgaacct catatag gctgaggttt  
gttctccagt gatgttcat gaggacgc cttgcgc accgtca atggccg cttaaga agcgggct ggaaattg cttttttgct  
gcctctgcc gcgcgattt tccccag tagcaatac cgatacccat caaagc agatccttt gtttgacat gattgtttc acatcag  
caaagtca aggttgata agaccaggt gtagcaat caagtcaga aatacctt gaaccctt ggcgaa gtacgttat ccgcttc  
acggaatg ettcagcat cgggtgt tttcatca acaattca aggatac ggtcgttc gggatcac gatcagt gatccaccgc  
tttttattg ccgagattc cgctgc agcctga agctgtct tttgcgtc cttcga aggtaaac ggtcttgc acaacgccgac  
agttaatg cgccta agtctttc gcgattt gtcgata accggtgc ggcacctgtt cctgttcc gccccata ccagctgtcac  
gaataccat gtcagcacctt taagtgtt tttcaatc tctctttg ctttctt cagcggcttttt tcccga ctccggattc gcacct  
gtcccaatc ctctagtc agctttgc gccgattt gcatttc acttctg cttttgac aggtta agactttg accgtccgtgtt acc  
gcgatactc tactcctt ggacttc attttca atcattc ggggta acgggggtt gttacc gccgctc taatcc gaataact  
taattgat gctaaacc gcccaatg tttgttctaa attcca aataagggc gggcggggc ggtattt ggattcccc ggggacc  
aaagtcga attacat gggcggc ggtttata agacgg gactgggg aaaaacctc ggcgttccc acttaatc ctttggggca  
tcccctc tcccccc ggggggt aaaaaaaaaa agccgcc gatccgttcca aatcccccccc atacggggggggat  
tgaaaggg gaattt gttata aggggaatttt gtaaac gcttttcaa accggaac gaacttc aaaaaaaaa accaaaagg  
gggggctt gggaaact taaaatg ccccc ggaaactc aggggtgcc actattt ggggggggg gccctttc gcccccc  
cggggaca aaggtca aggtcggggc aggggccttttcca agggctttt atattt gactacc ggaatttcaa agtgcga  
aaatgacc cgttaaac ggggggtccc ggtcggcc ctggag gttatfac gttggc gtaactaaa atgttttttat caat  
ttctaggtttttt gttgttcttag gggcccaattt gccaca atttag ggttagaa accggcctttt gcccttgg gttatctg  
ccctctttt ccttggcc gga

>141009-07\_A10\_pTG19-ftsZBs\_M13F-pUC.ab1 1691

caaacgtcgggaattcagctcgggtaccggggatccaagattggcccggcggccgatgttgagttcgaacaacat  
agacggcttagcatcaattaaagtaatcgagtaggagggcggcggtaacaacgccgtaaccgaatgattgaaaatgaagt  
gcaaggagtagagtatatcgcggtaaacacggacgctcaagctttaacctgtcaaaagcagaagtgaaaatgcaaatcg  
gcgcaaagctgactagaggattgggagcaggtgcgaatccggaagtcgggaaaaagccgctgaagaaagcaaagag  
cagattgaagaagcacttaaaggctgacatggtattcgtgacagctggtatggcggcggaacaggaacaggtgccgc  
accggttatcgcaaaatcgcgaaagacttaggcgattaactgtcggcgttgacaagaccgtttacctcgaaggacgc  
aaaagacagcttcaggctgcaggcgggaatctcggcaatgaaagaagcgggtgataactgatcgtgatcccgaacgacc  
gtatccttgaaattgtgatgaaaacacaccgatgctgaagcattccgtgaagcggataacgtacttcgccaaggggtcaa  
ggatttctgacttgattgctacacctggtcttatcaaccttgactttgctgatgtgaaaacaatcatgtcaaaacaaggatctgc  
tttgatgggtatcggattgctactggggaaaatcgcgcgagaggcagcaaaaaagcaatttcagcccgttcttgaa  
gcggccattgacgggtcgcgaaggcgtcctcatgaacatcactggaggaacaacctcagcctatatgaggttcaggaagc  
agcagacattgctgcttcggcgtctgatcaagacgtaaacatgatttccggttctgttattaatgaaaatctaaaagatgagatt  
gtggtgacagtgattgcaaccggctttatcgaacaagagaaggacgtgacgaagcctcagcgtccaagcttaaatcaag  
catcaaacacacaatcaaagtgtccgaaacgtgagccaaaacgtgaggagctcagcagcagacacagtaagccgcta  
cttcaaagccggctgatgatacgttgaatcccgaattcttaaaaaaccgaaaaaaccggtagaattcattcttggggatct  
cttaaatcacctggaggtggagtttcttaatggaggcgattaaactggcgaaccagggcaacgggttctctgtgggatatg  
gttctccaatcacaataaaaaccaaaaaagtaaacctgggggggctaaggagggaaccattaattttggctccgcctt  
cctccggacatgggggcttaagaaaacaccccaggaaaaaggaaataagggtgcctctcttcctcgtgttccgggggt  
ccccaggggtccaactgaaaatagaagaagaaaaagttaggtctccacaaaaaccaataaaaacagttcgtgcccttct  
ttttttgtttcttaattatcctttctttccctaattttaatttaagtaaaagaagggaagatccctgtccattcccacctt  
taggggaacaaatccataacaaggtctatggccggccctcattgaaccgaaaa

## APPENDIX B

### PHOSPHATE RELEASE ASSAY

#### Standard curve for free phosphate concentration

**Table B1** Free phosphate concentration standard.

Standard PO <sub>4</sub> <sup>3-</sup> (μM)	Absorbance (620 nm)	Standard deviation (SD)
10	0.022	0.003
20	0.044	0.001
30	0.068	0.001
40	0.090	0.004
50	0.119	0.003

**Not:** N=10

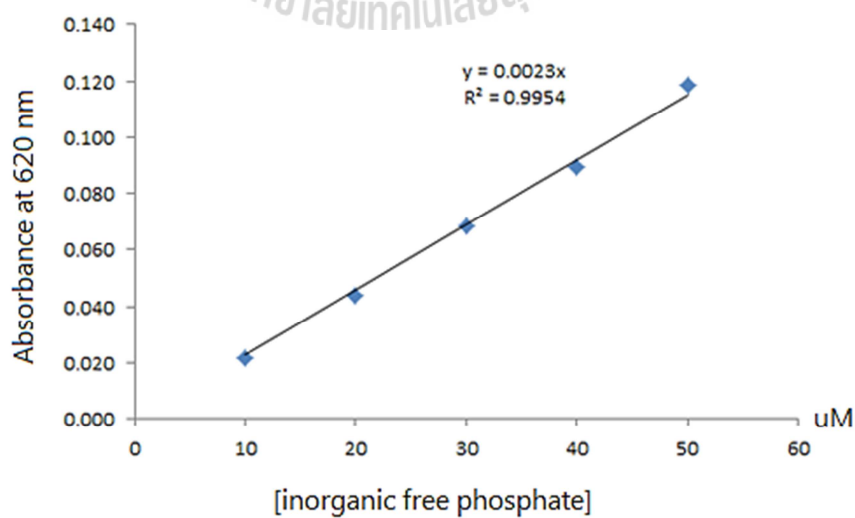


**Table B2** Effect of pH on ATP hydrolysis of the proteins.

pH	MreB	FtsZ	Lysozyme	BSA
pH 5.5	6.80	-0.50	0.20	0.50
pH 6.0	16.50	-1.70	0.35	0.15
pH 6.5	14.90	-1.32	-1.00	0.30
pH 7.0	31.11	-2.12	-1.12	-0.22
pH 7.5	33.70	-1.31	-0.92	0.21
pH 8.0	33.24	0.25	-0.51	-0.3

Not: N=10

**Table B3** Effect of pH on GTP hydrolysis of the proteins.

pH	MreB	FtsZ	Lysozyme	BSA
pH 5.5	20.64	9.00	0.71	0.32
pH 6.0	28.64	13.71	-0.90	0.61
pH 6.5	44.43	17.81	-1.30	-1.51
pH 7.0	39.81	11.15	-0.25	-1.09
pH 7.5	25.77	9.76	-0.91	1.05
pH 8.0	25.26	11.42	0.40	-1.43

Not: N=10

### T-value Equation

$$t = \frac{\bar{X}_1 - \bar{X}_2}{\sqrt{\left(\frac{(N_1 - 1)s_1^2 + (N_2 - 1)s_2^2}{N_1 + N_2 - 2}\right)\left(\frac{1}{N_1} + \frac{1}{N_2}\right)}}$$

**Table B4** Screening of natural compounds effect on ATP hydrolysis by MreB-Bs.

Sample	[PO <sub>4</sub> <sup>3-</sup> ] (μM)	Standard deviation (SD)
MreB + ATP	32.22	2.73
MreB + ATP + Apigenin	31.51	1.11
MreB + ATP + Baicalein	32.76	0.66
MreB + ATP + Luteolin	30.57	1.63
MreB + ATP + Mangostin	32.04	0.97
MreB + ATP + Naringenin	29.34	0.58
BSA + ATP	1.73	0.96
Lysozyme + ATP	0.03	2.19

**Not:** N=10

#### Statistics

MreB + ATP + Apigenin	The t-value is 0.40213. The p-value is 0.354074 The result is not significant at p < 0.05
MreB + ATP + Baicalein	The t-value is 0.4188. The p-value is 0.348438 The result is not significant at p < 0.05
MreB + ATP + Luteolin	The t-value is -0.33284. The p-value is 0.377986 The result is not significant at p < 0.05
MreB + ATP + Mangostin	The t-value is 0.10761. The p-value is 0.459744 The result is not significant at p < 0.05

**Table B5** Screening of natural compounds effect on GTP hydrolysis by MreB-Bs.

Sample	[PO <sub>4</sub> <sup>3-</sup> ] (μM)	Standard deviation (SD)
MreB + GTP	38.37	2.42
MreB + GTP + Apigenin	36.38	1.31
MreB + GTP + Baicalein	35.51	0.95
MreB + GTP + Luteolin	37.12	0.95
MreB + GTP + Mangostin	35.74	1.33
MreB + GTP + Naringenin	38.93	1.05
BSA + GTP	-1.50	0.39
Lysozyme + GTP	-1.30	1.36

**Not:** N=10

### Statistics

MreB + GTP + Apigenin	The t-value is 1.5872. The p-value is 0.09383 The result is not significant at p < 0.05
MreB + GTP + Baicalein	The t-value is 1.78269. The p-value is 0.074608 The result is not significant at p < 0.05
MreB + GTP + Luteolin	The t-value is 0.88195. The p-value is 0.213807 The result is not significant at p < 0.05
MreB + GTP + Mangostin	The t-value is 1.5822. The p-value is 0.094383 The result is not significant at p < 0.05
MreB + GTP + Naringenin	The t-value is -0.12525. The p-value is 0.453186 The result is not significant at p < 0.05

**Table B6** Screening of natural compounds effect on GTP hydrolysis by FtsZ-Bs.

Sample	[PO <sub>4</sub> <sup>3-</sup> ] (μM)	Standard deviation (SD)
FtsZ + GTP*	12.56	1.19
FtsZ + GTP + Apigenin*	8.38	0.67
FtsZ + GTP + Baicalein*	7.22	1.21
FtsZ + GTP + Luteolin	13.25	0.58
FtsZ + GTP + Mangostin	12.78	0.92
FtsZ + GTP + Naringenin	12.72	0.90
BSA + GTP	-1.50	0.39
Lysozyme + GTP	-1.30	1.36

**Not:** N=10

\*N=20

### Statistics

FtsZ + GTP + Apigenin	The t-value is 5.29673. The p-value is 0.00305 The result is significant at $p < 0.01$
FtsZ + GTP + Baicalein	The t-value is 5.43484. The p-value is 0.002781 The result is significant at $p < 0.01$
FtsZ + GTP + Luteolin	The t-value is -0.89731. The p-value is 0.21014 The result is not significant at $p < 0.05$
FtsZ + GTP + Mangostin	The t-value is -0.24936. The p-value is 0.407682 The result is not significant at $p < 0.05$
FtsZ + GTP + Naringenin	The t-value is -0.18151. The p-value is 0.432396 The result is not significant at $p < 0.05$

## APPENDIX C

### CHEMICAL PREPARATIONS

#### **10 N NaOH (200 ml)**

Dissolve 80 g NaOH in a final volume of 200 ml dH<sub>2</sub>O.

#### **1 M Tris-HCl (500 ml)**

1. Dissolve 60.55 g Tris base in 300 ml of dH<sub>2</sub>O.
2. Adjust the pH to the desired value with concentrated HCl.
3. Bring up the volume to 500 ml with dH<sub>2</sub>O.

#### **1 M Sodium acetate (200 ml)**

1. Dissolve 27.22 g sodium acetate in 100 ml of dH<sub>2</sub>O.
2. Add 6 ml of glacial acetic acid.
3. Adjust the pH to the desired value with 10 N NaOH.
4. Bring up the volume to 200 ml with dH<sub>2</sub>O.

#### **0.5 M MES (200 ml)**

1. Dissolve 19.52 g HEPES (free acid) in 100 ml of dH<sub>2</sub>O.
2. Adjust the pH to the desired value with 10 N NaOH.
3. Bring up the volume to 200 ml with dH<sub>2</sub>O.

**1 M HEPES (200 ml)**

1. Dissolve 41.66 g HEPES (free acid) in 100 ml of dH<sub>2</sub>O.
2. Adjust the pH to the desired value with 10 N NaOH.
3. Bring up the volume to 200 ml with dH<sub>2</sub>O.

**0.5 M EDTA, pH 8 (500 ml)**

1. Resuspend 93.05 g Na<sub>2</sub>•EDTA•2H<sub>2</sub>O (disodium dihydrate) in about 400 ml of dH<sub>2</sub>O.
2. Add about 9 g solid NaOH.
3. Once all the NaOH dissolves, slowly adjust the pH with 10 N NaOH.
4. Bring up the volume to 500 ml with dH<sub>2</sub>O.

**Note:** EDTA will not completely dissolve until the pH reaches 8.

**50X TAE buffer (1 L)**

Tris base 242.0 g

Glacial acetic acid 57.1 ml

0.5 M EDTA (pH 8.0) 100 ml

Bring up the volume to 1 L.

**6X DNA loading sample buffer (10 ml)**

Glycerol 3 g

Bromophenol blue 0.025 g

Xylene cyanol FF 0.025 g

Bring up the volume to 10 ml and store at 4 °C.

**SDS-PAGE preparation (30% gel)**

Acrylamide gel solution (100 ml)

acrylamide	29.4 g
bis-acrylamide	0.6 g

Separating gel (15% gel)

dH <sub>2</sub> O	2.9 ml
2 M Tris-HCl, pH 8.8	2 ml
10% SDS	0.1 ml
30% acrylamide gel solution	5 ml
10% (NH <sub>4</sub> ) <sub>2</sub> S <sub>2</sub> O <sub>8</sub>	50 µl
TEMED	5 µl

Stacking gel (4% gel)

dH <sub>2</sub> O	6.1 ml
0.5 M Tris-HCl, pH 6.8	2.5 ml
10% SDS	0.1 ml
30% acrylamide gel solution	1.3 ml
10% (NH <sub>4</sub> ) <sub>2</sub> S <sub>2</sub> O <sub>8</sub>	50 µl
TEMED	10 µl

**10X Running buffer (1 L)**

Tris base	30 g
Glycine	144 g
SDS	10 g

Bring up the volume to 1 L.

**5X Sample buffer**

SDS	1.0 g
Glycerol	5.0 ml
Bromophenol blue	25 mg
Tris base	242 mg
HCl	0.35 ml (adjust the pH to 6.8)
2-Mercaptoethanol	1.0 ml

Bring up the volume to 10 ml and store at 4 °C.

**Coomassie blue stain (1 L)**

Methanol	500 ml
Acetic acid	100 ml
Coomassie blue	0.5 g
dH <sub>2</sub> O	400 ml

Mix on stir plate until all coomassie blue is dissolved.

**De-stain (1 L)**

Methanol	400 ml
Acetic acid	100 ml

Bring up the volume to 1 L.

**10% SDS (100 ml)**

10 g SDS into 100 ml, heat to 68 °C for solubility, pH ~6.6.

**100 mg/ml ampicillin (10 ml)**

1. Weigh 1 g of ampicillin.
2. Bring up the volume to 10 ml and filter sterilizes (0.22  $\mu\text{m}$ ), store at -20 °C.

**1 M IPTG (10 ml)**

1. Weigh 2.38 g of IPTG (MW = 238.3 g/mol).
2. Bring up the volume to 10 ml and filter sterilizes (0.22  $\mu\text{m}$ ), store at -20 °C.

**20 mg/ml X-gal (1 ml)**

1. Weigh 20 mg of X-gal.
2. Bring up the volume to 1 ml with 100% DMF (dimethylformamide), store the stock solution at -20°C in the dark. Discard the stock solution if the color changes significantly.

**LB broth (1 L)**

Tryptone	10 g
Yeast extract	5 g
NaCl	5 g

Dissolve components in 1 L of dH<sub>2</sub>O and sterilize by autoclaving at 15 psi, at 121 °C for 15 minutes.

**LB agar (200 ml)**

Tryptone	2 g
Yeast extract	1 g
NaCl	1 g
Agar	4 g

Dissolve components in 200 ml of dH<sub>2</sub>O and sterilize by autoclaving at 15 psi, at 121 °C for 15 minutes.

**Blue-white selection LB agar plate**

1. Melt LB agar, and allow media to cool to 55 – 60 °C. Add ampicillin to final concentration of 100 µg/ml.
2. Gently swirl the flask to mix the ampicillin into the agar.
3. Pour a thin layer of LB agar ~10 ml into each plate.
4. Let each plate cool until its solid ~20 minutes.
5. Spread 40 µl of IPTG on top of the plate with spreader, let the plates dry in laminar flow.
6. Spread 40 µl of X-gal on top of the plate with a hockey stick spreader. This should take 30 minutes or so if the plate is dry.

**Ni-NTA resin regeneration**

1. Put all of the resin into a big column.
  2. Wash with 3 CV water.
  3. Wash with 3 – 5 CV of 0.5 M NaOH.
  4. Wash with water 5 CV make sure pH turn back to 6 – 7.
  5. Wash with 6 M guanidine hydrochloride and 25 mM imidazole, 2 CV each.
  6. Wash with 5 CV water immediately.
  7. Wash with 2 CV 100 mM EDTA.
  8. Wash with more than 5CV water.
  9. Re-charge the resin with 2 – 3 CV 100 mM NiSO<sub>4</sub> and keep resin in buffer for a couple hours with shaking.
  10. Wash the resin with more than 10 CV water.
  11. Wash with 2 CV 20% ethanol.
  12. Wash with 2 CV 50% ethanol.
  13. Wash with 2 CV 70% ethanol.
  14. Wash with 2 CV 50% ethanol.
  15. Wash with 2 CV 20% ethanol.
- Stock the resin in 20% ethanol in 4 degree.

## CURRICULUM VITAE

**NAME** Acting Sub-Lieutenant Sunaree Choknud

**DATE OF BIRTH** December 06, 1989

**PLACE OF BIRTH** Ubon Ratchathani

**EDUCATION 2015** M.Sc. in Biochemistry, School of Chemistry,  
Institute of Science, Suranaree University of  
Technology, Nakhon Ratchasima, Thailand

**2012** B.Sc. in Chemistry, Department of Chemistry,  
Faculty of Science, Ubon Ratchathani Rajabhat  
University, Ubon Ratchathani, Thailand

### PUBLICATION

Sunaree Choknud and Sakesit Chumnarnsilpa (2016). Screening of natural products effect on GTP hydrolysis of *Bacillus subtilis* FtsZ. **The 11<sup>th</sup> international Symposium of the Protein Society of Thailand.** August 3 – 5, Bangkok, Thailand: 215 – 221.

Sunaree Choknud, Chomphunuch Songsiriritthigul, and Sakesit Chumnarnsilpa (2015). The structural study of the C-terminal half of gelsolin. **The 10<sup>th</sup> International Symposium of the Protein Society of Thailand.** July 15 – 17, Bangkok, Thailand: 167 – 172.

Sunaree Choknud, Oratai Saisa-ard, and Kenneth J. Haller. (2012) Preparation and characterization of carboxylic acid adducts of gabapentin. **Engineering Journal.** 16(3): 29 – 36.